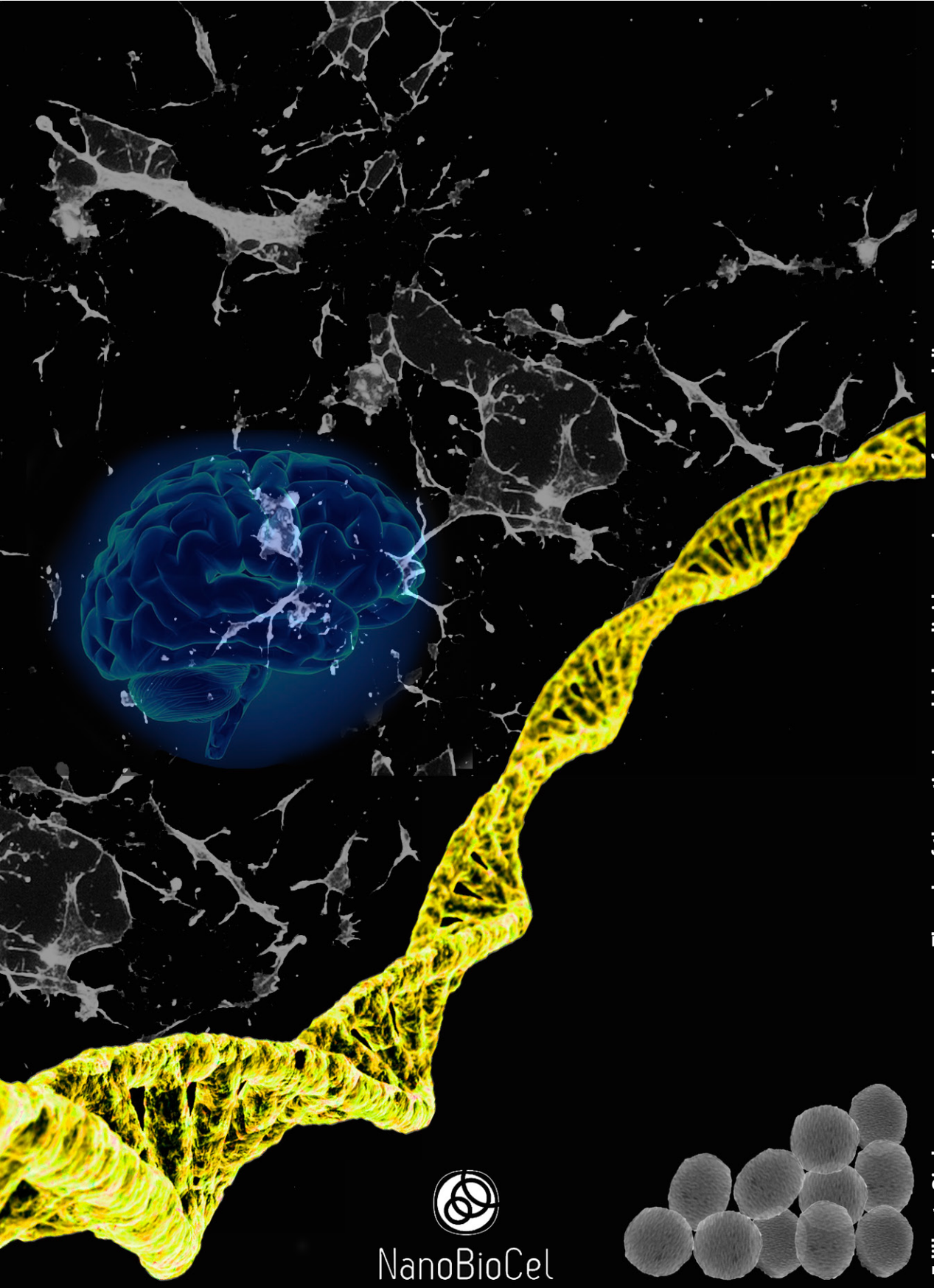

The role of the cationic and helper lipids on niosomes for gene delivery applications: Transfection of retina and brain as a main goal

Edilberto Ojeda Hernández

NanoBioCel

The role of the cationic and helper lipids on niosomes for gene delivery applications: Transfection of retina and brain as a main goal

Edilberto Ojeda Hernández

eman ta zabal zazu

Universidad del País Vasco

Euskal Herriko Unibertsitatea

The role of the cationic and helper lipids on niosomes for gene delivery applications: Transfection of retina and brain as a main goal

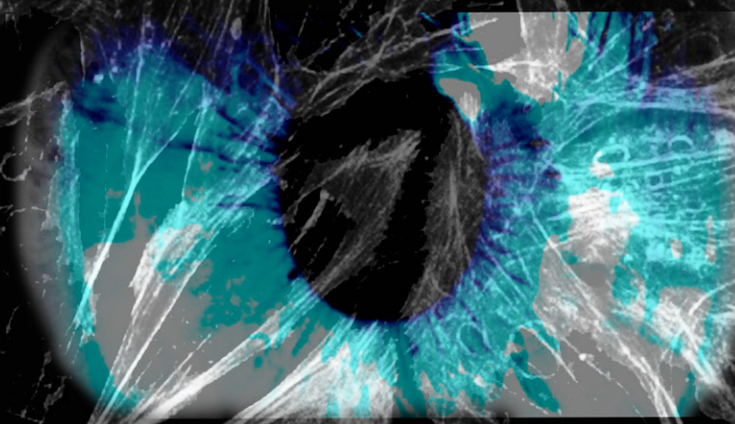

Edilberto Ojeda Hernández

Vitoria-Gasteiz 2016

eman ta zabal zazu
Universidad del País Vasco
Euskal Herriko Unibertsitatea

The role of the cationic and helper lipids on niosomes for gene delivery applications: Transfection of retina and brain as a main goal

Edilberto Ojeda Hernández
NanoBiocel Group, Laboratory of Pharmaceutics
University of the Basque Country (UPV/EHU)
Faculty of Pharmacy
Vitoria-Gasteiz 2016

NanoBioCel
Grupo de Micro y Nano Tecnologías, Biomateriales y Células

ACKNOWLEDGMENTS

La lista es larga y podría pasarme horas intentando escribir los nombres de cada uno de ustedes, digo horas porque con cada nombre se me vienen muchas memorias. Por tanto, es difícil poner nombres y apellidos para agradecer a cada uno. Sin embargo, cada uno de ustedes sabe del apoyo que me ha brindado a lo largo de estos años.

Sin duda alguna quiero agradecer a mi madre por brindarme su apoyo y amor incondicional y por estar siempre en los momentos más importantes de mi vida. A ella le debo la vida y gran parte de lo que soy. Todos mis logros se los dedico a ella con todo mi amor y en especial esta tesis doctoral, que sin su apoyo estos cuatro años hubieran sido aún más duros. Gracias por estar ahí una vez más, te debo más de lo que te puedes imaginar.

A mi familia que me han guiado, dado sus sabios consejos y que me han cobijado con su cariño y que sin duda me han ayudado a salir adelante, aunque miles de kilómetros y un océano están de por medio.

A mis apreciados amigos que sin duda han sido como una familia y que a pesar de la distancia, con algunos, siempre he podido contar con ellos en los buenos y malos momentos. Gracias por escuchar siempre, brindarme su apoyo, sabiduría y momentos inolvidables, gracias a todos ustedes. Gracias a todos ustedes por estar conmigo siempre que los necesito, a enseñarme que la vida hay que tomarla con sabiduría y alegría. Por nada de este mundo los cambiaría.

A mis compañeros del laboratorio de Farmacia y del CIEA por estar ahí cuando los experimentos salían mal, como es normal en un doctorado, y brindarme su apoyo, hombro y consejos en momentos de tensión. Y porque no todo es trabajo, gracias por los buenos momentos y recuerdos, por los cumpleaños, las sidrerías y las cenas inolvidables. También, quiero agradecer a aquellos con los que compartí y sigo compartiendo algo más que una relación de trabajo, a los que me ofrecieron su amistad y un hueco en sus cuadrillas.

To my labmates in Rome, Italy that made me feel part of the group during my stay. This thesis was also possible for their valuable contribution and hard work. Grazie a tutti per la vostra cortesia.

A mis tutores Gustavo Y José Luis por brindarme la oportunidad de desarrollarme como investigador y guiarme en el mundo de la ciencia. Este trabajo es el fruto de un gran esfuerzo y dedicación que no hubiera sido posible sin sus valiosos consejos y opiniones.

Muchas gracias a todos porque han hecho de este proyecto una realidad.

ACKNOWLEDGMENT FOR THE FINANCIAL SUPPORT

This thesis has been partially supported by the Basque Government (Consolidated Groups, IT-407-07) and the Univeristy of the Basque Country (UPV/EHU) (UFI 11/32). The intellectual and technical assistance from the ICTS "NANBIOSIS", more specifically, by the Drug Formulation Unit (U10) of the CIBER in Bioengineering, Biomaterials & Nanomedicine (CIBER-BBN) at the University of Basque Country (UPV/EHU) is acknowledge. Edilberto Ojeda Hernández gratefully acknowledges the support provided by The National Council of Science and Technology (CONACYT), Mexico for the fellowship grant.

ACKNOWLEDGMENT TO THE EDITORIALS

Authors would like to thank the editorials for granting permission to reuse their previously published articles in this thesis.

Ojeda et al. Organic & Biomolecular Chemistry. 2015;13:1068-1081

Ojeda et al. Biomaterials. 2016; 77: 267-279

Ojeda et al. International Journal of Pharmaceutics. 2016; 503: 115-126

Ojeda et al. Springer. 2016; 1445

Disfruta hoy, es más tarde de lo que parece
Enjoy right now, today might be already late

Anonymous

Table of Contents

1

Introduction

1.1. GENE THERAPY BACKGROUND

Gene therapy aims to cure or treat diseases through the molecular point of view, where DNA is delivered into the cell nucleus to produce or regulate defective genes. Moreover, gene therapy attempts to decrease the side effects or administration periods [1]. It has been described that gene therapy success mainly relies on an appropriate selection of the gene carrier since the delivery of naked DNA is an inefficient process. Within the requirements for the design of an appropriate gene carrier, we must consider that such carrier should be able to transport the DNA through the extracellular and intracellular barriers until the DNA reaches the cell nucleus, without compromising the integrity of the targeted cells or the genetic material itself [2]. Depending on the targeted cells, gene therapy is usually divided in two categories: 1) germ line gene therapy [3] and 2) somatic gene therapy [4]. Germ line therapy is the most restricted worldwide therapy since it implies the use of sperm or eggs, where any change in the DNA sequence will be passed to the next generation. On the other hand, somatic gene therapy targets any type of cells in the body but germ line cells and this therapy will only be focused on the individual patient.

Over the years, gene therapy has roused the interest of the scientist community. Such interest was based on important discoveries that led gene therapy be considered as a credible option. The first step for gene therapy took place in 1928 when Frederick Griffith [5] described the transformation of non-virulent pneumococcal bacteria type into virulent type *in vivo* and the subsequent discovery, in 1933, that this modification was caused by a substance called "transformation principle" [6]. Years later, in 1944, Avery and McCarty [7] purified such substance and concluded that the transformation of the *pneumococcus* bacteria was caused by deoxyribonucleic acid (DNA), whose double-helix structure was described by Watson and Crick in 1953. Finally, in 1961 Howard Temin discovered that virus could transfer genetic material and it could be inherited [8]. This important finding allowed considering the idea that gene transfer could be used as a tool towards the gene therapy. However, it was until 1973 when Rogers and Pfuderer conducted the first gene therapy trial [9,10]. Since then, more than 2000 clinic trials have been approved. Within gene therapy approaches there are two types of vectors: 1) viral vectors and 2) non-viral vectors, where the 70% of the clinical trials relies on viral vectors and, only, the 30% on non-viral vectors (Fig. 1) [11].

Despite the number of clinical trails above-mentioned, there are only four gene therapy products in the market, which are gene therapies based on viral vectors. In 2003, China approved the first gene therapy product, Gendicine™ followed by Oncorine™ in 2005, Glybera in 2012 in Europe and IMLYGIC™ in 2015 in USA (Table 1).

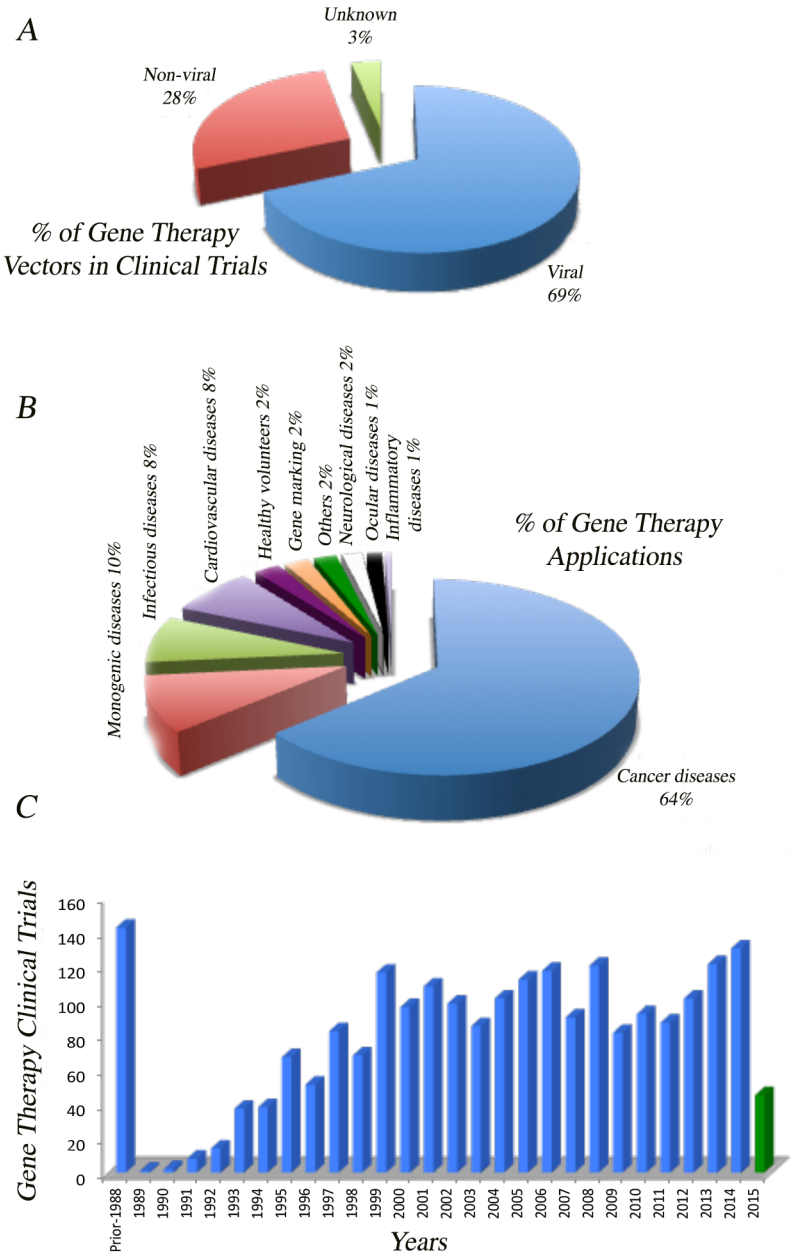

Figure 1. Statistical data of gene therapy clinical trials with viral and non-viral vectors. A) Distribution of clinical trials by type of vector. B) Distribution of clinical trials by application. C) Number of gene therapy clinical trials by year [11].

Gene therapy product	Type of vector	Therapeutic application
Gendicine™	Adenoviral vector	Head and neck squamous cell carcinoma treatment
Oncorine™	Adenoviral vector	Late stage refractory nasopharyngeal cancer treatment
Glybera	Adeno-associated viral vector	Severe lipoprotein lipase deficiency treatment
IMLYGIC™	Herpes simplex virus	Local treatment of unresectable cutaneous, subcutaneous and nodal lesions in patients with melanoma recurrent

Table 1. Gene therapy products in the market.

1.2. GENE DELIVERY VECTORS

Effective DNA delivery into the cells is a crucial step for a successful gene therapy. This step is subjected to the type of vector employed (See Table 2). Vectors for gene delivery purposes are classified in viral and non-viral vectors. Depending on the gene treated disorder or the complexity of the targeted cells such vectors must meet certain characteristics. Therefore, the election of the right vector can be a difficult task. Additionally, there are several factors that need to be addressed before gene vectors can be used to treat or cure diseases. Such factors include eluding invasive administrations, safe approaches to deliver the genetic material, production cost and effectiveness, where DNA protection from degradation, high cell internalization and long lasting gene expression are fundamental for the success of gene therapy [12] (Table 3).

Ideal gene vector	• DNA protection against enzymatic degradation • High cell internalization • DNA release into the cell nucleus • Non-immune response • Cell specificity • Long gene expression • Patient Safety • Low manufacture cost • Non-invasive administration

Table 2. Ideal gene vector characteristics.

Viral vectors	
Advantages	**Disadvantages**
• Transduction efficiency • Long lasting gene expression • More clinic trials • Commercialized products	• Safety • Low packaging capacity • Production cost • Genetic material integration • Immunogenicity • Broad tropism • Oncogenesis
Non viral vectors	
Advantages	**Disadvantages**
• Safety • High packaging capacity • Production cost • Easy to prepare • Low immunogenicity	• Low transfection efficiency • Few clinic trials • Short periods of gene expression

Table 3. Advantages and disadvantages of viral and non-viral vectors for gene therapy.

1.2.1. Viral vectors

Viral vectors are obtained from viruses that have been genetically modified, where the viral genome has been replaced with therapeutic human genes [13]. These vectors have

the capacity to integrate and non-integrate the genetic material into the genome. Currently, viral vectors represents around the 70% of the gene therapies in clinic trials [11]. This elevated number, clearly, represents the preference of researchers to viral vectors since these vectors have a highly cell internalization capacity and their efficiency to deliver, protect the genetic material and long lasting gene expression is also remarkable. Nevertheless, the use of viruses represents a constant hazard due to their ability to integrate the genetic material into the host genome, broad tropism, immunogenicity and oncogenesis. Additionally, the packaging capacity of these vectors is limited (between 8 and 38, some times around 150 kb, see table 4) [14,15] and their production cost is elevated [16].

Viral Vectors	Genetic material	Packaging capacity
Adenovirus	dsDNA	38 kb
Adeno-associated virus	ssDNA	4.8 kb
Retrovirus	RNA	8 kb
Lentivirus	RNA	8 kb
Herpesvirus	dsDNA	150 kb

Table 4. Type of genetic material employed by viral vectors and their packaging capacity [14-16].

1.2.2. Non-viral vectors

Non-viral vectors are those vectors prepared or obtained with synthetic or natural compounds as an alternative to viral vectors, such as electroporation, sonoporation, magnetofection or gene delivery mediated by dendrimers, polymers or lipid-based vectors (Table 5) [15,17].

Despite the low percentage of non-viral vectors that have reached clinic trials (Fig. 1A), researchers are constantly improving and developing new compounds and techniques that would help to deliver the genetic material with the above-mentioned non-viral vectors since these vectors are safer (low immune response), easier to prepare and use, and their production cost is lower than viral vectors [18]. Additionally, the size of the genetic material that can be carried with

Non-viral gene delivery vectors		
Physical delivery	Mechanical	DNA injection and gene gun [64,65]
	Electroporation	Electrical membrane cell disruption [66]
	Ultrasonic	Ultrasound waves to disrupt the cell membrane [67]
	Photoporation	Laser pulse to generate pores on the cell membrane [66]
	Hydroporation	Hydrodynamic pressure to penetrate the cell membrane [66]
	Magnetofection	Magnetic particles [68]
Chemical systems	Inorganic particles	Calcium phosphate, Silica, Gold [69-71]
	Polymers	PLL, PEI, Chitosan, Dendrimers, PLGA [72-76]
	Peptides	Cationic peptides: attach to lipoplexes and polyplexes to increase specificity [77]
	Cationic lipids	DOTAP, DOTMA, DOGS, DC-Chol [78,79]

Table 5. Non-viral vectors used in gene therapy research.

these vectors is basically unlimited. However, there are some drawbacks related to these carriers, for example, the difficulty to deliver the genetic material into the cell nucleus and the low gene expression [19]. Among the different non-viral options, cationic lipids represent an interesting option since their positive charge can increases the success of gene delivery due to their capacity to condensate the DNA and to fuse with the negatively charged cell membrane, which increases the probability to deliver the DNA into the cell nucleus (Fig. 2) [20,21].

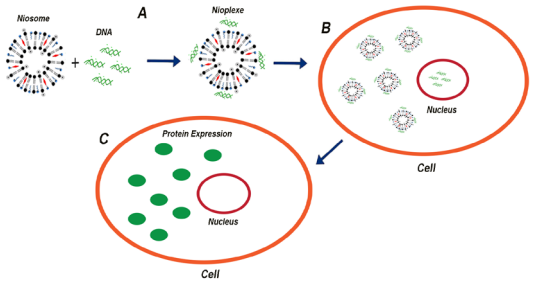

Figure 2. Gene therapy exemplification with non-viral vectors (Niosomes). A) The niosome is complex with DNA to form nioplexes. B) The nioplexes are internalized into the cell by different endocytic pathways and the DNA is delivered into the nucleus. C) Transfected cell, where the desired protein is expressed in the cytoplasm.

1.2.2.1. Cationic lipids

Since the introduction of the first cationic lipid in 1987, cationic lipids have been used to prepare nanoparticles for gene therapy purposes, for example liposomes and niosomes. Through the years, these cationic lipids have been structurally modified to increase their efficiency as gene vectors (Fig. 3) [22]. Moreover, the structural design of the cationic lipids plays an important role in relevant physicochemical parameters of nanoparticles, e.g. size, polydispersity index, morphology and superficial charge, where any change in such parameters can affect cell viability, cellular uptake, intracellular trafficking and nuclear entry [21,23]. Therefore, to obtain more efficient and less toxic cationic lipids for gene delivery applications, the chemical structure of cationic lipids needs to be deeply considered.

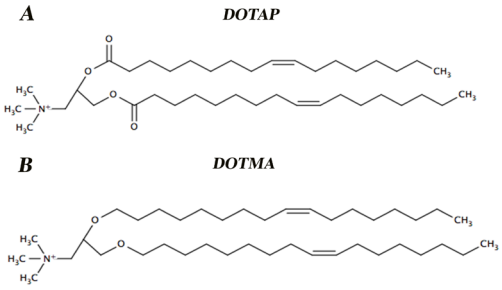

Figure 3. Two of the most studied cationic lipids for gene therapy purposes. A) Cationic lipid DOTAP. B) Cationic lipid DOTMA

Cationic lipids contain four functional domains: 1) Hydrophobic group. This group is usually derived from aliphatic hydrocarbon chains and often contains two linear aliphatic chains [21]. 2) Linker group. This part affects the flexibility, stability and biodegradability of the cationic lipid and its length determines the level of hydration [24]. 3) Backbone. It separates the polar head-group from the hydrophobic group; serinol and glycerol groups are the most popular units [23]. 4) Hydrophilic head-group. This domain is responsible

for the interaction with DNA and its condensation to form complexes due to electrostatic interactions (Fig. 4) [25].

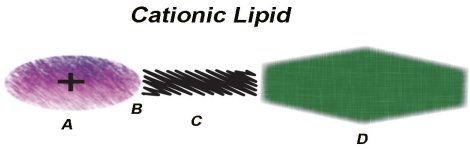

Figure 4. Cationic lipid basic structure. A) Hydrophobic group. B) Linker group. C) Backbone. C) Hydrophilic group.

1.2.2.2. Cationic lipid particles

Liposomes are normally prepared with phospholipids and they are morphologically spherical and small. Since liposomes are hydrophobic-hydrophilic and biodegradable, they are great candidates for drug delivery applications [1]. Liposomes can be prepared by several techniques e.g., mechanical dispersion, solvent dispersion or detergent removal method. Moreover, depending on the preparation technique the characteristics of liposomes, such as size, might differ. Liposomes are usually employed in the cosmetic and the pharmaceutical industry for delivery of molecules e.g., drugs or markers. Their use as gene delivery vectors became tangible when the cationic lipid DOTMA was employed to prepared liposomes capable to deliver DNA in different cell lines [26]. However, the use of liposomes in gene therapy is still limited due to their low solubility, short half-life, phospholipid oxidation, cell toxicity and low stability [27].

Niosomes are non-ionic surfactant carrier systems with a bilayer structure based on cationic lipids, which structure and physical properties clearly influence on the transfection efficiency and toxicity [23,28]. Moreover, niosomes are also prepared with non-ionic surfactants to form stable emulsions [29] and helper lipids that enhance the physicochemical properties of the mixture [30]. Structurally and physically, niosomes are similar to liposomes (Fig. 5). However, their difference relies on their compounds, i.e., niosomes are prepared using non-ionic surfactants instead of phospholipids. Additionally, these carriers are recognized for their low cost and superior chemical and storage stabilities. Nevertheless, their use in gene therapy is still limited since there are few reported results on their application for gene delivery purposes [31,32]. Therefore, the progress of niosomes as non-viral vectors is a challenging task, where further development is needed. See annex for detailed information about preparation and characterization of niosomes for gene delivery purposes.

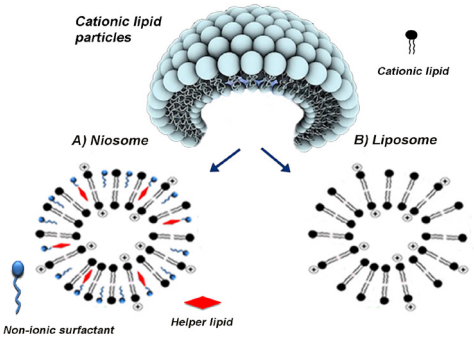

Figure 5. Structure of cationic lipid particles A) Niosome. B) Liposome

1.3. GENE DELIVERY BARRIERS

To deliver genes efficiently into the nucleus, vectors must circumvent several barriers that may difficult or impede such delivery. These barriers can be divided as extracellular and intracellular barriers. Once the vectors have passed the extracellular barriers and have been delivered in the desired region, intracellular barriers come into play and different factors might influence on the internalization process.

1.3.1. Extracellular barriers

Extracellular barriers are the first barriers that protect the integrity of the cells from foreign agents and it is important for any gene vector to overcome these barriers before a rapid clearance or degradation occurs (Fig. 6). The bloodstream is the preferred via for some gene delivery vectors since any organ or body compartment is connected to the circulatory system. However, the presence of enzymes and the non-specific binding to serum proteins (albumin, complement, immunoglobulins) and blood cells (erythrocytes, leukocytes, macrophages, platelets) are responsible for the degradation or aggregation of the DNA/vectors in the circulatory system, where naked DNA has shown short half-live (1.2 to 20 min.) [33-35]. On the other hand, when vectors are administered by the respiratory system, the alveolar macrophages in the lungs can make difficult the access of the gene vector to the targeted cells [36]. Moreover, the intervention of such barriers might end in the removal of the vectors by the reticuloendothelial system, liver, spleen and sometimes in the activation of the immune system, where inflammatory responses and complement activation are triggered [33,34]. Even thought non-viral vectors are generally exempted from the immune response, it has been observed that some vectors prepared with lipids, PEI or PEG can possibly activate the immune system [37-39].

Therefore, the consideration of the above mentioned extracellular barriers is important for a successful gene delivery, where the non-viral vectors characteristics, such as superficial charge or biodegradability and biocompatibility, might condition the implication of such barriers.

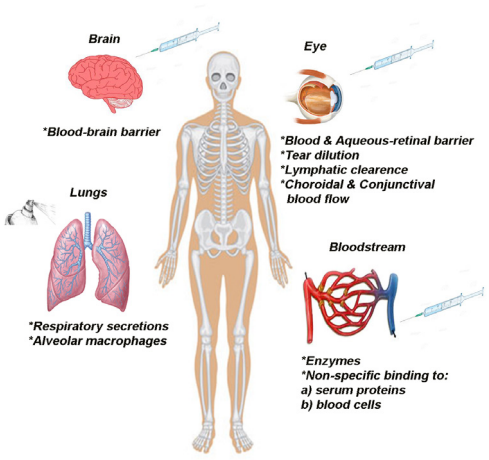

Figure 6. Extracellular barriers for gene delivery vectors

1.3.2. Additional barriers for specific organs

Some organs, such as the eye or brain, have their mechanisms (blood-retinal and blood-brain barrier) that isolate them from the rest of the organism, which difficult the gene delivery to such organs. The eye is an interesting organ for gene delivery applications due to its immune tolerance, which might cause to avoid rejection and inflammation from foreign antigens. Additionally, it is well known the genetic background of many devastating genetic diseases that affect this organ, such as leber congenital amaurosis, leber hereditary optic neuropathy, choroideremia, stargardt disease or retinoschisis [40,41]. However, ocular gene delivery represents a great challenge to the scientific community due to some barriers that need to be overcome before the targeted cell is reached. Some of these barriers include the layers of cornea, sclera, and blood aqueous and blood-retinal barriers, choroidal and conjunctival blood flow, lymphatic clearance, and tear dilution [42,43].

The brain is another important organ for gene delivery applications, where reside specialized cells (neurons and glial cells) protected with highly specialized barriers, for example the neurovascular unit, meninges, choroid plexus, neuroependyma and adult ependymal, to avoid any damage from foreign agents. Due to the specialized role of these cells, any disruption in their functionality might provoke several neurological disorders. Since several neural diseases have a known genetic origin, such as Parkinson, Huntington disease, and Alzheimer, among many others, gene therapy offers the alternative to address them from the molecular point of view [44-46]. Even though non-viral vectors, such as peptide nanoparticles and liposomes, have already opened a window for the treatment of neural diseases with some promising results [47-49], the complexity to bypass the brain barrier makes difficult to reach and transfect the brain cells.

1.3.3. Intracellular barriers

The study of the intracellular barriers is fundamental for the development of gene delivery vectors, where cellular uptake and intracellular trafficking studies are needed to understand how the vectors are processed when they are in contact with the cell membrane (Fig. 7 A) [1,37].

Proteins, phospholipid bilayers and microdomains constitute the cell membrane, which is the first cell barrier that any gene vector has to overcome. Such membrane is in charge to protect the cells components from the exterior by the restriction of the material exchange from the inside to the outside or vice versa. Overcome this barrier is crucial for gene therapy success since it will select how the external material will be processed through the membrane to its final fate [50]. The cell membrane can process the external material, e.g. non-viral vectors, into the cytoplasm by several endocytic pathways, where the most

studied are clathrin-mediated endocytosis (CME), caveolae-mediated endocytosis (CvME), macropinocytosis and the possible lysosomal intervention (Fig. 7B-D) [51-53]. CME is an energy dependent pathway that requires GTPasa dynamin. This pathway is characterized by the accumulation of clathrin structures around the engulfed pit, where these clathrin-coated vesicles are depolarized and turn into early endosomes followed by late endosomes and finally to lysosomes [54,55]. CvME, a GTPasa dynamin dependent process, is considered a non-acidic pathway that shows caveolae membrane microdomains formed by caveolins, cholesterol and sphingolipids. When these pits are processed through membrane by this pathway, they become caveosomes and avoid the lysosomes. However, there are some findings that suggest that caveosomes also fuses to the lysosomes [56-58]. Macropinocytosis is a process generated by actin-driven invaginations, where there are not coating structures to form the macropinosomes. It is believed that macropinosomes fuse with lysosomes. Additionally, there is evidence that macropinosomes can suffer a partial acidification without lysosomal fusion and be driven out the cell for a possible cell reenter (recycling process). This pathway is considered an efficient route since invaginations are large and the particles that show nonselective endocytosis can be easily internalized through this pathway [59-61]. Lysosomes are in charge of molecule degradation in the cell cytoplasm, where such degradation inside the lysosomes is possible due to their high proton concentration (pH $\leq$ 5). Their intervention, among other factors, will depend on the type of analyzed cells, i.e., phagocytic specialized cells (macrophages) will show higher amounts of lysosomes compared to less specialized phagocytic cells (pituitary cells). It is believed that the final destination of any material inside the lysosomes is the degradation [62]. However, there are findings that suggest that certain materials are able to scape through the pH-buffering effect, which provokes osmotic swelling and rupture due to the protonation of the entrapped material and a subsequent influx of ions and water [63].

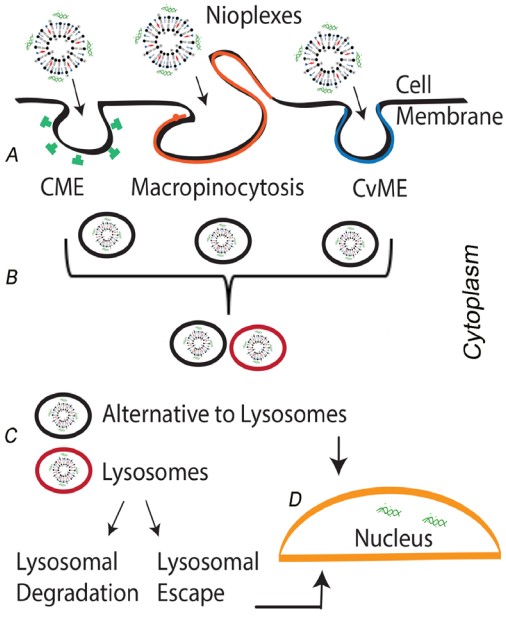

Figure 7. Cell internalization processes of non-viral vectors (nioplexes). A) Cell uptake through CME, Macropinocytosis and CvME. B) Endocytic pathway canalization of nioplexes. C) Endocyted nioplexes can and cannot follow the lysosomal degradation. D) DNA delivery into the cell nucleus

1.4. REFERENCES

1. Yin H, Kanasty RL, Eltoukhy AA, Vegas AJ, Dorkin JR, Anderson DG. Non-viral vectors for gene-based therapy. Nat Rev Genet 2014;15:541-555.
2. Pezzoli D, Chiesa R, De Nardo L, Candiani G. We still have a long way to go to effectively deliver genes! J Appl Biomater Funct Mater 2012;10:82-91.
3. Matthews QL, Curiel DT. Gene therapy: human germline genetic modifications--assessing the scientific, socioethical, and religious issues. South Med J 2007;100:98-100.
4. Bank A. Human somatic cell gene therapy. Bioessays 1996;18:999-1007.
5. Griffith F. The Significance of Pneumococcal Types. J Hyg (Lond) 1928;27:113-159.
6. Alloway JL. Further Observations on the use of Pneumococcus Extracts in Effecting Transformation of Type in Vitro. J Exp Med 1933;57:265-278.
7. Avery OT, Macleod CM, McCarty M. Studies on the Chemical Nature of the Substance Inducing Transformation of Pneumococcal Types : Induction of Transformation by a Desoxyribonucleic Acid Fraction Isolated from Pneumococcus Type Iii. J Exp Med 1944;79:137-158.
8. Temin HM. Mixed infection with two types of Rous sarcoma virus. Virology 1961;13:158-163.
9. Rogers S, Pfuderer P. Use of viruses as carriers of added genetic information. Nature 1968;219:749-751.
10. Rogers S, Lowenthal A, Terheggen HG, Columbo JP. Induction of arginase activity with the Shope papilloma virus in tissue culture cells from an argininemic patient. J Exp Med 1973;137:1091-1096.
11. Wiley J. Gene Therapy Clinical Trials Worldwide. 2015;2015.
12. Rodríguez-Gascon A., del Pozo-Rodríguez A., Solinís M.A. Non-viral delivery systems in gene therapy, In: Dr. Francisco Martin, editor. Gene Therapy - Tools and Potential Applications: InTech, 2013.
13. Walther W, Stein U. Viral vectors for gene transfer: a review of their use in the treatment of human diseases. Drugs 2000;60:249-271.
14. Thomas CE, Ehrhardt A, Kay MA. Progress and problems with the use of viral vectors for gene therapy. Nat Rev Genet 2003;4:346-358.
15. Nayerossadat N, Maedeh T, Ali PA. Viral and nonviral delivery systems for gene delivery. Adv Biomed Res 2012;1:27-9175.98152. Epub 2012 Jul 6.
16. Sun S, Rao VB, Rossmann MG. Genome packaging in viruses. Curr Opin Struct Biol 2010;20:114-120.
17. Ramamoorth M, Narvekar A. Non viral vectors in gene therapy- an overview. J Clin Diagn Res 2015;9:GE01-6.
18. Kamimura K, Suda T, Zhang G, Liu D. Advances in Gene Delivery Systems. Pharmaceut Med 2011;25:293-306.
19. Charbel Issa P, MacLaren RE. Non-viral retinal gene therapy: a review. Clin Experiment Ophthalmol 2012;40:39-47.
20. Chung H, Kim TW, Kwon M, Kwon IC, Jeong SY. Oil components modulate physical characteristics and function of the natural oil emulsions as drug or gene delivery system. J Controlled Release 2001;71:339-350.
21. Byk G, Dubertret C, Escriou V, Frederic M, Jaslin G, Rangara R, et al. Synthesis, activity, and structure--activity relationship studies of novel cationic lipids for DNA transfer. J Med Chem 1998;41:229-235.
22. Martin B, Sainlos M, Aissaoui A, Oudrhiri N, Hauchecorne M, Vigneron JP, et al. The design of cationic lipids for gene delivery. Curr Pharm Des 2005;11:375-394.
23. Zhi D, Zhang S, Wang B, Zhao Y, Yang B, Yu S. Transfection efficiency of cationic lipids with different hydrophobic domains in gene delivery. Bioconjug Chem 2010;21:563-577.
24. Mahidhar YV, Rajesh M, Chaudhuri A. Spacer-arm modulated gene delivery efficacy of novel cationic glycolipids: design, synthesis, and in vitro transfection biology. J Med Chem 2004;47:3938-3948.
25. Karmali PP, Chaudhuri A. Cationic liposomes as non-viral carriers of gene medicines: resolved issues, open questions, and future promises. Med Res Rev 2007;27:696-722.
26. Felgner PL, Gadek TR, Holm M, Roman R, Chan HW, Wenz M, et al. Lipofection: a highly efficient, lipid-mediated DNA-transfection procedure. Proc Natl Acad Sci U S A 1987;84:7413-7417.
27. Akbarzadeh A, Rezaei-Sadabady R, Davaran S, Joo SW, Zarghami N, Hanifehpour Y, et al. Liposome:

classification, preparation, and applications. Nanoscale Res Lett 2013;8:102-276X-8-102.
28. Ma B, Zhang S, Jiang H, Zhao B, Lv H. Lipoplex morphologies and their influences on transfection efficiency in gene delivery. J Control Release 2007;123:184-194.
29. Huang Y, Rao Y, Chen J, Yang VC, Liang W. Polysorbate cationic synthetic vesicle for gene delivery. J Biomed Mater Res A 2011;96:513-519.
30. Mochizuki S, Kanegae N, Nishina K, Kamikawa Y, Koiwai K, Masunaga H, et al. The role of the helper lipid dioleoylphosphatidylethanolamine (DOPE) for DNA transfection cooperating with a cationic lipid bearing ethylenediamine. Biochim Biophys Acta 2013;1828:412-418.
31. Rajera R, Nagpal K, Singh SK, Mishra DN. Niosomes: a controlled and novel drug delivery system. Biol Pharm Bull 2011;34:945-953.
32. Puras G, Mashal M, Zarate J, Agirre M, Ojeda E, Grijalvo S, et al. A novel cationic niosome formulation for gene delivery to the retina. J Control Release 2014;174:27-36.
33. Cullis PR, Chonn A, Semple SC. Interactions of liposomes and lipid-based carrier systems with blood proteins: Relation to clearance behaviour in vivo. Adv Drug Deliv Rev 1998;32:3-17.
34. Sakurai F, Nishioka T, Saito H, Baba T, Okuda A, Matsumoto O, et al. Interaction between DNA-cationic liposome complexes and erythrocytes is an important factor in systemic gene transfer via the intravenous route in mice: the role of the neutral helper lipid. Gene Ther 2001;8:677-686.
35. Houk BE, Hochhaus G, Hughes JA. Kinetic modeling of plasmid DNA degradation in rat plasma. AAPS PharmSci 1999;1:E9.
36. McCray PB,Jr, Wang G, Kline JN, Zabner J, Chada S, Jolly DJ, et al. Alveolar macrophages inhibit retrovirus-mediated gene transfer to airway epithelia. Hum Gene Ther 1997;8:1087-1093.
37. Wang T, Upponi JR, Torchilin VP. Design of multifunctional non-viral gene vectors to overcome physiological barriers: dilemmas and strategies. Int J Pharm 2012;427:3-20.
38. Dow SW, Fradkin LG, Liggitt DH, Willson AP, Heath TD, Potter TA. Lipid-DNA complexes induce potent activation of innate immune responses and antitumor activity when administered intravenously. J Immunol 1999;163:1552-1561.
39. Semple SC, Harasym TO, Clow KA, Ansell SM, Klimuk SK, Hope MJ. Immunogenicity and rapid blood clearance of liposomes containing polyethylene glycol-lipid conjugates and nucleic Acid. J Pharmacol Exp Ther 2005;312:1020-1026.
40. Farrar GJ, Millington-Ward S, Chadderton N, Mansergh FC, Palfi A. Gene therapies for inherited retinal disorders. Vis Neurosci 2014;31:289-307.
41. Lipinski DM, Thake M, MacLaren RE. Clinical applications of retinal gene therapy. Prog Retin Eye Res 2013;32:22-47.
42. Herrero-Vanrell R, Vicario de la Torre M, Andrés-Guerrero V, Barbosa-Alfaro D, Molina-Martínez IT, Bravo-Osuna I. Nano and microtechnologies for ophthalmic administration, an overview. Journal of Drug Delivery Science and Technology 2013;23:75-102.
43. Diebold Y, Calonge M. Applications of nanoparticles in ophthalmology. Prog Retin Eye Res 2010;29:596-609.
44. Bertram L, Tanzi RE. The genetic epidemiology of neurodegenerative disease. J Clin Invest 2005;115:1449-1457.
45. Tsuji S. Genetics of neurodegenerative diseases: insights from high-throughput resequencing. Hum Mol Genet 2010;19:R65-70.
46. Simonato M, Bennett J, Boulis NM, Castro MG, Fink DJ, Goins WF, et al. Progress in gene therapy for neurological disorders. Nat Rev Neurol 2013;9:277-291.
47. Yurek DM, Fletcher AM, Smith GM, Seroogy KB, Ziady AG, Molter J, et al. Long-term transgene expression in the central nervous system using DNA nanoparticles. Mol Ther 2009;17:641-650.
48. Ajmani PS, Tang F, Krishnaswami S, Meyer EM, Sumners C, Hughes JA. Enhanced transgene expression in rat brain cell cultures with a disulfide-containing cationic lipid. Neurosci Lett 1999;277:141-144.
49. Geisert EE,Jr, Del Mar NA, Owens JL, Holmberg EG. Transfecting neurons and glia in the rat using pH-sensitive

immunoliposomes. Neurosci Lett 1995;184:40-43.
50. Lynn F., Gottfried and David A. Dean. Extracellular and intracellular barriers to non-viral gene transfer. In: Prof. Ming Wei, editor. Novel Gene Therapy Approaches: InTech, 2013.
51. Zhao F, Zhao Y, Liu Y, Chang X, Chen C, Zhao Y. Cellular uptake, intracellular trafficking, and cytotoxicity of nanomaterials. Small 2011;7:1322-1337.
52. Marchini C, Pozzi D, Montani M, Alfonsi C, Amici A, Amenitsch H, et al. Tailoring lipoplex composition to the lipid composition of plasma membrane: a Trojan horse for cell entry? Langmuir 2010;26:13867-13873.
53. Cardarelli F, Pozzi D, Bifone A, Marchini C, Caracciolo G. Cholesterol-dependent macropinocytosis and endosomal escape control the transfection efficiency of lipoplexes in CHO living cells. Mol Pharm 2012;9:334-340.
54. Le Roy C, Wrana JL. Clathrin- and non-clathrin-mediated endocytic regulation of cell signalling. Nat Rev Mol Cell Biol 2005;6:112-126.
55. Rappoport JZ. Focusing on clathrin-mediated endocytosis. Biochem J 2008;412:415-423.
56. Kirkham M, Parton RG. Clathrin-independent endocytosis: new insights into caveolae and non-caveolar lipid raft carriers. Biochim Biophys Acta 2005;1746:349-363.
57. Kiss AL, Botos E. Endocytosis via caveolae: alternative pathway with distinct cellular compartments to avoid lysosomal degradation? J Cell Mol Med 2009;13:1228-1237.
58. Nassoy P, Lamaze C. Stressing caveolae new role in cell mechanics. Trends Cell Biol 2012;22:381-389.
59. Luzio JP, Parkinson MD, Gray SR, Bright NA. The delivery of endocytosed cargo to lysosomes. Biochem Soc Trans 2009;37:1019-1021.
60. Xiang S, Tong H, Shi Q, Fernandes JC, Jin T, Dai K, et al. Uptake mechanisms of non-viral gene delivery. J Control Release 2012;158:371-378.
61. Lim JP, Gleeson PA. Macropinocytosis: an endocytic pathway for internalising large gulps. Immunol Cell Biol 2011;89:836-843.
62. Settembre C, Ballabio A. Lysosome: regulator of lipid degradation pathways. Trends Cell Biol 2014;24:743-750.
63. Varkouhi AK, Scholte M, Storm G, Haisma HJ. Endosomal escape pathways for delivery of biologicals. J Control Release 2011;151:220-228.
64. Herweijer H, Wolff JA. Progress and prospects: naked DNA gene transfer and therapy. Gene Ther 2003;10:453-458.
65. Yang CH, Shen SC, Lee JC, Wu PC, Hsueh SF, Lu CY, et al. Seeing the gene therapy: application of gene gun technique to transfect and decolour pigmented rat skin with human agouti signalling protein cDNA. Gene Ther 2004;11:1033-1039.
66. Wells DJ. Gene therapy progress and prospects: electroporation and other physical methods. Gene Ther 2004;11:1363-1369.
67. Chen ZY, Lin Y, Yang F, Jiang L, Ge S. Gene therapy for cardiovascular disease mediated by ultrasound and microbubbles. Cardiovasc Ultrasound 2013;11:11-7120-11-11.
68. Prosen L, Prijic S, Music B, Lavrencak J, Cemazar M, Sersa G. Magnetofection: a reproducible method for gene delivery to melanoma cells. Biomed Res Int 2013;2013:209452.
69. Ghosh PS, Kim CK, Han G, Forbes NS, Rotello VM. Efficient gene delivery vectors by tuning the surface charge density of amino acid-functionalized gold nanoparticles. ACS Nano 2008;2:2213-2218.
70. Haynes MT, Huang L. Lipid-coated calcium phosphate nanoparticles for nonviral gene therapy. Adv Genet 2014;88:205-229.
71. Choi EW, Shin IS, Lee CW, Youn HY. The effect of gene therapy using CTLA4Ig/silica-nanoparticles on canine experimental autoimmune thyroiditis. J Gene Med 2008;10:795-804.
72. Rimann M, Luhmann T, Textor M, Guerino B, Ogier J, Hall H. Characterization of PLL-g-PEG-DNA nanoparticles for the delivery of therapeutic DNA. Bioconjug Chem 2008;19:548-557.
73. Moffatt S, Wiehle S, Cristiano RJ. A multifunctional PEI-based cationic polyplex for enhanced systemic p53-mediated gene therapy. Gene Ther 2006;13:1512-1523.
74. Agirre M, Zarate J, Puras G, Ojeda E, Pedraz JL. Improving transfection efficiency of ultrapure oligochitosan/

DNA polyplexes by medium acidification. Drug Deliv 2015;22:100-110.
75. Chaplot SP, Rupenthal ID. Dendrimers for gene delivery--a potential approach for ocular therapy? J Pharm Pharmacol 2014;66:542-556.
76. Bala I, Hariharan S, Kumar MN. PLGA nanoparticles in drug delivery: the state of the art. Crit Rev Ther Drug Carrier Syst 2004;21:387-422.
77. Liang X, Shi B, Wang K, Fan M, Jiao D, Ao J, et al. Development of self-assembling peptide nanovesicle with bilayers for enhanced EGFR-targeted drug and gene delivery. Biomaterials 2016;82:194-207.
78. Balazs DA, Godbey W. Liposomes for use in gene delivery. J Drug Deliv 2011;2011:326497.
79. Ciani L, Ristori S, Salvati A, Calamai L, Martini G. DOTAP/DOPE and DC-Chol/DOPE lipoplexes for gene delivery: zeta potential measurements and electron spin resonance spectra. Biochimica et Biophysica Acta (BBA) - Biomembranes 2004;1664:70-79.

2

Objectives

2. OBJECTIVES

Gene therapy has become an area of interest due to the possibility to achieve a therapeutic effect by the delivery of normal functioning gene into the cells. Within gene delivery vectors, non-viral vectors offer a safer way to deliver genetic material compared to viral vectors. Moreover, non-viral vectors have attracted attention for their potential application in the treatment or cure of inherent disorders, such as retinal and neurological disorders, among many others. Nevertheless, non-viral vectors have shown low transfection efficiencies and the transient gene expression rises concerns about the application of these vectors in the clinics. Among non-viral carriers, lipidic systems, such as niosomes are a promising option to vectorize many kinds of drugs. Unfortunately, their use is limited since the comprehension about the mechanisms that involve their gene delivery efficacy, such as components and their effect on the targeted cells, is still in progress.

Consequently, the main objective of this thesis is to elaborate safe and efficient niosome particles for gene delivery in retina and brain.

1. To study the influence of the polar head-group of cationic lipids with a serinol backbone structure on niosomes and the study of the physicochemical and biological parameters related to transfection efficiency and viability in different cell lines.

2. To design cationic niosomes to transfect efficiently rat brain cells after cortical administration and rat retina cells after intravitreal and subretinal administration.

3. To understand the role of the helper lipids in the intracellular disposition and the transfection efficiency of niosomes designed for gene delivery in retinal pigment epithelial cells

3

Niosomes based on synthetic cationic lipids for gene delivery: The influence of polar head-groups on the transfection efficiency in HEK-293, ARPE-19 and MSC-D1 cells

Niosomes based on synthetic cationic lipids for gene delivery: The influence of polar head-groups on the transfection efficiency in HEK-293, ARPE-19 and MSC-D1 cells

Ojeda, E[1,2]; Puras, G[1,2]; Agirre, M[1,2]; Zárate, J[1,2]; Grijalvo, S[2,3]; Pons, R[2,3]; Eritja, R[2,3]; Martinez-Navarrete, G[2,4]; Soto-Sanchez, C[2,4]; Fernández, E[2,4] and Pedraz, JL[1,2]

[1] NanoBioCel Group, University of Basque Country, Vitoria, Spain.
[2] Networking Research Centre of Bioengineering, Biomaterials and Nanomedicine (CIBER-BBN)
[3] Institute of Advanced Chemistry of Catalonia, IQAC-CSIC, Barcelona, Spain.
[4] Neuroprothesis and Neuroengineering Research Group, Miguel Hernández University, Spain

Organic & Biomolecular Chemistry. 2015;13:1068-1081

ABSTRACT

We designed niosomes based on three lipids that differed only on the polar-head group to analyze the influence on the transfection efficiency. These lipids were characterized in terms of small-angle X-ray scattering before being incorporated into the niosomes, which were characterized in terms of pK_a, size, zeta potential, morphology and physical stability. Nioplexes were obtained upon the addition of plasmid. Different ratios (w/w) were selected to analyze the influence of this parameter on size, charge and on the ability to condense, release and protect the DNA. *In vitro* transfection experiments were performed in HEK-293, ARPE-19 and MSC-D1 cells. Our results show that the chemical composition of the cationic head-group clearly affects to the physicochemical parameters of the niosomes and specially, to the transfection efficiency. Only niosomes based on cationic lipids with a dimethyl amino head group (Lipid 3) showed transfection capacity when compared with their counterparts amino (Lipid 1) and tripetide head-groups (Lipid 2). Regarding cell viability, we clearly observed that nioplexes based on the cationic lipid 3 had a more deleterious effect than their counterparts, especially in ARPE-19 cells at 20/1 and 30/1 ratios. Similar studies could be extended to other series of cationic lipids in order to progress in the research of safe and efficient non-viral vectors for gene delivery purposes.

Keywords: Cationic lipids, gene therapy, niosomes, non-viral vectors, transfection.

3.1. INTRODUCTION

Gene therapy has become one of the main areas of interest for scientists, because it focuses on the possibility of delivering a normal functioning gene into the cell in order to have a therapeutic effect [1]. However, efficient delivery and expression of genes into cells is not as easy as it seems. The entry of the DNA into cells and the protection of the genetic material against enzymatic digestion before reaching the nucleus, are two important factors that may clearly hampers this process. Other factors to be considered for the development of effective gene carriers include the intracellular trafficking and the subsequent entry into the nucleus in order to express the desirable molecule [2].

Basically, there are two main gene carrier systems classified as viral and non-viral vectors. Viral vectors rely on the use of viruses as carriers due to their natural ability to insert genetic material into the cells. However, some serious concerns such as immunogenicity, oncogenicity and the high cost of production jeopardize their use in human beings [3]. On the other hand, non-viral vectors based on cationic lipids or polymers offer a safer way to deliver genetic material, as they exhibit lower risk of antigen-specific immune and inflammatory response. Moreover they are cheaper and easier to elaborate, and the size of DNA inserted is theoretically unlimited [4]. However, non-viral vectors are less effective than viral vectors as gene cariers Therefore, research on the design of safe and effective novel non-viral vectors merits special attention for the research community.

Niosomes are non-ionic surfactant vesicles with a bilayer structure that have been effectively used to vectorize many kinds of drugs [5,6]. Unfortunately, these outcomes have not been the same for gene therapy purposes where their use is still limited; however some promising results have been recently reported in the literature for retinal gene delivery purposes [7]. Therefore, research on niosomes as non-viral vectors represents a challenge topic to be further developed. Compared with liposomes, niosomes are recognized for their low cost and superior chemical and storage stabilities. The structure and physical properties of niosomes are similar to liposomes, with the only difference that niosomes are prepared using non-ionic surfactants instead of phospholipids.

Basically, there are three main components in a niosome formulation: a) Non-ionic surfactants such as polysorbate 80 and span that form stable emulsions [8], b) helper lipids such as cholesterol or squalene that enhance the physicochemical properties of the lipid emulsion [9,10] and c) cationic lipids, which structure and physical properties clearly influence on the transfection efficiency and toxicity [11].

Most of the cationic lipids employed for gene delivery purposes contain four functional domains: a hydrophilic head-group, a hydrophobic domain, a linker, and a backbone domain. The hydrophobic group is usually derived from aliphatic hydrocarbon chains.

Classically, the hydrophobic domain often contains two linear aliphatic chains, because it has been reported that cationic lipids containing one or three carbon chains tend to be more toxic and show poor transfection efficiencies [12]. The linker group influences on the flexibility, stability, and biodegradability of the cationic lipid, while its length determines the level of hydration [13]. The backbone separates the polar-head group from the hydrophobic group, being serinol and glycerol groups the more popular units [14]. Finally, the hydrophilic head-group is responsible of the interaction with DNA and its condensation to form complexes due to electrostatic interactions [15].

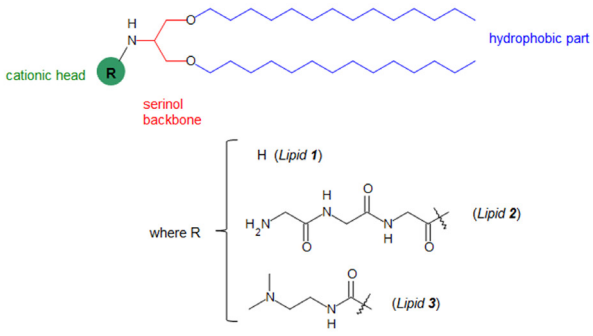

Figure 1. General structure for the novel amino lipid-based serinol derivatives (lipids 1, 2 and 3) containing the same backbone, hydrophobic part and several cationic heads.

In the present study, we designed niosome vectors based on three synthetic amino lipids containing polysorbate 80 as non-ionic surfactant and squalene as helper lipid. Our three cationic lipids were synthesized containing the same serinol backbone with two identical fully hydrocarbonated alkyl chains, varying only the cationic head structure with an amino (Lipid 1), a tripeptide (Lipid 2) and a dimethyl amino group (Lipid 3) (Fig. 1) in order to study the influence of the polar-head group on the transfection efficiency and cell viability.

The amino polar-head group (Lipid 1) was selected based on the excellent transfection results obtained when it was incorporated to a glycerol derivative cationic lipid7. The dimethyl amino group (Lipid 3) is considered as one of the most suitable pendant groups for cationic lipids to be used in transfection experiments, for this reason was selected as a polar-head group. Finally, the tripeptide group (Lipid 2) was selected as polar head group as this compound has a lower pK_a than dimethyl amino and amino groups and it may form potential intermolecular H-bonds. These novel cationic lipids were analyzed by small-angle X-ray scattering (SAXS). Niosomes prepared by oil-in-water emulsion (o/w) and film-

hydration technique were characterized in terms of pKa, size, zeta potential, morphology and physical stability. Upon the addition of the pCMS-EGFP reported plasmid, we obtained nioplexes at different cationic lipid/DNA ratios (w/w). The influence of cationic lipid/DNA ratios on particle size, zeta potential and on the ability to condense, release and protect the DNA from enzymatic digestion was analyzed. *In vitro* experiments were performed with the most promising formulations to evaluate the transfection efficiency and viability in HEK-293, ARPE-19 and MSC-D1 cells. Delivery carriers prepared by biomolecular assembly and conjugations have been extensively reported in the literature [16-18].

3.2 MATERIAL AND METHODS

3.2.1. Materials

All reagents, solvents and chemicals used in this study were of the highest purity available and were used as received. DNase I, sodium dodecyl sulphate (SDS), squalene and PBS were purchased from Sigma-Aldrich (Madrid, Spain). Polysorbate 80 (Tween 80) was provided by Vencaser (Bilbao, Spain). All reactions were carried out under inert atmosphere of argon. Flash column chromatography was carried out on silica gel SDS 0.063-0.2 mm/70-230 mesh. 1H and 13C NMR spectra were recorded at 25ºC on a Varian Mercury 400 MHz spectrometer using deuterated solvents. Tetramethylsilane (TMS) was used as an internal reference (0 ppm) for 1H spectra recorded in CDCl3 and the residual signal of the solvent (77.1 ppm) for 13C spectra. For CD3OD and d6-DMSO the residual signal of the solvent was used as a reference. Chemical shifts are reported in part per million (ppm), coupling constants (J) in Hz and multiplicity as follows: s (singlet), d (doublet), t (triplet), q (quadruplet), quint (quintuplet), m (multiplet) and br (broad signal). Electrospray ionization mass spectra (ESI-MS) were recorded on a Micromass ZQ instrument with single quadrupole detector coupled to an HPLC, and high-resolution (HR) ESI-MS on an Agilent 1100 LC/MS-TOF instrument (Servei d'Espectrometría de Masses, Universitat de Barcelona). Cell culture reagents were purchased from LGC Promochem (Barcelona, Spain). Opti-MEM® I reduced medium, antibiotic/antimicotic solution and LipofectamineTM 2000 transfection reagents were acquired from Invitrogen (San Diego, California, USA). Retinal pigmented epithelial cells (ARPE-19), human embryonic kidney cells (HEK-293) and mouse bone marrow mesenchimal stem cells (MSC-D1) were obtained from the American Type Culture Collection (ATCC).

3.2.2. Synthesis of cationic lipids

3.2.2.1.Synthesis of tert-butyl-N-[2-tetradecyloxy-1-(tetradecyloxymethyl)ethyl]carbamate (5)

Diol 4 (500 mg; 2.61 mmol) and tetradecylalkyl bromide (4.2 mL, 15.6 mmol) were dissolved in toluene (2.0 mL). Then, Bu4NHSO4 (444 mg; 1.305 mmol) was added along with a 50% solution of NaOH (3.0 mL). The mixture was heated at 60 ºC with vigorous stirring overnight. The reaction was diluted with AcOEt (15 mL) and the organic layer was washed with water (3 x 10 mL). The organic layer was dried on anhydrous MgSO4 and solvent was evaporated obtaining the corresponding crude that was purified by flash chromatography (Hex 100% to Hex/AcOEt 10%).

Yield 54%;1H -NMR (400 MHz, CDCl3) d 4.89 (broad s, NH), 3.50 (m, 1H;CH-N), 3.41 (m, 8H; 4 CH2-O), 1.54 (s, 9H; 3 CH3-C), 1.44(s, 9H; 3 CH3-C), 1.28 (m, 48H; alkyl chain), 0.88 (t, J = 6.7 Hz, 6H; 2 CH3); The spectra shows rotamers; 13C-NMR (125 MHz, CDCl3) d 146.7 (CO), 85.1 (C-O), 71.3 (CH2-O), 69.1 (CH2-O), 31.8 (CH-N), 29.7, 29.6, 29.6, 29.4, 29.3, 28.3, 27.3, 26.1, 22.6 (alkyl chain), 14.0 (CH3); ESI-MS for C36H74NO4 m/z 584.5612 (calculated) 584.5608 (M+H)+(found); C72H146N2NaO8 m/z 1190.0971 (calculated) 1190.0974 (2M+Na)+ (found).

3.2.2.2. Synthesis of 1,3-di(tetradecyloxy)propan-2-amine (Lipid 1)

N-protected alkyl diol 5 (300 mg; 0.514 mmol) was dissolved in a mixture of dichloromethane: trifluoroacetic acid (4:0.5; v/v). The reaction was stirred at room temperature for 30 minutes. The solvent was evaporated obtaining the corresponding amine derivative in its trifluoroacetate form. The crude was re-dissolved in AcOEt (5 mL) and carbonate on polymer support (20 eq) was added. Mixture was stirred for 1 hour at room temperature. The resin was filtered off and the solvent was evaporated, obtaining the expected Lipid 1, which was used without further purification.

Yield 100%; 1H -NMR (400 MHz, CDCl3) d 3.43 (m, 6H; 3 CH2-O); 3.30 (m, 2H; CH2-O); 3.15 (m, 1H; CH-N); 1.26 (m, 48H; alkyl chain); 0.88 (t, J = 6.7 Hz; 6H; 2 CH3); 13C-NMR (125 MHz, CDCl3) d 71.9 (CH2-O), 66.7 (CH2-O), 51.8 (CH2-O), 31.8 (CH-N), 29.7, 29.6, 29.6, 29.5, 29.3, 29.3, 29.1, 25.8, 22.6 (alkyl chain), 14.0 (CH3); ESI-MS for C31H65NO2 m/z 484.5135 (calculated) 484.5136 (M+H)+ (found).

3.2.2.3. Synthesis of tert-butyl-N-[2-oxo-2-[[2-oxo-2-[[2-oxo-2-[[2-tetradecyloxy-1-(tetradecyloxymethyl)-ethyl]amino]ethyl]amino]ethyl]amino]ethyl]carbamate (6)

Previously, Boc-triglycine (2.0 eq) and N-hydroxysuccinimide (2.2 eq) were dissolved in dichloromethane (3 mL). Reaction was stirred for 5 minutes and EDC (2.4 eq) was added. The reaction was stirred overnight at room temperature. The organic layer was washed with water (3 x 5 mL) and dried over anhydrous MgSO4. The solvent was evaporated and crude was used in the next step without further purification. Amine alkyl diol 3 (100

mg; 0.206 mmol) was added over the activated tripeptide. Reaction was heated at 60 ºC and stirred overnight. The solvent was evaporated and the resultant crude was purified by flash chromatography (DCM/MeOH 5%).

Yield 86 %, 1H-NMR (400 MHz, CDCl3) ḍ 7.04 (broad m, NH), 6.04 (broad d, NH), 5.54 (broad s, NH), 4.18 (broad s, NH), 3.99 (d, J = 5.7 Hz, 2H; CH2), 3.90 (d, J = 5.7 Hz, 2H; CH2), 3.83 (d, J = 5.7 Hz, 2H; CH2), 3.51 (m, 4H; 2 CH2-O), 3.42 (m, 5H; CH-N and 2 CH2-O), 2.39 (t, J = 5.9 Hz, 2H), 1.54 (m, 4H; 2 CH2), 1.44 (s, 9H; 3 CH3-C); 1.26 (m, 44H; alkyl chain), 0.88 (t, J = 7.0 Hz, 6H; 2 CH3); 13C-NMR (125 MHz, CDCl3) ḍ 168.5 (CO), 166.8 (CO), 165.7 (CO), 164.7 (CO), 76.2 (C-O), 67.4 (CH2-O), 64.7 (CH2-O), 49.7 (CH2-N), 44.9 (CH2-N), 39.0 (CH2-N), 38.9 (CH-N), 27.9 (CH3-C), 25.8, 25.7, 25.6, 25.5, 25.3, 24.3, 22.0, 21.4, 18.7, 14.5, 13.4, 10.1, 7.8 (alkyl chain); ESI-MS for C42H82N4O7 m/z 755.6256 (calculated) 755.6260 (M+H)+, C42H82N4NaO7 777.6072 (calculated) 777.6076 (M+Na)+ C84H164N8NaO14 1532.2251 (calculated) 1532.2251 (2M+Na)+ (found)

3.2.2.4. Synthesis of [[2-[(2-aminoacetyl)amino]acetyl]amino]-N-[2-tetradecyloxy-1(tetradecoxymethyl)-ethyl]-acetamide (Lipid 2)

Boc-protected alkyl tripeptide 6 (70 mg; 0.093 mmol) was dissolved in a mixture of dichloromethane:trifluoroacetic 10%. The reaction was stirred at room temperature for one hour. Solvent was removed until dryness. The corresponding trifluoroacetate salt was dissolved in a mixture of AcOEt:MeOH (3:2) and carbonate on polymer support (20 eq) was added. The reaction was stirred for one hour at room temperature. The resin was filtered off and solvent was evaporated obtaining the corresponding Lipid 2, which was used without further purification.

Yield 100%, 1H-NMR (400 MHz, CDCl3) ḍ 7.97 (broad s, NH), 7.14 (broad s, NH), 6.27 (broad d, NH), 4.09 (broad s, NH2), 3.92 (m, 2H; CH2-N), 3.84 (m, 2H; CH2-N), 3.44 (m, 2H; CH2-N), 3.34 (m, 8H; 4 CH2-O), 1.46 (m, 2H; CH2-C), 1.18 (m, 44H; alkyl chain), 0.80 (t, J = 6.8 Hz, 6H; 2 CH3); 13C-NMR (125 MHz, CDCl3) ḍ 173.7 (CO), 169.3 (CO), 168.2 (CO), 71.5 (CH2-O), 68.8 (CH2-O), 48.9 (CH2-NH2), 42.8 (CH2-N), 31.9 (CH2-N), 29.7 (CH-N), 29.6, 29.5, 29.5, 29.4, 29.3, 26.0, 22.6 (alkyl chain), 14.0 (CH3-C); ESI-MS for C37H74N4O5 m/z 655.5732 (calculated) 655.5731 (M+H)+ (found).

3.2.2.5 Synthesis of 1-(2-dimethylaminoethyl)-3-[2-tetradecyloxy-1-(tetradecoxymethyl)-ethyl]urea (Lipid 3)

Previously, p-nitrophenyl-chloroformate (2.5 eq) and the di-alkylated amine 1 (50 mg; 0.103 mmol) were dissolved in a mixture of tetrahydrofurane and dichloromethane (1:1) (3 mL). The reaction was cooled at 0 ºC and DIEA (2.5 eq) was carefully added dropwise. The

solution was heated at room temperature and stirred for 4 hours. The solvent was removed and the resultant crude was used in the next step without further purification. Crude was dissolved in DMF (3 mL) and the corresponding amine derivative (1.1 eq) was added dropwise. The reaction was stirred overnight at room temperature. Finally, solvent was removed and the resultant crude was purified by flash chromatography (DCM:MeOH 5% to 10%) obtaining the expected Lipid 3.

Yield 88%, 1H-NMR (400 MHz, CDCl3) d 5.03 (broad s, NH), 4.98 (broad s, NH), 3.52 (d, J = 4.4 Hz, 1H; CH-NH), 3.50 (d, J = 4.4 Hz, 1H; CH-NH), 3.42 (m, 8H; 4 CH2-O), 3.25 (m, 2H; CH2-N), 2.44 (t, J = 5.9Hz, 2H; CH2-N), 2.26 (s, 6H; 2 CH3-N), 1.54 (m, 4H; 2 CH2), 1.27 (m, 44H; alkyl chain); 0.88 (t, J = 6.7 Hz, 6H; 2 CH3); 13C-NMR (125 MHz, CDCl3) d 158.1 (CO), 71.3 (CH-N), 69.8 (CH2-O), 58.8 (CH2-O), 49.6 (CH2-N), 45.0 (CH2-N), 37.8 (CH3-N), 31.9, 29.7, 29.6, 29.5, 29.3, 26.1, 22.6, 14.0 (CH3). The spectra shows rotamers; ESI-MS for C36H75N3O3 m/z 598.5881 (calculated) 598.5888 (M+H)+ (found).

3.2.3. Small Angle X-ray Scattering (SAXS) analysis of cationic lipids

SAXS patterns were recorded simultaneously using a S3-MICRO (Hecus X-ray systems GMBH Graz. Austria) coupled to a GENIX-Fox 3D X-ray source (Xenox. Grenoble) which produces a detector-focused X-ray beam with λ=0.1542 nm Cu Kα-line at greater than 97% purity and less than 0.3% Kα. The transmitted scattering was detected using a PSD 50 Hecus at small-angle regime (0.09 nm-1 < q < 6 nm-1). Temperature was controlled through a Peltier TCCS-3 Hecus. The dry lipid samples (5–10 mg) were inserted in a glass capillary with 1mm diameter and 10 μm wall thickness (Hilgenberg, Germany) and HEPES buffer was added and mixed with the lípid derivatives. The capillaries were incubated at 25 ºC and 37 ºC for 24 h at least. The SAXS scattering curves were plotted as a function of the scattering vector modulus, $q = 4\pi/\lambda \sin(\theta/2)$, where θ is the scattering angle and λ the wavelength of the incident radiation. The system scattering vector was calibrated by measuring a standard silver behenate sample. Scattering curves were mainly smeared by the detector width because we used a detector-focused small beam (300 x 400 μm full width at half maximum), which widens the peaks without a noticeable effect on peak position. The instrumentally smeared experimental SAXS curves were fitted to numerically smeared models for beam size and detector width effects. Least squares routine based on the Levenberg-Marquardt scheme was used. The bilayer was fitted using a three-Gaussian profile based on the MCG model [19,20].

Specifically, the bilayer is calculated as a sumation of the head-groups contribution (in the form of a Gaussian centred at ±Zh, amplitude σh and maximum contrast electron density $\tilde{p}_H = (p_H - p_{H_2O})$), the methyl groups contribution (in the form of a Gaussian centred at 0 with amplitude σc and maximum electron density $\tilde{p}_C = (p_C - p_{H_2O})$). In addition to these two

contributions and, as a difference with the original model reported by Pabst et al. [20] a third contribution corresponding to an error function centred at the bilayer centre and negative contrast electron density contribution $\tilde{p}_{CH_2} = (p_{CH_2} - p_{H_2O})$ corresponding to the difference in electron density between the bilayer methylene and the outer water [21].

$$p(Z) = \tilde{p}_H \exp\left[(-Z - Z_H)^2 / 2\sigma^2{}_H\right] + \tilde{p}_C \exp\left[(-Z)^2 / 2\sigma^2{}_C\right] + p_{CH_2}(Z)$$

eq. 1 where the methylene contributions is a mirrowed error function centred at the polar/ non polar interface,

$$p_{CH_2}(Z > 0) = \tilde{p}_{CH_2} \frac{1}{\sqrt{\pi}} \int_Z^\infty e^{-(t - Z_{CH_2})^2} dt$$

eq. 2

The unidimensional Fourier transform of the corresponding electronic profile has been numerically evaluated. The structure is modelled according to the modified Caillé model as in Pabst et al. [20] (equation 3) and the global intensity is calculated according to equation 4, where Ndiff corresponds to a fraction of uncorrelated bilayers.

$$S(q) = N + 2\sum_{k=1}^{N-1} (N - k) \cos(kdq)\, e^{-(d/2\pi)^2 q^2 n_1 \gamma} (\pi k)^{-(d/2\pi)^2 q^2 n_1}$$

eq. 3

$$I(q) = |F(q)^2 S(q)| / q^2 \quad \text{eq. 4}$$

The parameters in equation 3 correspond to N, total number of correlated bilayers, d repetition distance, η1 the Caillé parameter and γ to the Euler constant.

3.2.4. Preparation of niosomes

Niosomes based on three different synthetic cationic lipids were prepared using both the o/w emulsification and the film-hydration techniques. In the o/w emulsification technique, 5 mg of the cationic lipid were gently grinded with 20 µl of squalene to obtain a fine powder. Then, 1 ml of dichloromethane was quickly added and emulsified with 5 ml aqueous phase containing non-ionic surfactant polysorbate 80 (0.5%, w/w). The emulsion was obtained by sonication (Branson Sonifier 250, Danbury) during 60 s at 50 W in ice bath. The organic solvent was removed from the emulsion by evaporation under magnetic agitation for 4 h. Upon dichloromethane evaporation, a dispersion containing the nanoparticles was formed by precipitation of the cationic nanoparticles in the aqueous medium. In the Film-Hydration technique, 5 mg of the cationic lipid were gently grinded with 20 µl of squalene to obtain a fine powder. Then, 1 ml of dichloromethane was added and thoroughly mixed to obtain the organic phase. Then, the solvent was evaporated under magnetic agitation for 4 h. Under DCM evaporation, the lipid film obtained was hydrated with 5 ml aqueous phase containing non-ionic surfactant polysorbate 80 (0.5%, w/w). The emulsion was obtained by

sonication (Branson Sonifier 250, Danbury) during 60 s at 50 W in ice bath. We obtained the same niosome concentration using both techniques (1mg cationic lipid/ml).

3.2.5. Plasmid propagation and preparation of nioplexes

pCMS-EGFP plasmid was propagated in Escherichia coli DH5-α and purified using the Qiagen endotoxin-free plasmid purification Maxi-prep kit (Qiagen, Santa Clarita, CA, USA) according to the manufacturer's instructions. Concentration of pDNA was quantified by measuring absorbance at 260 nm using a NanoDrop® (ND-1000 Spectrophotometer, Thermo Fisher Scientific Inc. Denver, USA). The purity of the plasmid was verified by agarose gel electrophoresis in Tris Borate-EDTA buffer, pH 8.0 (TBE buffer). DNA bands were detected using GelRed™ (Biotium, Hayward, California, USA) to stain DNA and images were observed with a ChemiDoc™ MP Imaging System (Bio-Rad, USA).

The nioplexes (Niosome/DNA vectors) were elaborated by mixing an appropriate volume of a stock solution of pCMS-EGFP plasmid (0.5 mg/ml) with different volumes of the niosome suspensions (1mg cationic lipid/ml). The mixture was left for 30 min at room temperature to enhance electrostatic interaction between the cationic lipids of the niosomes and the negatively charged plasmid. The Niosome/DNA ratio was referred as the ratio of cationic lipid to DNA (w/w). The stock solutions of cationic lipid (1 mg/ml) correspond to the following molar concentrations: 2.07 mM (Lipid 1, MW 484), 1.53 mM (Lipid 2, MW 655), and 1.67 mM (Lipid 3, MW 598). The stock solution of plasmid pCMS-EGFP of 0.5 mg/ml was estimated to be around 0.137 micromolar (pCMS-EGFP, 5541 bp, average MW 3657060).

3.2.6. TNS fluorescence titration assay for the determination of the pKa value of the niosomes

Fluorescent measures were recorded on a SpectraMax M5 spectrophotometer (Molecular Devices) with the excitation wavelength (λex) set at 321 nm and the emission wavelength (λem) set at 445 nm. Niosomes were diluted to 75 μM cationic lipids (1, 2 and 3) in 100 μL of buffer solutions containing 10 mM HEPES, 10 mM MES, 10 mM ammonium acetate and 150 mM NaCl with pH ranging between 2.5 and 11.1. A stock solution of TNS dissolved in DMSO was added to the above buffer solution to obtain a 1 μM TNS solution. Solutions were mixed thoroughly and the resultant fluorescence was measured at room temperature. Fluorescence values are results from triplicate measurements. The fluorescence of TNS (normalized) was plotted against pH. Curves were fitted using a sigmoid function. The pKa values of the cationic lipids were calculated as the pH values at which TNS fluorescence is half-maximal fluorescence intensity.

3.2.7. Size and zeta potential measurements

The hydrodynamic diameter of the niosomes and nioplexes were determined by Dynamic Light Scattering (DLS) using a Zetasizer Nano ZS (Malvern Instrument, UK). Briefly, 50 µl of the niosomes or nioplexes were resuspended into 950 µl of 0.1 mM NaCl solution to determined size and PDI. All measurements were carried out in triplicate. The particle size reported as hydrodynamic diameter was obtained by cumulative analysis.

The zeta potential was obtained by Lasser Doppler Velocimetry (LDV) using a Zetasizer Nano ZS (Malvern Instrument, UK). Samples were resuspended (50 µl) into 0.1 mM NaCl (950 µl) using folded capillary cells for zeta analysis. The Smoluchowski approximation was used to support the calculation of the zeta potential from the electrophoretic mobility. Zeta potential measurements were run in triplicate. Only data that met the quality criteria according with the software program (DTS 5.0) were included in the study.

3.2.8. Cryo-TEM microscopy of niosomes

The morphology of niosomes was observed by Cryo-TEM microscopy. Briefly, one drop of the sample solution was vitrified by rapid freezing in liquid ethane using a Vitrobot Markt IV (FEI). This vitrified sample grid was transferred through 655 Turbo Pumping Station (Gatan) to a 626 DH Single Tilt Liquid Nitrogen Cryo-holder (Gatan), where was maintained about -180ºC. Copper grid (300 mesh Quantifoils) was hydrophilized by glow-discharge treatment. The sample was examined in a TEM, TECNAI G2 20 TWIN (FEI), operating at an accelerating voltage of 200 KeV in a bright-field and low-dose image mode.

3.2.9. Physical stability study of niosomes

The physical stability of niosomes based on three different synthetic cationic lipids was determined by monitoring the particle size and zeta potential after storage for 100 days at 4°C and 25°C. All samples were measure in triplicate.

3.2.10. Agarose gel electrophoresis studies of nioplexes

Naked DNA or nioplexes at different ratios (20 µl, containing 200 ng of the plasmid) were subjected to electrophoresis on an agarose gel (0.8%). The gel was immersed in a tris-acetate-EDTA buffer and exposed for 30 min to 120 V. DNA bands were stained with GelRed™ (Biotium, Hayward, California, USA) and images were observed with a TFX-20M transilluminator (Vilber-Lourmat, Germany). To analyze the release of DNA from the formulation, 12 µl of a 7% SDS solution was added to the samples to get a final SDS concentration of 3.5% in each well. The pDNA protection capacity of the vectors against enzymatic digestion was analyzed by adding the DNase I enzyme to the vector formulations

(final concentration of 1 U DNase I/2.5 µg DNA). Afterwards, the mixtures were incubated at 37° C for 30 min and finally, 12 µl of a 7% SDS solution was added to analyze the released DNA. The integrity of the DNA in each sample was compared to a control of untreated DNA.

3.2.11. Cell culture and *in vitro* transfection protocols

HEK-293, ARPE-19 and MSC-D1 cells were seeded in 24 well plates at an initial density of 15 x 104, 10 x 104, and 8 x 104 cells/well, with 300 µl of EMEM containing 10% horse serum, 300 µl of D-MEM/F-12 containing 10% bovine serum, and 300 µl of DEMEM containing 10% horse serum, respectively. Cells were adhered overnight to reach 70-90% of confluence at the time of transfection. Then, the regular growth medium was removed and the cells were exposed to nioplexes resuspended in Opti-MEM® transfection medium at different cationic lipid/DNA ratios, containing all of them 1.25 µg of the plasmid. Each formulation was used in triplicate. After 4 h of incubation at 37ºC, the nioplexes were replaced by 500 µl of regular growth medium. Cells were allowed to grow for 72 h until flow cytometry analysis. Following the manufacturer's protocol, lipofectamineTM 2000 was used in combination with pDNA, as transfection positive control.

3.2.12. Transfection efficiency and cell viability measurement

Flow cytometry analysis was conducted using a FACSCalibur system flow cytometer (Becton Dickinson Bioscience, San Jose, USA) in order to quantify the % of EGFP positive cells. Cells were washed twice in PBS and detached from the microplate with 200 µl of trypsin/EDTA and 400 µl of normal growth medium were added. The pellets were resuspended in growth medium, diluted in FACSFlow liquid and directly introduce to the flow cytometer. Transfection efficiency was expressed as the percentage of EGFP positive cells at 525 nm (FL1). Control samples (non-transfected cells) were displayed on a forward scatter (FCS) versus side scatter (SSC), dot plot to establish a collection gate and exclude cell debris. Other examples containing Lipofectamine transfected cells, and non-transfected cells were used as controls to compensate FL2 signal in FL1 channels. For each sample 10,000 events were collected.

Cell viability of the three cell lines was evaluated using the Cell Counting Kit-8 (CCK-8; Dojingo Molecular Technologies, Inc, Gaithersburg, MD) according with the manufacturer´s protocol. Briefly, cells were exposed to nioplexes under the same conditions as described before. 72 h later, 10 µl of CCK-8 solution was added to 200 µl of medium in each well, and the plate was incubated 4 h at 37°C and 5% CO2. Relative cell viability percentage (%) was calculated based on the absorbance (Infinite M200 microplate reader, Tecan GENios, Switzerland) observed at 450 nm. Each formulation was used in triplicate.

3.3. RESULTS AND DISCUSSION

3.3.1. Synthesis of ionizable amino lipids

The synthesis of the three proposed ionizable amino lipids (1, 2 and 3) is displayed in Fig. 2. The synthesis started with the double alkylation of the N-protected diol 4 in the presence of tetradecyl bromide and sodium hydroxide (50%) by using the transfer-phase catalyst reaction. This reaction afforded the alkylated compound 5 with moderate yields (54%). Then, N-Boc deprotection in acid conditions (CH2Cl2 / TFA 10%) and subsequent treatment with Amberlyte IRA-900 yielded in quantitative form the expected di-alkylated amine 1 (Lipid 1) in its free form.

Further amine functionalization with an activated Boc-Gly-Gly-Gly-OH afforded the protected N-Boc-dialkylated tripeptide 6 with good yields. Boc-deprotection using the same acid conditions described before achieved the expected Lipid 2 in quantitive yield. Finally, a N,N-dimethylethylenediamine residue was successfully introduced into the Lipid 1 by activating 1 with p-nitrophenyl chloroformate. This reaction generated the expected Lipid 3 with good yields (For more details see the supporting information section 1).

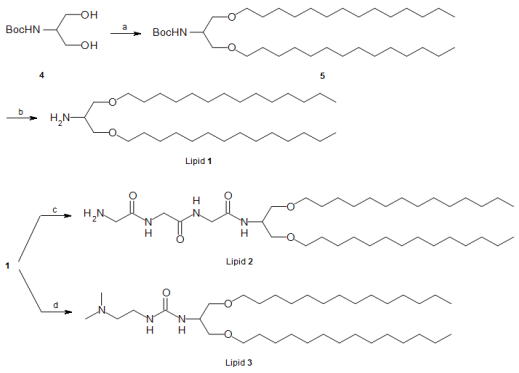

Figure 2. Synthetic strategy for the synthesis of the ionizable lipids 1, 2 and 3.

3.3.2. Small Angle X-ray Scattering (SAXS) analysis of cationic lipids

In Fig. 3-A, we show the SAXS curves at 25 ºC corresponding to the three amino lipids. No significant differences were observed at 37 ºC (data not shown). For the lipid 1 three equidistant peaks can be clearly observed while for lipid 2 up to 4 equidistant peaks are apparent. In contrast, for lipid 3 the three observed peaks are not equidistant and the peaks appear at positions q1: 2 q1: 4 q1. In this case the peak that should appear at 3 q1 is absent due to the bilayer form factor. The presence of equidistant peaks is the sign of a lamellar structuring of the system; therefore, we have fitted a modified Caillé Gausian model to the SAXS curves. In this model, the bilayer structure is calculated with two Gausian corresponding to the polar heads at both sides of the bilayer and one Gausian at the center of the bilayer corresponding to the low density methyl terminal groups of the hydrophobic

chains. In addition, the contribution of the methylene groups of the hydrocarbon chains is provided by a symmetric error function [21]. The layered structure is calculated using the modified Caillé structure factor as found in the literature [19,20]. The electronic profiles are shown in Fig. 3-B, and the main parameters of the fit in Table 1 (this material is available in the supporting Information section 2). Lipid 1 is the one that shows a most clear methylene dip at the center of the bilayer, this is usually associated to strong order in the hydrophobic domain (the so-called gel phase found for phospholipids). The lipid 3 also shows a distinct low electronic density region at the center of the bilayer, albeit less defined than lipid 1, while the dip has completely disappeared for lipid 2. This corresponds to a more fluid hydrophobic domain for lipid 2. The other remarkable difference between the lipids is the amount of water hydrating the polar heads. While lipid 1 is hydrated by at most 1 water molecule and there is virtually no water in the liquid crystal, the liquid crystals formed by lipid 2 and lipid 3 contain similar amount of water, around 11 water molecules per lipid. There is, however, a striking difference between water location in the liquid crystal formed by lipid 2 and lipid 3. As it can be observed in Fig. 3-B, the high electronic density of lipid 2 is distributed, reaching the limit of the bilayer while that of lipid 3 remains quite tightly bound to the hydrophobic domain of the bilayer. The meaning of this is that the polar region of lipid 3 contains almost no water and most of the water between the bilayers is free.

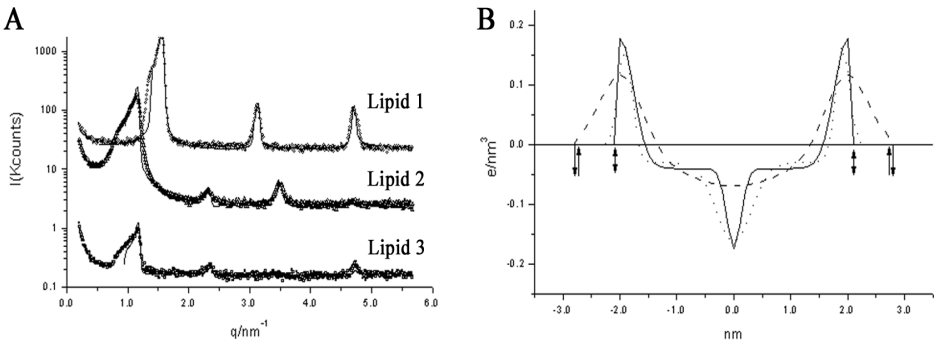

Figure 3. A) Scattered intensity at 25 ºC of the lipids after incubation with HEPES buffer. The lines correspond to the best fit of correlated lamellae, see text for the details. The curves have been scaled by factors of 10, the original scale corresponds to lipid 3. B). Electron density contrast relative to water perpendicular to the bilayer for lipid 1 (full line, upper-down arrow), Lipid 2 (dashed line, down arrow) and lipid 3 (dotted line, up arrow) as obtained from the fits of the scattering curves of figure A. The arrows mark the limit of the corresponding layer.

3.3.3. Determination of niosomal pKa by fluorescence

Liposomal pKa have been used to predict the efficacy of formulations containing ionizable amino lipids to encapsulate and mediate delivery of different cargoes into cells [22]. This parameter, in particular, has been used both in rational design of lipids [23] and

structure-activity relationship (SAR) studies in order to analyze combinatorial libraries of lipids by varying the amino cationic head group, linker or hydrophobic chains and thereby designing more efficient vehicles for *in vivo* applications.

There are two different approaches that have been reported in order to measure amino lipid pKa values: 1) potentiometric titration of amino lipids prepared in niosomes and 2) the effect of 2-(p-toluidino)-6-naphtalene sulfonic acid (TNS) fluorescence at different pH [24].

In our case, the use of the second approach allowed us to determine the acid dissociation constant of our niosome formulations containing the ionizable amino lipids 1, 2 and 3, respectively by in situ TNS fluorescence titration from pH 2.5 to 11.0 (Fig. 4-A, 4-B and 4-C). As displayed in Fig. 4, the amino lipids (1–3) containing the same hydrophobic alkyl region and serinol backbone but modifying only the cationic head group was sufficient to affect the pKa value for the corresponding niosomes. Therefore, the half-maximal fluorescence intensity afforded niosomal pKa values that ranged from 6.63 to 7.00 (lipid 1, pKa=7.00; lipid 2, pKa=6.63 and lipid 3, pKa=6.72, respectively). As displayed in Fig. 1, lipids 1 and 2 have a primary amino group. Lipid 1 has a higher pKa than lipid 2. This is consistent with the presence of the electron-withdrawing amide groups in lipid 2 that lower the pKa. Moreover, lipid 3 is a tertiary amine with electron-withdrawing groups and for this reason the pKa is higher than the lipid 2. It has been suggested that the optimal pKa of cationic lipid for transfection should be < 7.0 as in this way a large number of amino groups would be neutral at physiological pH 7.4 [23]. If this suggestion is correct, then the pKa of the amino lipids described in this work could fall the optimal range for transfection.

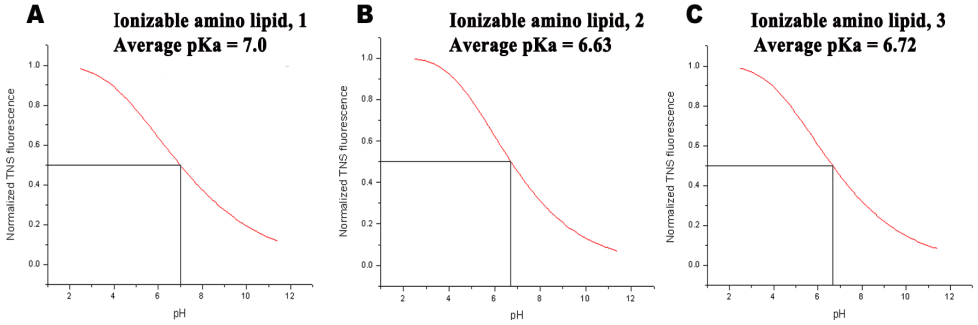

Figure 4. In situ TNS fluorescence titration to determining the pka of niosomes bases on three cationic lipids. A) Sigmoidal curve showing TNS fluorescence as a function of pH in the presence of lipid 1 (75 μM), TNS (1 μM) and buffer solution (total volume 100 μL), B) Sigmoidal curve showing TNS fluorescence as a function of pH in the presence of lipid 2 (75 μM), TNS (1 μM) and buffer solution (total volume 100 μL), C) Sigmoidal curve showing TNS fluorescence as a function of pH in the presence of lipid 3 (75 μM), TNS (1 μM) and buffer solution (total volume 100 μL).

3.3.4. Particle size, zeta potential and morphology evaluation of niosomes

It has been widely reported that the uptake and transfection efficiency of non-viral vectors strongly depends on the method of elaboration, which clearly impact on some physicochemical parameters including size, zeta potential and morphology [25]. Therefore, we prepared niosomes based on the three synthesized amino lipids by o/w emulsion and film-hydration techniques. Resulted niosomes were characterized in terms of size, zeta potential and morphology (Fig. 5). We observed that zeta potential values were similar between both techniques for the three niosome formulations (Fig. 5-A, lines). Interestingly, the highest zeta potential values were obtained when niosomes were based on lipid 3 (≈ +30mV), independently of the elaboration technique. Regarding particle size values (Fig. 5-A, bars), we did not find differences between the niosomes when these were elaborated by the film hydration technique (values around 200 nm). However, smaller particle sizes were obtained when niosomes based on the lipid 2 were formulated by the film-hydration technique (≈ 150 nm).

In addition to the size and charge, the homogeneity of the suspension containing nanoparticles should be also considerate since this parameter affects to the formation of the

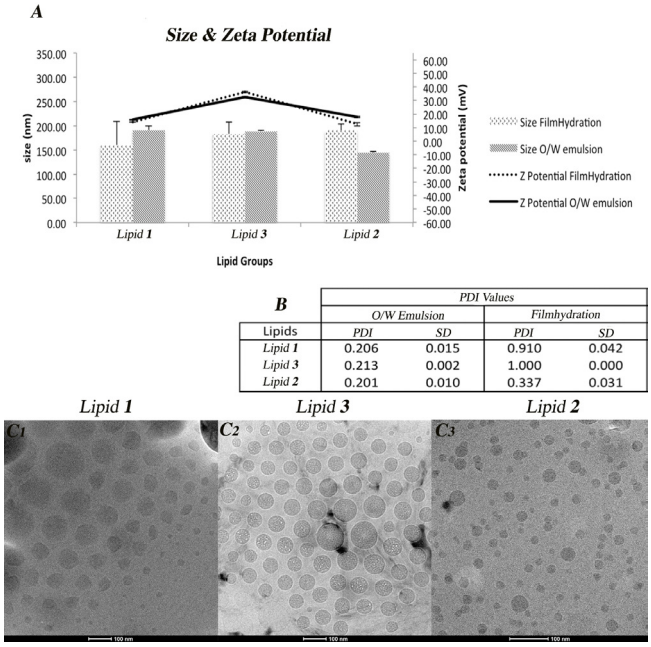

Figure 5. Physicochemical characterization of niosomes based on lipids 1, 3 and 2. A) Size and Zeta potential values. B) PDI values. Each value represents the mean ± standard deviation of three measurements. C) Cryo-TEM images of niosomes prepared by the o/w emulsion technique. Niosomes were based on lipid 1 (C1), lipid 3 (C2) and lipid 2 (C3). Scale bar = 100 nm.

nioplexes (after the addition of plasmid) and the subsequent cell internalization processes [26]. We determined the polydispersity index (PDI) as a measure of homogeneity (Fig. 5-B). Our data clearly revealed that the lowest PDI values were obtained when niosomes were prepared by the O/W emulsion technique, and these values were similar, independently of the lipid employed to formulate the niosomes. However, when niosomes were elaborated by the film-hydration technique, PDI values were extremely high, especially for niosomes elaborated with the lipids 1 and 3 (0.9 and 1.0 values respectively), which indicates that these suspensions had a very broad size distribution. Therefore, the cumulative analysis to determine particle size does not apply to scenario. Consequently, we discarded for the following experiments the niosomes that were prepared using film-hydration technique.

To get a direct evidence of the niosomes formation, we examined niosomes elaborated by the O/W emulsion technique with the three cationic lipids under a Cryo-TEM microscope (Fig. 5-C). In our experimental conditions, all niosomes, especially those elaborated with the lipid 3 (Fig. 5-C2) adopted a spherical and homogeneous morphology, which is the most favorable structure from an energetic point of view. In all niosome formulations, sizes reported by Cryo-TEM (around 100 nm or less) were slightly smaller than the sizes reported by dynamic light scattering (around 200 nm, Fig. 5-A, bars). Such differences in the sizes of the niosomes could be explained by the sample manipulation required to perform Cryo-TEM analysis.

3.3.5. Physical stability of niosomes

Instability of niosomes can be seen as a merging of one or more particles and thus formation of aggregates that result in an increase on the particle size throughout the testing period. Therefore, the bigger is the size, the more unstable the niosomal system is. Normally, the electrostatic repulsions among the vesicles are due to the surface charge. As a rule of thumb, high surface charges of the vesicles (above 20 mV, absolute value) should provide enough electrostatic repulsion to prevent the formation of aggregates [10].

We measured the physical stability of niosomes based on the three cationic lipids by monitoring the particle size and the zeta potential after storage for 100 days at 4°C and 25°C (Fig. 6). Our data shows that stability of niosomes strongly depended on the storage temperature and on the cationic lipid used to elaborate the niosomes. Clear decreases on the zeta potential value along the time was observed when niosomes based on lipid 1 and especially on lipid 2, was stored at 25°C. In the case of niosomes based on the lipid 2, the decrease on zeta potential led to a clear increase in the particle size, resulting in unstable niosomes due to the reduction of the electrostatic repulsions [27]. However, zeta potential and size of niosomes based on the lipid 3 did no vary too much along the time when stored at 25°C, which clearly

indicates that the polar head-group of the cationic lipid strongly affects to the niosome stabilities. When samples were stored in the refrigerator at 4°C, we did not observe a clear decrease on the zeta potential value along the time, with the exception of niosomes based on the lipid 2 which clearly was unstable after 100 days of storage at 4°C. Again, a decrease in the zeta potential value led to a clear increase in the particle size. Temperature can lead to changes in the crystalline structure of lipids due to changes in zeta potential, as previously reported [28]. In conclusion, niosomes based on lipids 1, 2 and 3 were more stable when were stored at 4°C, specially, niosomes based on the lipid 3, which size and zeta potential values did not strongly vary along the 100 days duration of the study.

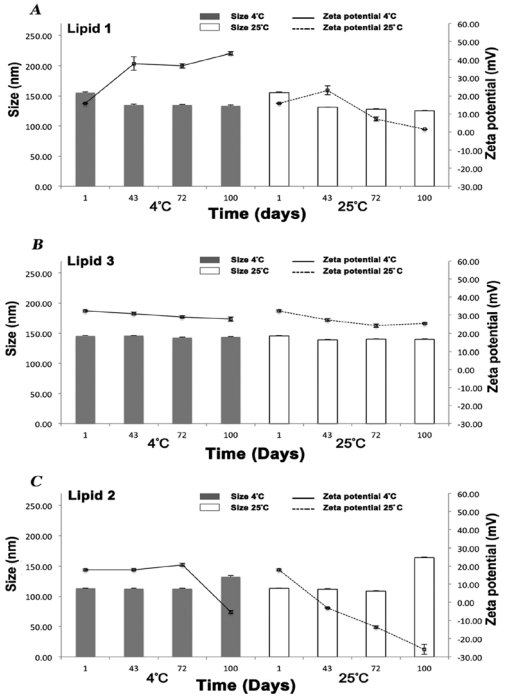

Figure 6. Physical stability of niosomes based on lipid 1 (A), lipid 3 (B) and lipid 2 (C), following storage at 4°C and 25°C for 100 days. Particle size (bars) and zeta potential (lines) of niosomes based on cationic lipids; A) lipid 1, B) lipid 3 and C) lipid 2. Each value represents the mean ± standard deviation (SD) from three independent experiments.

3.3.6. Characterization of nioplexes in terms of size and zeta potential

Adding DNA to the niosomes at different cationic lipid/DNA ratios (w/w) formed nioplexes that were characterized by charge and size parameters (Fig. 7). A clearer decrease in zeta potential value (Fig. 7, lines) was observed in the three niosome formulations when DNA was added at a cationic lipid/DNA mass ratio of 1/1. For niosomes based on the lipid 1, the charges oscillated from 18 to -35 mV, for niosomes based on the lipid 2, these charges oscillated from 19 to -48 mV and for niosomes based on the lipid 3, charges oscillated from 31 to -41 mV. Interestingly, in all nioplexes formulations, zeta potential values increased proportionally to the cationic lipid/DNA mass ratio, reaching the maximum values at the highest cationic lipid /DNA ratio 30/1 (+8 mV, + 10mV and +22mV for nioplexes based on lipid 1, 2 and 3 respectively). This increase in the charge was more evident for the nioplexes prepared with the lipid 3. The clear relationship between the cationic lipid/DNA mass ratio and the superficial charge demonstrates that at an appropriate mass ratio, cationic niosomes were able to bind and neutralize the negative charges of the DNA [29], resulting in positively

charged nioplexes that can easily interact with the negatively charged cell surfaces, inducing early steps of the endocytosis process, which finally increases transfection efficiency [30].

Regarding the size of nioplexes (Fig. 7, bars), results in general showed that the increase of the cationic lipid /DNA ratios from 1:1 to 30:1 did not significantly affect to the final size, with some exceptions such as niosomes based on cationic lipid 1 at 25:1 and 30:1 ratios (Fig 7-A). These slight increases in the final size could be due to the achievement of a final zeta potential value near to 0, which results in less compacted and bigger nioplexes. In general, most of the nioplexes showed a final size value under 200 nm, which has been report to be adequate for intracellular uptake and therefore transfection [31]. It is generally accepted that the mass ratio influences on the particle size of nioplexes [29]. However in our experimental conditions, we did not find relevant differences, probably because the final particle size of the resulted nioplexes may depend on a delicate balance between the ability of the cationic niosome to precondense with the DNA which reduces the particle size, and the greater space demanded by the niosome itself, which increases the particle size [7].

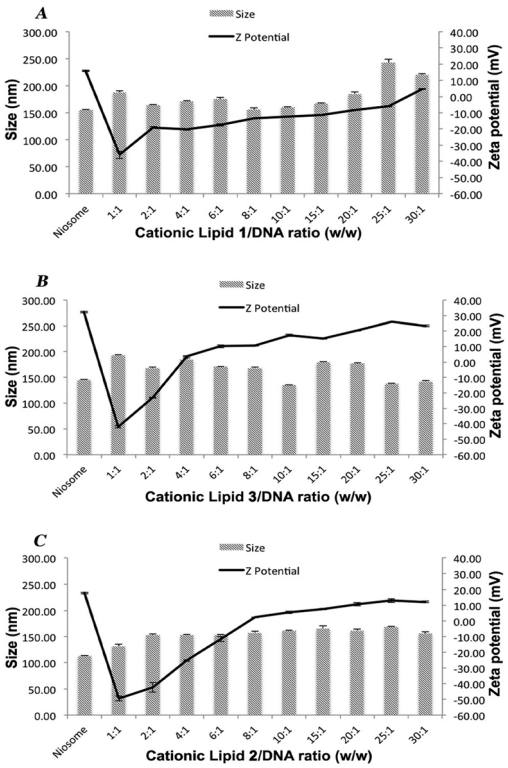

Figure 7. The influence of the cationic lipid/DNA ratio (w/w) on the particle size (bars) and zeta potential (lines) of niosomes based on: A) lipid 1, B) lipid 3 and C) lipid 2. Each value represents the mean ± standard deviation of three measurements.

3.3.7. Agarose gel electrophoresis studies of nioplexes

To further analyze the electrostatic interactions between the niosomes based on the three cationic lipids and the DNA, we performed an agarose gel electrophoresis assay, since an optimum balance between DNA condensation and release is mandatory to enhance transfection efficiency [32]. Additionally, DNA can be easily degraded by enzymes in the cytosol before reaching the nucleus [33]. Therefore, we studied the DNA protection capacity of niosomes based on the three cationic lipids against DNase enzymatic digestion, in order

to design efficient non-viral carriers for gene delivery purposes. Based on the data obtained in Fig. 7, we selected 6/1, 10/1, 20/1 and 30/1 cationic lipid/DNA mass ratios to perform the agarose gel electrophoresis studies, since at cationic lipid/DNA mass ratios below 6/1, the zeta potential values of resulted nioplexes were negatives when nioplexes were formulated with lipid 1 and lipid 2. Data of agarose gel electrophoresis assays are shown in Fig 8.

Nioplexes based on cationic lipid 1 (Fig. 8-A) failed to condense and therefore, to protect the DNA against enzymatic digestion. Clear SC bands on lanes 4, 7, 10 and 13, suggest that unbound DNA was able to migrate through the gel at 6/1, 10/1, 20/1 and 30/1 cationic lipid/DNA mass ratios, respectively. As expected, DNA was easily released from the niosomes based on cationic lipid 1 upon the addition of SDS at all ratios studied, because clear SC and OC bands (in some cases comparable to control lane 2, free DNA) were observed on lanes 5, 8, 11 and 14. Interestingly, faint SC band observed at all mass ratios suggested that the DNA was partially digested upon exposition to DNases when niosomes were formulated with the lipid 1, which anticipates poor performance in next *in vitro* transfection experiments.

Regarding nioplexes based on the cationic lipid 3 (Fig. 8-B), we clearly observed that the condensation capacity was superior to that observed when niosomes were formulated with lipid 1 (Fig. 8-A) since most of the DNA remained retained in the well and not clear SC bands were observed on lanes 4, 7, 10 and 13. Additionally, protection capacity increased

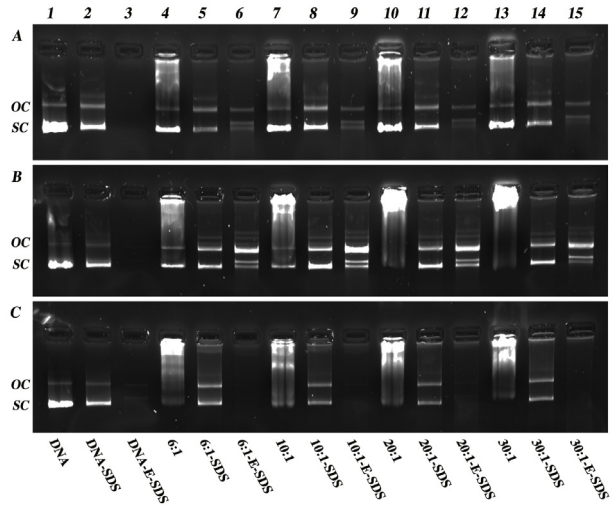

Figure 8. Binding, protection, and SDS-induced release of DNA from niosomes at different cationic lipid/DNA ratios (w/w) visualized by agarose electrophoresis. OC: open circular form, SC: supercoiled form. Lanes 1-3 correspond to free DNA; lanes 4-6, cationic lipid/DNA ratio 6/1; lanes 7-9, cationic lipid/DNA ratio 10/1; lanes 10-12, cationic lipid/DNA ratio 20/1; lanes 13-15, cationic lipid/DNA ratio 30/1. Nioplexes were treated with SDS (lanes 2,5,8,11 and 14) and DNase I + SDS (lanes 3,6,9,12 and 15). A) Nioplexes based on cationic lipid 1, B) Nioplexes based on cationic lipid 3, C) Nioplexes based on cationic lipid 2.

proportionally to the cationic lipid/DNA mass ratios. Therefore, at low mass rations (6/1, lane 4) niosomes were no so efficient to condense DNA. When SDS was added, niosomes were able to release the DNA at all cationic lipid mass ratios analyzed (lanes 5, 8, 11 and 14), which reveals that electrostatic interactions between niosomes based on the lipid 3 and DNA are strong enough to condense DNA, but at the same time, DNA can be easily released from the niosomes upon the addition of SDS, which is an optimal condition for gene delivery purposes [34]. Protection assays against enzymatic digestion revealed that niosomes based on cationic lipid 3 not only condensed and released the DNA, but also efficiently protected the DNA against enzymatic digestion at all ratios, since clear SC bands, the most bioactive form [35], were observed on lanes 6, 9, 12 and 15.

Nioplexes based on the cationic lipid 2 (Fig. 8-C) clearly failed to protect the DNA, as observed by the absence of SC or even OC bands on lanes 6, 9, 12 and 15, despite the fact that niosomes condensed and released properly the DNA after the addition of SDS. Protection capacity of DNA against enzymatic digestion is a mandatory issue that merits special attention for the design of efficient gene delivery vectors [36]. We hypothesize that electrostatic interactions between the cationic lipid 2 and DNA are efficient to condense the DNA, but are not strong enough to protect the DNA. The absence of DNA bands on lane 3 (Fig 8-A, B and C) confirms that the enzyme worked properly in all experiments carried out.

3.3.8. *In vitro* transfection experiments in HEK-293, ARPE-19, and MSC-D1 cells

One of the main goals of non-viral gene delivery systems is to emulate transfection efficiencies obtained with viral vectors. Therefore, the synthesis and development of new safe and efficient non-viral vector carriers represents an attractive challenge for the scientific community that need to be overcome in order to beat gene therapy based on viral vectors.

A single vector is unlikely to be optimal for all applications, since lipofection efficiency is a cell dependent process [37,38]. Therefore, transfection efficiency needs to be studied and evaluated in different cell lines, as we have presented in the current study. Human embryonic kidney cells (HEK-293) have been extensively used as a well-known and easy to transfect model [39]. Human retinal pigment epithelial cells (ARPE-19) are more difficult to transfect cells [36]. These cells are essentials for neural retina homeostasis and play a major role in genetic ocular diseases associated with senescence and dystrophies of the photoreceptors [40]. Finally, mesenchymal stem cells (MSC-D1) have shown flattering characteristics for different medicine applications due to their capacity of differentiation (osteocytes, chondrocytes or adipocytes) and their ability to produce immunosuppression upon transplantation to name just a few. Therefore, MSC-D1 cells represent an attractive model for the development of safe non-viral vectors carriers despite the lack of articles

reported on the literature [41].

Transfection results are shown on Fig. 9-A. As can be observed, only those nioplexes based on cationic lipid 3 showed relevant percentages of transfection. In all cases, the highest percentages were obtained in HEK-293, reaching 33% of transfection at the cationic lipid/DNA ratio 10/1. This value is clearly superior to the maximum transfection values obtained in both ARPE-19 (8% at 10/1 ratio) and MSC-D1 cells (1% at 20/1 ratio). Such differences found on transfection values among the cells could be explained by the different cell line dependent barriers that nucleic acids need to face before reaching the cellular machinery for protein synthesis, such as cellular uptake, structural changes caused by interactions with cellular lipids and posterior intracellular trafficking processes [2,42-44].

The lack of transfection observed when cationic lipids 1 and 2 were used to obtain nioplexes in the three cell lines suggests that the polar head-group of the cationic lipid plays a pivotal role on transfection efficiency. Therefore, minor structural changes performed in the cationic lipid head-groups, such as the inclusion of one additional methylene moiety, are able to change dramatically gene transfer efficiencies, as previously reported by Singh et al. [45]. Moreover, these differences obtained in transfection efficiencies with our three formulations

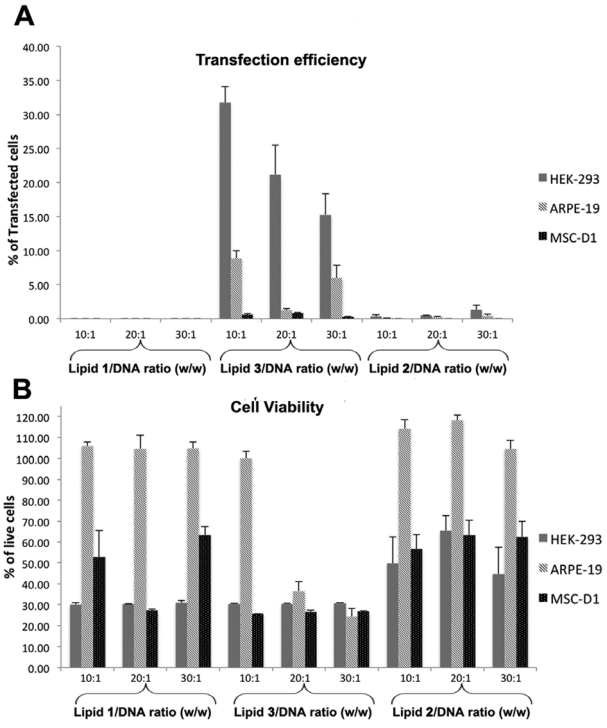

Figure 9. *In vitro* transfection experiments of nioplexes based on cationic lipids 1, 3 and 2 in HEK-293, ARPE-19 and MSC-D1 cells. A) Transfection efficiency at different cationic lipid/DNA ratios (w/w). B) Cell viability at different cationic lipid/DNA ratio (w/w).

might be hypothesized to several causes such as particle hydrophobicity, electrostatic interactions, lipid structures, or formation of aggregates between nioplexes [46,47].

More specifically, the presence of the dimethylaminoethyl moiety as hydrophilic cationic head in the lipid 3 was able to impart efficiently cellular uptake of pDNA. Reported transfection experiments performed with other cell lines *in vitro* and/or *in vivo* using the same modification and other dimethylamino derivatives have shown the importance to maintain this cationic head into the lipid structure, probably due to the easiness of these amino lipids to ionize and the tendency to interact with biomembranes [48,49]. Thus, niosome pKa value for niosomes based on cationic lipid 3 (pKa=6.72, Fig. 4-C) confirmed the correlation between activity and ionization behavior. Besides the dissociation effect observed for the lipid 3, the interaction between the cationic lipid and the DNA can influence on the transfection efficiency. In fact, this structuring promotion is not only due to the lipid itself, but also to the compounds that are used to prepare the niosomes, such as the squalene which can promote the inverted hexagonal phase by facilitating the lamellar to inverted hexagonal phase transition of phospholipids causing the endosome swelling and promote membrane fusion [50]. Surprisingly, this superior transfection property described before for the lipid 3 was not observed for niosomes containing the lipids 1 and 2 which did not promote delivery of DNA *in vitro* even having similar dissociation constants (pKa=7.00 and 6.63 for lipid 1 and 2, respectively; Fig. 4-A, B). This lack of activity could be attributed to both molecular shape of the cationic lipid and the formation of closed-pack units based on electrostatic interactions and van der Waals' attractions (Fig. 3-B) [51]. Consequently, these nioplexes might be unable to adopt the hexagonal morphology because of niosome packing that could become more stabilized and thereby inactivating the delivery process [52]. As a consequence, these results also evidenced that pKa constant is a necessary but not sufficient condition for having a good DNA delivery into the cell [48]. When examining other relevant physicochemical properties for gene deliver purposes such as size, zeta potential or morphology (Fig. 5), we found that niosomes based on the cationic lipid 3 were about 200 nm (Fig. 5-A, bars), had spherical and homogeneous morphology (Fig. 5-C2), and the zeta potential value was higher (around + 30 mV) than the obtained with their counterparts lipid 1 and 2 (around + 20 mV, Fig. 5-A, lines). The higher superficial charge of niosomes based on the lipid 3 could explain the highest stability of this formation due to electrostatic repulsion forces that avoid variations over the time on size and zeta potential values, as observed on Fig. 6-B. Finally, nioplexes obtained upon the addition of DNA at different cationic lipid/DNA ratios (w/w), were more positively charged when the cationic lipid 3 was used (Fig. 7-B), which could support the data obtained in the agarose gel electrophoresis studies. According to this, only nioplexes formulated with the lipid 3 were able to condense, release and protect the DNA against enzymatic digestion

at appropriate cationic lipid/DNA mass ratios 10/1, 20/1 and 30/1 (Fig. 8-B). All these data highlight that cationic lipid head groups play a relevant role on transfection efficiency since minor structural changes are able to dramatically affect this process. However, not only transfection efficiency needs to be assessed when developing novel non-viral vector carriers for gene delivery purposes. The introduction of foreign DNA into the cell is not a natural process. Therefore, transfection is an inherent toxic process by itself. Additionally, cationic lipids toxicity is a highly cell dependent process that has been classically attributed to the induction of apoptosis and could limit the application in the clinic [53].

Results related to cell viability are summarized in Fig. 9-B. We observed a clearly cell-dependent toxicity effect, being ARPE-19 the cells that better tolerated the nioplexes formulations at most ratio studied (with the exception lipid 3, ratio 30:1). Other reported cell viability studies performed with other niosomes based on a glycerol backbone instead of a serinol backbone have also shown that ARPE-19 cells tolerate the nioplexes better than HEK-293 cells [7]. Cell-dependent toxicity effect observed could be probably due to differences in membrane composition as well as differences in phagocytic activity and processing of the nioplexes among the cells studied.

Regarding the cytotoxic effect among our three nioplexes formulations, we clearly observed that nioplexes based on the cationic lipid 3 had a more deleterious effect than their counterparts, especially in ARPE-19 cells at 20/1 and 30/1 ratios. This toxic effect of nioplexes based on the cationic lipid 3 could be explained by the higher zeta potential of these vectors, which could destabilize cell membranes.

To summarize, our data revealed that cationic lipid chemical structure of the hydrophilic group clearly influenced not only on transfection efficiency but also on cell viability. Therefore, the detailed study of this domain is a mandatory issue for the research community in order to design more efficient and safe non-viral vectors based on cationic lipids.

3.4. CONCLUSION

In the present study, we designed niosomes based on three different cationic lipids, which differed only on the polar-head group. Our results show that the chemical composition of the cationic head-group clearly affects to the physicochemical parameters of the niosomes and specially, to the transfection efficiency. Only niosomes based on cationic lipids with a dimethyl amino head group (Lipid 3) showed transfection capacity when compared with their counterparts amino (Lipid 1) and tripetide head-groups (Lipid 2). However, niosomes based on cationic lipid 3 showed a more deleterious effect than their counterpart lipids, especially in ARPE-19 cells at 20/1 and 30/1 ratios. Therefore, we hypothesize that changing the actual ether bond (linker domain) of cationic lipid 1 by a biodegradable ester bond could rend into better tolerated niosome formulations maintaining transfection efficiency, since ether bounds are too stable to be biodegraded, which results in higher toxicity compounds compared to ester bounds [54]. In any case, further studies will be required to support this assumption.

3.5. ACKNOWLEDGMENTS

This project was partially supported by the University of the Basque Country UPV/EHU (UFI 11/32), the National Council of Science and Technology (CONACYT), Mexico, Reg. # 217101, the Spanish Ministry of Education (Grant CTQ2010-20541, CTQ2010-14897), the Basque Government (Department of Education, University and Research, predoctoral BFI-2011-2226 grant), the Generalitat de Catalunya (2009SGR208, 2009SGR1331) and the Instituto de Salud Carlos III. Technical and human support provided by SGIker (UPV/EHU) is gratefully acknowledged. Authors also wish to thank the intellectual and technical assistance from the platform for Drug Formulation (NANBIOSIS) CIBER-BBN.

3.6. REFERENCES

1. Anderson WF. Human gene therapy. Nature 1998;392:25-30.

2. del Pozo-Rodriguez A, Pujals S, Delgado D, Solinis MA, Gascon AR, Giralt E, et al. A proline-rich peptide improves cell transfection of solid lipid nanoparticle-based non-viral vectors. J Control Release 2009;133:52-59.

3. Verma IM. A tumultuous year for gene therapy. Mol Ther 2000;2:415-416.

4. Charbel Issa P, MacLaren RE. Non-viral retinal gene therapy: a review. Clin Experiment Ophthalmol 2012;40:39-47.

5. Rajera R, Nagpal K, Singh SK, Mishra DN. Niosomes: a controlled and novel drug delivery system. Biol Pharm Bull 2011;34:945-953.

6. Paolino D, Muzzalupo R, Ricciardi A, Celia C, Picci N, Fresta M. *In vitro* and *in vivo* evaluation of Bola-surfactant containing niosomes for transdermal delivery. Biomed Microdevices 2007;9:421-433.

7. Puras G, Mashal M, Zarate J, Agirre M, Ojeda E, Grijalvo S, et al. A novel cationic niosome formulation for gene delivery to the retina. J Control Release 2014;174:27-36.

8. Liu F, Yang J, Huang L, Liu D. New cationic lipid formulations for gene transfer. Pharm Res 1996;13:1856-1860.

9. Chung H, Kim TW, Kwon M, Kwon IC, Jeong SY. Oil components modulate physical characteristics and function of the natural oil emulsions as drug or gene delivery system. J Controlled Release 2001;71:339-350.

10. Huang Y, Rao Y, Chen J, Yang VC, Liang W. Polysorbate cationic synthetic vesicle for gene delivery. J Biomed Mater Res A 2011;96:513-519.

11. Ma B, Zhang S, Jiang H, Zhao B, Lv H. Lipoplex morphologies and their influences on transfection efficiency in gene delivery. J Control Release 2007;123:184-194.

12. Byk G, Dubertret C, Escriou V, Frederic M, Jaslin G, Rangara R, et al. Synthesis, activity, and structure--activity relationship studies of novel cationic lipids for DNA transfer. J Med Chem 1998;41:229-235.

13. Mahidhar YV, Rajesh M, Chaudhuri A. Spacer-arm modulated gene delivery efficacy of novel cationic glycolipids: design, synthesis, and *in vitro* transfection biology. J Med Chem 2004;47:3938-3948.

14. Zhi D, Zhang S, Wang B, Zhao Y, Yang B, Yu S. Transfection efficiency of cationic lipids with different hydrophobic domains in gene delivery. Bioconjug Chem 2010;21:563-577.

15. Karmali PP, Chaudhuri A. Cationic liposomes as non-viral carriers of gene medicines: resolved issues, open questions, and future promises. Med Res Rev 2007;27:696-722.

16. Zhao F, Shen G, Chen C, Xing R, Zou Q, Ma G, et al. Nanoengineering of stimuli-responsive protein-based biomimetic protocells as versatile drug delivery tools. Chemistry 2014;20:6880-6887.

17. Wang K, Yan X, Cui Y, He Q, Li J. Synthesis and *in vitro* behavior of multivalent cationic lipopeptide for DNA delivery and release in HeLa cells. Bioconjug Chem 2007;18:1735-1738.

18. Yan X, Li J, Mohwald H. Templating assembly of multifunctional hybrid colloidal spheres. Adv Mater 2012;24:2663-2667.

19. Haba E, Pinazo A, Pons R, Perez L, Manresa A. Complex rhamnolipid mixture characterization and its influence on DPPC bilayer organization. Biochim Biophys Acta 2014;1838:776-783.

20. Pabst G, Rappolt M, Amenitsch H, Laggner P. Structural information from multilamellar liposomes at full hydration: full q-range fitting with high quality x-ray data. Phys Rev E Stat Phys Plasmas Fluids Relat Interdiscip Topics 2000;62:4000-4009.

21. Kucerka N, Nieh MP, Katsaras J. Asymmetric distribution of cholesterol in unilamellar vesicles of monounsaturated phospholipids. Langmuir 2009;25:13522-13527.

22. Kanasty R, Dorkin JR, Vegas A, Anderson D. Delivery materials for siRNA therapeutics. Nat Mater 2013;12:967-977.

23. Semple SC, Akinc A, Chen J, Sandhu AP, Mui BL, Cho CK, et al. Rational design of cationic lipids for siRNA delivery. Nat Biotechnol 2010;28:172-176.

24. Zhang J, Fan H, Levorse DA, Crocker LS. Ionization behavior of amino lipids for siRNA delivery: determination of ionization constants, SAR, and the impact of lipid pKa on cationic lipid-biomembrane interactions. Langmuir

2011;27:1907-1914.
25. Tros de Ilarduya C, Sun Y, Duzgunes N. Gene delivery by lipoplexes and polyplexes. Eur J Pharm Sci 2010;40:159-170.
26. Caracciolo G, Caminiti R, Digman MA, Gratton E, Sanchez S. Efficient escape from endosomes determines the superior efficiency of multicomponent lipoplexes. J Phys Chem B 2009;113:4995-4997.
27. Caracciolo G, Amenitsch H. Cationic liposome/DNA complexes: from structure to interactions with cellular membranes. Eur Biophys J 2012;41:815-829.
28. Heurtault B, Saulnier P, Pech B, Proust JE, Benoit JP. Physico-chemical stability of colloidal lipid particles. Biomaterials 2003;24:4283-4300.
29. Paecharoenchai O, Niyomtham N, Ngawhirunpat T, Rojanarata T, Yingyongnarongkul BE, Opanasopit P. Cationic niosomes composed of spermine-based cationic lipids mediate high gene transfection efficiency. J Drug Target 2012;20:783-792.
30. Resina S, Prevot P, Thierry AR. Physico-chemical characteristics of lipoplexes influence cell uptake mechanisms and transfection efficacy. PLoS One 2009;4:e6058.
31. Ferrari A, Pellegrini V, Arcangeli C, Fittipaldi A, Giacca M, Beltram F. Caveolae-mediated internalization of extracellular HIV-1 tat fusion proteins visualized in real time. Mol Ther 2003;8:284-294.
32. Delgado D, del Pozo-Rodriguez A, Solinis MA, Rodriguez-Gascon A. Understanding the mechanism of protamine in solid lipid nanoparticle-based lipofection: the importance of the entry pathway. Eur J Pharm Biopharm 2011;79:495-502.
33. Midoux P, Monsigny M. Efficient gene transfer by histidylated polylysine/pDNA complexes. Bioconjug Chem 1999;10:406-411.
34. Ochoa GP, Sesma JZ, Diez MA, Diaz-Tahoces A, Aviles-Trigeros M, Grijalvo S, et al. A novel formulation based on 2,3-di(tetradecyloxy)propan-1-amine cationic lipid combined with polysorbate 80 for efficient gene delivery to the retina. Pharm Res 2014;31:1665-1675.
35. Remaut K, Sanders NN, Fayazpour F, Demeester J, De Smedt SC. Influence of plasmid DNA topology on the transfection properties of DOTAP/DOPE lipoplexes. J Control Release 2006;115:335-343.
36. del Pozo-Rodriguez A, Delgado D, Solinis MA, Gascon AR, Pedraz JL. Solid lipid nanoparticles for retinal gene therapy: transfection and intracellular trafficking in RPE cells. Int J Pharm 2008;360:177-183.
37. Leventis R, Silvius JR. Interactions of mammalian cells with lipid dispersions containing novel metabolizable cationic amphiphiles. Biochim Biophys Acta 1990;1023:124-132.
38. Gao X, Huang L. A novel cationic liposome reagent for efficient transfection of mammalian cells. Biochem Biophys Res Commun 1991;179:280-285.
39. Thomas P, Smart TG. HEK293 cell line: a vehicle for the expression of recombinant proteins. J Pharmacol Toxicol Methods 2005;51:187-200.
40. Bejjani RA, BenEzra D, Cohen H, Rieger J, Andrieu C, Jeanny JC, et al. Nanoparticles for gene delivery to retinal pigment epithelial cells. Mol Vis 2005;11:124-132.
41. Corsi K, Chellat F, Yahia L, Fernandes JC. Mesenchymal stem cells, MG63 and HEK293 transfection using chitosan-DNA nanoparticles. Biomaterials 2003;24:1255-1264.
42. Pozzi D, Caracciolo G, Caminiti R, De Sanctis SC, Amenitsch H, Marchini C, et al. Toward the rational design of lipid gene vectors: shape coupling between lipoplex and anionic cellular lipids controls the phase evolution of lipoplexes and the efficiency of DNA release. ACS Appl Mater Interfaces 2009;1:2237-2249.
43. Pozzi D, Marchini C, Cardarelli F, Rossetta A, Colapicchioni V, Amici A, et al. Mechanistic understanding of gene delivery mediated by highly efficient multicomponent envelope-type nanoparticle systems. Mol Pharm 2013;10:4654-4665.
44. Pozzi D, Marchini C, Cardarelli F, Salomone F, Coppola S, Montani M, et al. Mechanistic evaluation of the transfection barriers involved in lipid-mediated gene delivery: interplay between nanostructure and composition. Biochim Biophys Acta 2014;1838:957-967.
45. Singh RS, Chaudhuri A. Single additional methylene group in the head-group region imparts high gene transfer

efficacy to a transfection-incompetent cationic lipid. FEBS Lett 2004;556:86-90.
46. Brunner S, Sauer T, Carotta S, Cotten M, Saltik M, Wagner E. Cell cycle dependence of gene transfer by lipoplex, polyplex and recombinant adenovirus. Gene Ther 2000;7:401-407.
47. Lin AJ, Slack NL, Ahmad A, George CX, Samuel CE, Safinya CR. Three-dimensional imaging of lipid gene-carriers: membrane charge density controls universal transfection behavior in lamellar cationic liposome-DNA complexes. Biophys J 2003;84:3307-3316.
48. Jayaraman M, Ansell SM, Mui BL, Tam YK, Chen J, Du X, et al. Maximizing the potency of siRNA lipid nanoparticles for hepatic gene silencing *in vivo*. Angew Chem Int Ed Engl 2012;51:8529-8533.
49. Heyes J, Palmer L, Bremner K, MacLachlan I. Cationic lipid saturation influences intracellular delivery of encapsulated nucleic acids. J Control Release 2005;107:276-287.
50. Goni FM, Alonso A. Membrane fusion induced by phospholipase C and sphingomyelinases. Biosci Rep 2000;20:443-463.
51. Bennett MJ, Aberle AM, Balasubramaniam RP, Malone JG, Malone RW, Nantz MH. Cationic lipid-mediated gene delivery to murine lung: correlation of lipid hydration with *in vivo* transfection activity. J Med Chem 1997;40:4069-4078.
52. Smisterova J, Wagenaar A, Stuart MC, Polushkin E, ten Brinke G, Hulst R, et al. Molecular shape of the cationic lipid controls the structure of cationic lipid/dioleylphosphatidylethanolamine-DNA complexes and the efficiency of gene delivery. J Biol Chem 2001;276:47615-47622.
53. Yingyongnarongkul BE, Radchatawedchakoon W, Krajarng A, Watanapokasin R, Suksamrarn A. High transfection efficiency and low toxicity cationic lipids with aminoglycerol-diamine conjugate. Bioorg Med Chem 2009;17:176-188.
54. Aberle AM, Tablin F, Zhu J, Walker NJ, Gruenert DC, Nantz MH. A novel tetraester construct that reduces cationic lipid-associated cytotoxicity. Implications for the onset of cytotoxicity. Biochemistry 1998;37:6533-6540.

4

The influence of the polar head-group of synthetic cationic lipids on the transfection efficiency mediated by niosomes in rat retina and brain

The influence of the polar head-group of synthetic cationic lipids on the transfection efficiency mediated by niosomes in rat retina and brain

Ojeda, E[1,2]; Puras, G[1,2]; Agirre, M[1,2]; Zarate, J[1,2]; Grijalvo, S[2,3]; Eritja, R[2,3]; Martinez-Navarrete, G[2,4]; Soto-Sánchez, C[2,4]; Diaz-Tahoces, A[2,4]; Aviles-Trigueros, M[5]; Fernández, E[2,4] and Pedraz, JL[1,2]

[1] NanoBioCel Group, University of Basque Country (UPV/EHU), Vitoria-Gasteiz, Spain.
[2] Biomedical Research Networking Center in Bioengineering, Biomaterials and Nanomedicine (CIBER-BBN), Vitoria-Gasteiz, Spain
[3] Institute of Advanced Chemistry of Catalonia, IQAC-CSIC, Barcelona, Spain.
[4] Neuroprothesis and Neuroengineering Research Group, Miguel Hernández University, Spain
[5]Laboratory of Experimental Ophthalmology, Faculty of Medicine, University of Murcia, Regional Campus of International Excellence "Campus Mare Nostrum", Murcia, Spain

Biomaterials. 2016; 77: 267-279

ABSTRACT

The development of novel non-viral delivery vehicles is essential in the search of more efficient strategies for retina and brain diseases. Herein, optimized niosome formulations prepared by oil-in water (o/w) and film-hydration techniques were characterized in terms of size, PDI, zeta potential, morphology and stability. Three ionizable glycerol-based cationic lipids containing a primary amine group (lipid 1), a triglycine group (lipid 2) and a dimethylamino ethyl pendent group (lipid 3) as polar head-groups were part of such niosomes. Upon the addition of pCMS-EGFP plasmid, nioplexes were obtained at different cationic lipid/DNA ratios (w/w). The resultant nioplexes were further physicochemically characterized and evaluated to condense, release and protect the DNA against enzymatic digestion. In vitro experiments were performed to evaluate transfection efficiency and cell viability in HEK-293, ARPE-19 and PECC cells. Interestingly, niosome formulations based on lipid 3 showed better transfection efficiencies in ARPE-19 and PECC cells than the rest of cationic lipids showed in this study. *In vivo* experiments in rat retina after intravitreal and subretinal injections together with in rat brain after cerebral cortex administration showed promising transfection efficiencies when niosome formulations based on lipid 3 were used. These results provide new insights for the development of non-viral vectors based on cationic lipids and their applications for efficient delivery of genetic material to the retina and brain.

Keywords: Niosomes, gene delivery, non-viral vector, cationic lipid, retina, brain

4.1. INTRODUCTION

Gene therapy is a challenging field that is emerging as a promising strategy for the treatment of several diseases [1]. Concretely, non-viral vectors have attracted the interest of the scientific community because, compared to viral vectors, they offer a safer way to deliver genetic material, as they do not exhibit antigen-specific immune and inflammatory response, are cheaper, easy to elaborate and the size of DNA inserted is theoretically unlimited [2]. Nevertheless, their low transfection efficiencies and the transient gene expression are the main concerns that these carriers have to overcome to reach clinical practice. There is a wide range of non-viral vectors described in the literature, such as those composed of polymers, lipids or peptides [3-5]. Among lipidic systems, liposomes are the most common vectors. However, our research group has previously described that niosomes are a promising alternative to liposomes for gene delivery purposes. Niosomes are carrier systems that form vesicles with a bilayer structure and compared to liposomes they are recognized for their low cost and superior chemical and storage stabilities. Nevertheless, few reports have been focused on their application for gene delivery purposes [6,7].

Unlike liposomes, which are elaborated with phospholipids, niosomes for gene delivery purposes are typically based on non-ionic surfactants to form more stable emulsions. In addition, helper lipids are also added to the formulations to enhance the physicochemical properties of the emulsion and finally, the cationic lipids, whose structural and physical properties clearly influence the transfection efficiency and toxicity [8-10].

Cationic lipids for gene delivery purposes usually contain four functional domains (hydrophobic group, linker group, hydrophilic head-group and backbone), which affect some important physicochemical parameters, such as the flexibility, stability, biodegradability, the level of hydration, interaction with DNA and its condensation [11-14]. In our previous work [15] the influence of the polar head-group on transfection efficiency together with cell viability was studied in HEK-293, ARPE-19 and MSC-D1 cells. Although promising results were obtained, such studies were performed with lipids containing a serinol backbone, which due to its low biodegradability reduced significantly cell viability. Therefore in the present manuscript, we have modified the serinol backbone by a glycerol one in order to improve the design of the niosomes formulation for *in vivo* retinal and brain delivery purposes.

Regarding the applications of gene therapy, the eye has favorable characteristics for this type of therapy, such as small size, immune-privileged position and well-defined compartmentalized anatomy, which minimize potential adverse reactions [16]. Additionally, most of the devastating inherent diseases in the eye are well described and their genetic background is also well known. However, at present few effective treatments are available for inherent retinal diseases. Therefore, research on the design of novel formulations for gene

delivery to the retina represents a promising approach in order to translate animal research into clinical trials [17]. On the other hand, neurological disorders are the most difficult diseases to treat with clinical pharmacological approaches, mainly due to the complexity of the nervous system and the different brain physical barriers that drugs need to overcome after systemic administration [18]. Gene therapy represents a promising alternative to the traditional pharmacological approaches to face many devastating genetic diseases of the brain, such as Batten disease [19], Canavan disease [20] or Parkinson´s disease [21]. In the past few years many gene transfer methods have been developed to treat retinal and brain diseases. However, all gene clinical trials are based on viral vectors that generate moderate optimism to drive the field forward. Therefore, we present an alternative and a safer approach to confront inherent retinal and brain disorders by the use of niosomes as non-viral carriers for gene delivery purposes.

Consequently, in the present study, we designed niosomes vectors for retinal and brain delivery purposes based on three synthetic ionizable cationic lipids containing polysorbate 80, as a non-ionic surfactant and squalene, as a helper lipid. These cationic lipids had three different functional domains: 1) an hydrophobic tail formed by two saturated hydrocarbonated alkyl chains of fourteen atoms of carbons in length; 2) a polar head formed by an amino group (lipid 1), a glycine triglycine (lipid 2) and a dimethylaminoethyl group (lipid 3) and 3) a glycerol-based building block. Niosomes prepared by the oil-in-water emulsion (o/w) and film-hydration techniques were characterized in terms of size, PDI, zeta potential, morphology and physical stability. Upon the addition of the pCMS-EGFP reporter plasmid, we obtained nioplexes at different cationic lipid/DNA ratios (w/w). The influence of cationic lipid/DNA ratios on particle size, zeta potential and the ability to condense, release and protect DNA from enzymatic digestion was analyzed. *In vitro* experiments were performed and analyzed by flow cytometry to evaluate the most promising formulations in terms of transfection efficiency, viability and mean fluorescence intensity (MFI) in human embryonic kidney 293 cells (HEK-293), retinal pigment epithelia 19 cells (ARPE-19) and rat primary embryonic cerebral cortex cells (PECC). In order to move forward and according to the previous characterization results of the niosome formulations and nioplexes, we carried out some preliminary *in vivo* studies by confocal microscopy to evaluate transfection efficiency of the most promising formulation in the rat retina after intravitreal and subretinal injection and in the rat brain after injection in the cerebral cortex.

4.2. MATERIAL AND METHODS

4.2.1. Material

All reactions were carried out under an inert atmosphere of argon. Flash column chromatography was carried out on silica gel SDS 0.063–0.2 mm/70–230 mesh. 1H and 13C NMR spectra were recorded at 25 °C on a Varian Mercury 400 MHz spectrometer using deuterated solvents. Tetramethylsilane (TMS) was used as an internal reference (0 ppm) for 1H spectra recorded in CDCl3 and the residual signal of the solvent (77.1 ppm) for 13C spectra. For CD3OD and d6-DMSO the residual signal of the solvent was used as a reference. Chemical shifts are reported in parts per million (ppm), coupling constants (J) in Hz and multiplicity as follows: s (singlet), d (doublet), t (triplet), q (quadruplet), quint (quintuplet), m (multiplet) and br (broad signal). Electrospray ionization mass spectra (ESI-MS) were recorded on a Micromass ZQ instrument with a single quadrupole detector coupled to an HPLC, and high resolution (HR) ESI-MS on an Agilent 1100 LC/MS-TOF instrument (Servei d'Espectrometría de Masses, Universitat de Barcelona). HEK-293 cells, ARPE-19 cells, Eagle's Minimal Essential medium with Earle's BSS and 2 mM L-glutamine (EMEM) were obtained from the American Type Culture Collection (ATCC). Dulbecco's Modified Eagle's medium Han's Nutrient Mixture F-12 (1:1), Trypsine, Hank's Balanced Salt Solution (HBSS), Neurobasal medium (NB), Fetal bovine Serum (FBS), B27® and GlutamaxTM supplements and Penicillin-Streptomycin (Pen/Strep) antibiotics were purchased from Gibco® (San Diego, California, US). The plasmid pCMS-EGFP was purchased from PlasmidFactory (Bielefeld, Germany). The gel electrophoresis materials and gel red solution were acquired from Bio-Rad (Madrid, Spain). DNase I, sodium dodecyl sulfate (SDS), squalene, polysorbate 80, PBS and paraformaldehyde were purchased from Sigma-Aldrich (Madrid, Spain), and dichloromethane (DCM) was purchased from Panreac (Barcelona, Spain). Opti-MEM® reduced medium, antibiotic/antimycotic solution and LipofectmanineTM 2000 transfection reagent were acquired from Invitrogen (San Diego, California, US). The BD Viaprobe kit was obtained from BD Biosciences (Belgium).

4.2.2. Synthesis of ionizable cationic amino lipids

The synthesis of the ionizable cationic amino lipids is summarized in supplementary data scheme S1. Synthesis of tert-butyl-N-[2-[[2-[[2-[2,3-di(tetradecoxy)propylamino]-2-oxo-ethyl]amino]-2-oxo-ethyl]-amino]-2-oxo-ethyl]carbamate (3). Firstly, the carboxylic acid activation was carried out as follows: glycine tripeptide (2.0 eq) and N-hydroxysuccinimide (2.1 eq) were dissolved in DCM (3 mL) and the solution was stirred for a couple of minutes. Then, EDC (2.2 eq) was added. The reaction was stirred overnight at room temperature. The organic layer was washed with water (3 x 5 mL) and dried over anhydrous MgSO4. The

combined organic layers were reduced in vacuo and the anticipated crude was used in the next step without further purification. Cationic lipid 1 (compound 2) (100 mg; 0.206 mmol) was added over the activated tripeptide. Reaction was heated at 60 ºC and stirred overnight. The solvent was evaporated and the resultant crude was purified by flash chromatography (DCM/MeOH 5%).

Synthesis of 2-[[2-[(2-aminoacetyl)amino]acetyl]amino]-N-[2,3-di(tetradecoxy) propyl]-acetamide (4, lipid 2). Boc-protected alkyl tripeptide 3 (50 mg; 0.066 mmol) was dissolved in DCM (1 mL) and trifluoroacetic acid was subsequently added (10%). The solution was stirred for one at room temperature. The solvent was removed until dryness. Finally, the anticipated trifluoroacetate salt was dissolved in a mixture of AcOEt:MeOH (3:2) and carbonate on polymer support (20 eq) was added. The mixture was stirred for one hour at room temperature. The resin was filtered off and solvent was reduced until dryness obtaining the corresponding cationic lipid 4, which was used without further purification.

Synthesis of 1-(2-dimethylaminoethyl)-3-[2,3-di(tetradecoxy)propyl]urea (5, lipid 3). Previously, p-nitrophenyl-chloroformate (2.5 eq) and amino diol 2 (100 mg; 0.206 mmol) were dissolved in a mixture of tetrahydrofurane and DCM (1:1) (6 mL). The reaction was cooled at 0 ºC and DIEA (2.5 eq) was carefully added dropwise. The solution was stirred for 4 hours and heated at room temperature. The solvent was removed and the resultant crude was used in the next step without further purification. The yellow crude was dissolved in DMF (3 mL) and the corresponding dimethylamine derivative (1.1 eq) was added dropwise. The reaction was stirred overnight at room temperature. Finally, solvent was removed and the resultant crude was purified by flash chromatography (DCM:MeOH 5% to 10%).

4.2.3. Preparation of niosomes and nioplexes

Niosomes based on three different synthetic cationic lipids were prepared using the o/w emulsification and the film-hydration techniques, as previously reported [15]. In the o/w emulsification technique, the cationic lipid (5 mg) was gently grounded with 23 µl of squalene and then emulsified in an aqueous phase containing polysorbate 80 (0.5%, w/w). The emulsion was obtained by sonication (Branson Sonifier 250, Danbury) for 30 s at 50 W. The organic solvent was removed from the emulsion by evaporation under magnetic agitation for 3 h. In the film-hydration technique, the lipid compounds (5 mg cationic lipid and 23 µl squalene) were grounded in DCM, and then the solvent was evaporated under magnetic agitation for 3 h. Then, the lipid film was hydrated with the aqueous phase containing the non-ionic surfactant polysorbate 80 (0.5%, w/w), and the emulsion was obtained by sonication for 30 s at 50 W. The final cationic lipid concentration was 1mg/ml.

The nioplexes (niosome/DNA vectors) were elaborated by mixing an appropriate

volume of a stock solution of the pCMS-EGFP plasmid (0.5 mg/ml), which was propagated and purified as previously reported [15] with different volumes of the niosome suspensions for 30 min at room temperature. The niosome/DNA ratio was referred as the ratio of cationic lipid to DNA (w/w). The stock solutions of cationic lipids (1 mg/ml) correspond to the following molar concentrations: 2.07 mM (Lipid 1, MW 484), 1.53 mM (Lipid 2, MW 654), and 1.67 mM (Lipid 3, MW 598). The stock solution of plasmid pCMS-EGFP (0.5 mg/ml) was estimated to be around 0.137 micromolar (pCMS-EGFP, 5541 bp, average MW 3657060).

4.2.4. Size and zeta potential of niosomes and nioplexes and Cryo-TEM analysis of niosomes

Dynamic Light Scattering (DLS) and Laser Doppler Velocimetry (LDV) were applied to measure hydrodimanyc diameter and zeta potential of the niosomes and nioplexes in a Zetasizer Nano ZS (Malvern Instrument, UK). Particle size reported as hydrodynamic diameter was obtained by Z-average (cumulants means). Niosomes or nioplexes were resuspended 0.1 mM NaCl solution. All measurements were carried out in triplicate. Only data that met the quality criteria according to the software program were included in the study. Cryo Transmission Electron Microscopy (Cryo-TEM) was employed to analyze the morphology of niosomes, as previously described [15].

4.2.5. Physical stability study of niosomes

Niosomes based on three different synthetic cationic lipids were storage for 100 days at 4 °C and 25 °C. Their physical stability was determined by monitoring the particle size and zeta potential during storage time. All samples were measured in triplicate.

4.2.6. Agarose gel electrophoresis studies of nioplexes

In order to analyze the ability of the niosomes to condensate, release and protect the DNA, we carried out an agarose gel electrophoresis assay with the nioplexes at different cationic lipid/DNA ratios (200 ng of DNA per well). The agarose gel (0.8%) was immersed in a Tris-acetate-EDTA buffer and exposed for 30 min to 120 V. DNA bands were stained with GelRedTM (Biotium, Hayward, California, USA) and images were observed with a ChemiDocTM MP Imaging System. SDS 3.5% solution and DNase I enzyme (1 U DNase I per 2.5 μg DNA) were added to the samples to evaluate the release and protection, respectively. The integrity of the DNA in each sample was compared to a control of untreated DNA.

4.2.7. Cell culture and *in vitro* transfection protocols

HEK-293 and ARPE-19 cells were seeded in 24 well plates at an initial density of

15×104 and 10×104 cell per well, with 300 µl of EMEM containing 10% horse serum and 300 µl of D-MEM/F-12 containing 10% bovine serum, respectively. Cells were incubated overnight to achieve 70-90% of confluence at the time of transfection. Experimental procedures for PECC cells were carried out conformed to the directive 2010/63/EU of the European Parliament and of the Council, and the RD 53/2013 Spanish regulation on the protection of animals use for scientific purposes and was approved by the Miguel Hernandez University Committee for Animal use in Laboratory. Dissociated cultures of hippocampal neurons were obtained from E17.5 rat embryos (Sprague Dawley) and preserved in HBSS during extraction. Then, trypsin was added to the medium and incubated in a bath at 37°C for chemical dissociation. Subsequently, the tissue was mechanically dissociated in NB/FBS and the cell density was determined using a hemocytometer. Cells were seeded on glass coverslips (Thermo Scientific) at approximately 100,000 cells/well cell density in a 12 well plate (Corning Incorporated) and maintained in a NB/FBS medium supplemented with B27, Glutamax and Pen/Strep (1:100 dilution) in an incubator at 37°C and 5% CO2. At the time of transfection assay, the regular growth mediums were removed from ARPE-19, HEK-293 and PECC cells, and the cells were exposed to nioplexes resuspended in Opti-MEM® transfection medium at different cationic lipid/DNA ratios. The amount of plasmid for each well was 1.25 µg. Each formulation was used in triplicate. After 4 h of incubation at 37°C, the nioplexes were replaced by 300 µl of regular growth medium. Cells were allowed to grow for 72 h until flow cytometry analysis. Following the manufacturer's protocol, LipofectamineTM 2000 was used in combination with pDNA as a transfection positive control.

4.2.8. Transfection efficiency and cell viability

Flow cytometry analysis was conducted using a FACSCalibur system flow cytometer (Becton Dickinson Bioscience, San Jose, USA) in order to quantify the percentage of EGFP positive cells. Cells were washed twice with PBS and detached from the microplate with 200 µl of trypsin/EDTA. Once the cells were detached, 400 µl of their respective normal growth medium were added and directly introduced into the flow cytometer. Transfection efficiency was expressed as the percentage of EGFP positive cells at 525 nm (FL1) after excluding dead cells. MFI data were obtained from live positive cells at 525 nm (FL1). Cell viability of the cells was evaluated using 5 µL of BD-Via Probe reagent in each sample and positive cells were excluded from the EGFP expression analysis. The fluorescent signal corresponding to dead cells was measured at 650 nm (FL3). Control samples (non-transfected cells) were displayed on a forward scatter (FSC) versus side scatter (SSC) dot plot to establish a collection gate and exclude cells debris. Control samples containing LipofectamineTM 2000 transfected cells without BD-Via Probe, and non-transfected cells with BD-Via Probe were

used to compensate FL2 signal in FL1 and FL3 channels. For each sample 10,000 events were collected. Each formulation was analyzed in triplicate.

4.2.9. *In vivo* studies in rats

Adult male Sprague Dawley rats (6-7 weeks old, 200-300 g weight) were used as experimental animals. All experimental procedures were carried out in accordance with the Spanish and European Union regulations for the use of animals in research and the Association for Research in Vision and Ophthalmology (ARVO) statement for the use of animals in ophthalmic and vision research and supervised by the Miguel Hernandez University Standing Committee for Animal Use in Laboratory. The surgical procedures used for the administration of the vectors in the retina and brain have been described elsewhere [22,23].

4.2.10. Intravitreal and subretinal injections

Six adult male Sprague Dawley rats were use for this assay; three rats received injection of nioplexes by intravitreal and three by subretinal route. Injections were performed under an operating microscope (Zeiss OPMI® pico; Carl Zeiss Meditec GmbH, Jena, Germany) with the aid of a Hamilton microsyringe (Hamilton Co., Reno, NV). A bent 34-gauge needle was used to inject into the vitreous of the left eye, closely adjacent to the ora serrata without touching the lens. In order to deliver the formulation into the subretinal space, the needle was passed through the sclerotomy 2 mm posterior to ora serrata and in a tangential direction toward the posterior retinal pole along the subretinal space. Successful administration was confirmed by the appearance of a partial retinal detachment by direct ophthalmoscopy of the eye fundus. The untreated right eye, served as a control. Seven days post-injection, the rats were sacrificed and perfused with saline solution (0.9%) followed by paraformaldehyde (4%) in phosphate buffer (0.1M, pH 7.2-7.4) at 4ºC.

4.2.11. Evaluation of EGFP expression in rat retinas

All preparations were mounted as follows. Both eyes from each group were enucleated and immersed for 1 hour in a solution of PBS with paraformaldehyde (4%). Later, the retinas were dissected as whole-mounts by making four radial cuts. Retinal orientation was maintained by making the deepest radial cut in the superior retina. The retinas were post-fixed for 1 hour in the same fixative medium, rinsed with PBS, and mounted in poly-L-lysine coated microscope slides with the vitreal side facing up, covered with anti-fading mounting media containing glycerol (50%) and p-phenylenediamine (0.04%) in sodium carbonate buffer (0.1 M, pH 9.0). In order to identify retinal nuclei, the samples were stained

with Hoechst 33342. 5 µg/ml of dye was added to the samples and left for 5 minutes, then samples were thoroughly washed with PBS (0.1 M) and covered with anti-fading mounting media. EGFP expression and Hoechst 33342 staining were evaluated with a Leica TCS SPE spectral confocal microscope (Leica Microsystems GmbH, Wetzlar, Germany). Images were processed, montaged and composed digitally using ImageJ, (National Institutes of Health, Bethesda, MD) and Adobe® Photoshop® CS5.1 (Adobe Systems Inc, San Jose, CA) software. Hoechst 33342 staining was pseudocolored in red for better contrast.

4.2.12. Brain administration

Data were obtained from male Sprague-Dawley adult rats. Surgical analgesia was induced by buprenorphine (0.025 mg/kg, s.c) and anesthesia and sedation were induced by a cocktail of ketamine HCl (40 mg/kg, i.p) and diazepam (5 mg/kg, i.p). Subsequently, the anesthesia was continued and maintained with a mix of oxygen and 2 % of isofluorane for the rest of the surgery. The effect of the anesthesia was continuously evaluated by monitoring heart rate, blinking and toe pinch reflexes. Rats were pre-treated with dexamethasone (1 mg/kg, i.p) 24 hours previous to the surgery and administered again 20 minutes before and 24 hours after surgery. Briefly, we drilled a small craniotomy while 0.8 µl of nioplexes were incubated for 30 min at room temperature. Then, the nioplexes were injected inside the cerebral cortex with a microsyringe (Hamilton company, 33-gauge needle) 1 mm. Once the procedure was finished, the animals were housed in their own cages for 3 days. A post-surgery treatment with antibiotics (enroflorxacine 25 mg/kg, s.c), anti-inflammatory and analgesic drugs (meloxicam 2mg/kg, s.c) was administrated.

4.2.13. Evaluation of EGFP expression in the rat brain

Intracardiac perfusion with phosphate buffer solution followed by paraformaldehyde (4%) was performed for an initial fixation. Then, the brains were preserved in paraformaldehyde (4%) and cryoprotected in sucrose solution (30%) with PBS before slicing. A cryostat (HM 550; Microm International GmbH, Walldorf, Germany) was used to obtain slices of 20 µm from coronal frozen sections adjacent to the injection area. Once the slices were mounted for immunohistochemistry processing, sections were incubated in normal bovine serum (10%) (Jackson, West Grove, PA, USA) with Triton X-100 (0.5%) for blocking of non-specific staining. Then, the samples were incubated overnight at room temperature with chicken anti-GFP (Invotrogen, 1:100) and rabbit anti-NeuN (Millipore, 1:300) antibodies diluted in PBS containing Triton-X100 (0.5%). Later, sections were washed in PBS and incubated for 1 hour with Alexa Fluor 488-conjugated donkey anti-rabbit IgG and Alexa fluor 555-conjugated donkey anti-chicken IgG (Invitrogen, 1:100). Hoechst 33342 was used to label the cell

nuclei. Finally, sections were mounted for imaging and analyzed with a Leica TCS SPE fluorescence microscope (Leica, Microsystems GmbH, Germany). Hoechst 33342 staining was pseudocolored in red for better contrast.

4.3. RESULTS AND DISCUSSION

4.3.1. Synthesis of ionizable cationic amino lipids

The search of pH-responsive drug delivery systems is one of the main strategies that have been used to carry out more efficient processes of drug release in acid environment. This mechanism normally protects therapeutic molecules at physiological pH whereas accelerates such release in the presence of acid pH caused by late endosomes or lysosomes in which pH can vary from 6.5 to 4.5, respectively. This pH dependence on mediating cellular internalization has been recently reported for eliciting gene silencing *in vivo* [24]. In this systematic study, a tight correlation between acid dissociation constant (pKa) value and activity of cationic lipid-based combinatorial libraries was determined by optimizing several variables like lipid-chain unsaturation, linker chemistry and polar head nature. Interestingly, an optimum pKa (6.2-6.5) was established as an ideal value in order to design new liposomal drug delivery systems [24].

Specifically, this optimal relationship between pKa and silencing activity was successfully found for amino lipid derivatives containing dimethylaminoethyl as a cationic pendent group. This correlation in the transfection activity was also observed in our recent work based on serinol amino lipid derivatives [15]. These findings made us to consider the possibility of introducing this potential modification in our glycerol-based cationic lipid 1 (Fig. 1) which efficiently promoted cellular uptake with improved values compared to commercially available cationic lipids. As comparison purposes, we also selected triglycine tripeptide in its free amine form in order to investigate further additional effects that could govern transfection efficiency processes when increased the polar-pendent group electronic nature.

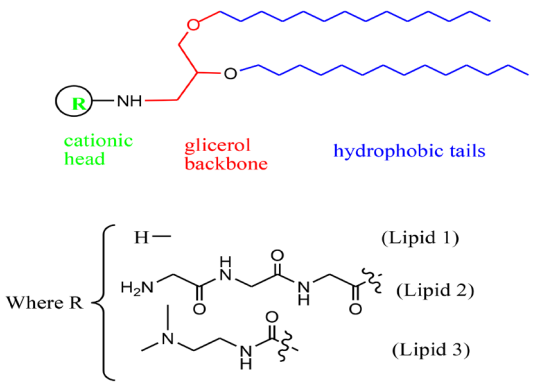

Figure 1. Chemical structures of cationic lipids.
Lipid 1: 2, 3-bis (tetradecyloxy) propan-1-amine
Lipid 2: 2-amino-N-(((((2, 3-bis (tetradecyloxy) propyl) carbamoyl) methyl) carbamoyl) methyl) acetamide
Lipid 3: 1-(2-dimethylaminoethyl)-3-[2,3-di (tetradecoxy) propyl] urea

The synthetic strategy for obtaining our small library of glycerol-based cationic lipids is displayed in scheme S1

(see supplementary part for additional details). The synthesis of the cationic lipid 1 (compound 2) was previously reported by our research group [7]. In order to further functionalize the free amine group of the amino lipid 2 with a triglycine peptide, carboxylic acid activation with 1-Ethyl-3-(3-dimethylaminopropyl)carbodiimide (EDC) and N-Hydroxysuccinimide (NHS) was carried out by using standard activation protocols. Thus, the anticipated Boc-protected-tripeptide-amino lipid 3 was obtained with moderate yields after purifying by flash chromatography (70%). Final Boc-deprotection was efficiently done with acid treatment (10% trifluoroacetic acid) in DCM, which afforded the corresponding free amine in its trifluoroacetate form. Treatment with carbonate polymer support liberated the amine and the expected triglycine-amino lipid derivative 4 (cationic lipid 2) was obtained after resin filtration (87%). Finally, the introduction of the dimethylaminoethyl pendent group was accomplished by activating the amine group from amino lipid 2 with p-nitrophenyl-chloroformate according to well-stablished protocols [15]. Final nucleophilic reaction introduced the corresponding dimethylaminoethyl residue and generated the expected urea derivative 5 (cationic lipid 3) with moderate yield (65%). Since these modifications have not been studied yet, we tentatively chose these three pendant groups in order to be incorporated to the glycerol building block (lipid 1, lipid 2 and lipid 3).

4.3.2. Particle size, PDI, zeta potential and morphology of niosomes

Niosomes based on the three cationic lipids prepared by o/w emulsion and film-hydration techniques were characterized in terms of Z-average (cumulants) size, PDI, zeta potential and morphology (Fig. 2). We observed that zeta potential values were similar in both techniques for the niosome formulations based on lipid 1 (+47 mV) and lipid 3 (+43 and +36 mV for o/w emulsion and film-hydration, respectively) (Fig. 2A lines). On the other hand, for the niosomes prepared with the lipid 2, there was a considerable difference of 20 mV in the zeta potential between the two techniques (+37 and +59 mV for o/w emulsion and film-hydration, respectively) (Fig. 2A, lines). In any case, all niosome formulations exhibited positive zeta values over 30 mV, which enhanced the formation of stable suspensions due to the repulsion among the positively charged particles [25]. Additionally, these positive charges also allowed an easy interaction with the negatively charged cell surfaces to increase cell uptake [26].

Regarding particle size values (Fig. 2A, bars), we did not find remarkable differences between the niosomes when they were elaborated by the o/w emulsion or film-hydration technique. In all cases, the particle size was around 200 nm. As a homogeneity parameter of the suspensions, we determined the polydispersity index (PDI) (Fig. 2B). Lower PDI values (0.19, 0.17 and 0.21 for lipid 1, 2 and 3, respectively) were found in niosomes prepared by

o/w emulsion when they were compared to niosomes prepared by film-hydration technique (0.35, 0.99 and 0.51 for lipid 1, 2 and 3, respectively), which showed that the size distribution of niosomes prepared by the o/w emulsion was narrower than the size distribution obtained by film-hydration technique. Since it has been previously reported that narrow distribution of the PDI values enhances the uptake and posterior internalization process of the nanoparticles [27,28], we decided to discard the niosomes prepared by the film-hydration technique for the following experiments.

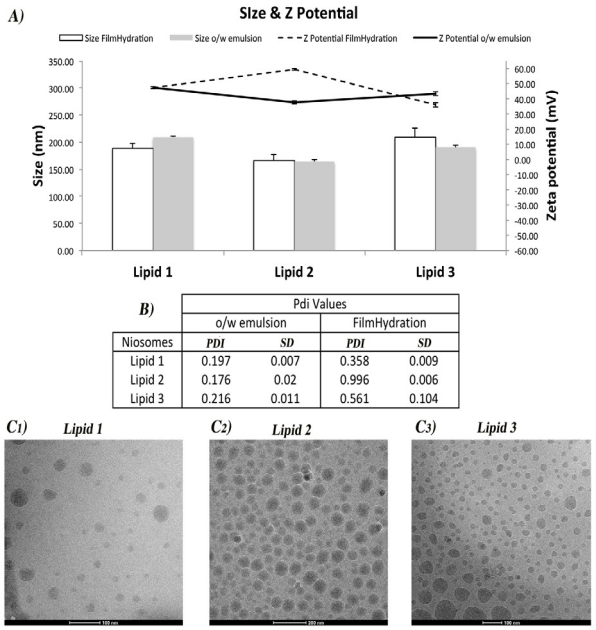

B)	Pdi Values			
	o/w emulsion		FilmHydration	
Niosomes	*PDI*	*SD*	*PDI*	*SD*
Lipid 1	0.197	0.007	0.358	0.009
Lipid 2	0.176	0.02	0.996	0.006
Lipid 3	0.216	0.011	0.561	0.104

Figure 2. Physicochemical characterization of niosomes based on lipid 1, 2 and 3. A) Z-average (cumulants) size (white and gray bars, which correspond to niosomes prepared by film-hydration and o/w emulsion techniques, respectively) and zeta potential values (dotted and continuous lines which correspond to niosomes prepared by film-hydration and o/w emulsion techniques, respectively). B) PDI values. Each value represents the mean ± standard deviation of three measurements. C) Cryo-TEM images of niosomes prepared by the o/w emulsion technique. C1) Niosomes based on lipid 1, C2) niosomes based on lipid 2 and C3) niosomes based on lipid 3. Scale bar for figures C1 and C3=100nm and for figure C2=200nm.

The morphology of niosomes based on the three cationic lipids and elaborated by the o/w emulsion technique was analyzed by Cryo-TEM (Fig. 2 C1, C2 and C3). We observed that all niosomes adopted a spherical and homogeneous morphology. Additionally, the size observed in all niosome formulations by Cryo-TEM (around 100 nm) appeared to be smaller than the sizes reported by dynamic light scattering (around 200 nm, Fig. 2A, bars). Differences in the reported size between DLS and Cryo-TEM techniques could be explained by the treatment of the sample when are processed by both analyses [15].

Based on the data obtained from the physicochemical properties of the niosome formulations, such as size (around 200 nm, Fig. 2A bars), zeta potential (over +37 mV, Fig 2A lines), morphology (spherical and homogeneous, Fig. 2C 1,2,3) and the significant differences in the PDI values (Fig. 2B), we determined that the niosomes prepared by o/w emulsion technique were the most suitable candidates for the following assays.

4.3.3. Physical stability of niosomes

Physical stability of niosomes based on the three cationic lipids prepared by o/w emulsion technique is represented on Fig. 3, as a measure of particle size and zeta potential value over the time at 4 and 25ºC. Regarding zeta potential data, all the niosomes stored at 4ºC did not show relevant changes (Fig. 3 A, B and C lines), especially niosomes based on lipid 2 (+40 mV, Fig. 3B continued line). On the other hand, when formulations were stored at 25ºC, remarkable decreases on the zeta potential values were found on niosomes elaborated with lipid 1 and 3 from +40 to -20 mV (Fig. 3A dot line) and from +43 to +2 mV (Fig. 3C dot line), respectively. This decrease at temperatures around 25ºC can be explained by the re-orientation of crystalline structure of the lipids at high temperatures that is followed by a change on the particle surface, which reduces the zeta potential [29]. The size of the niosomes, as shown in Fig. 3 (gray bars), remained stable for all conditions at 4ºC. However at 25ºC storage temperature, niosomes based on lipid 3 increased their size (250 nm) after 100 days (Fig. 3C, white bars). This increase of the particle size can be caused by gradual diminution of the positive charges of the particles that decreases electrostatic repulsion and generates aggregates [25].

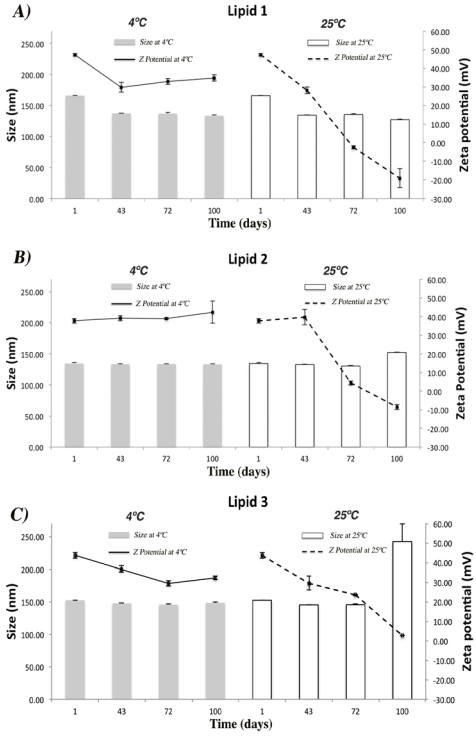

Figure 3. Physical stability of niosomes based on lipid 1 (A), lipid 2 (B) and lipid 3 (C) following storage at 4ºC and 25ºC for 100 days. Gray and white bars correspond to Z-average (cumulants) size obtained at 4ºC and 25ºC, respectively, while continuous and dotted lines correspond to zeta values obtained at 4ºC and 25ºC. Each value represents the mean ± standard deviation (SD) from three independent experiments.

In general, more stable formulations over the time in terms of size and charge were achieved at 4ºC, where the positive superficial charge of niosomes last longer time. At this temperature condition, the high charges avoid the formation of niosome aggregates due to electrostatic repulsion forces. These findings about the zeta potential and size of the niosomes suggest that storage temperature plays an important role in the stability of our niosomes. Moreover, these data also highlighted the participation of the polar head-groups in the physical stability of niosomes, where the implication is more evident in the zeta potential values at 25ºC. Similar results were observed in previous reported data [15].

4.3.4. Characterization of nioplexes in terms of zeta potential and size

Nioplexes formed by the addition of DNA to the niosomes at different cationic lipid/DNA ratios (w/w) were characterized in terms of charge and size (Fig. 4). The results showed a significant decline in zeta potential values (Fig. 4, lines) in the three niosomes formulations when DNA was added at 1/1 cationic lipid/DNA mass ratio (w/w). These changes were observed especially for niosomes based on lipid 2; zeta potential value decreased from +31 mV to -57 mV (Fig. 4B, line). However, we observed a constant increment of the zeta potential values in all nioplexes formulations with the increment of cationic lipid/DNA proportion. The maximum positive zeta potential values were observed at 30/1 cationic lipid/DNA ratio (w/w) (+35 mV, +31 mV and +27 mV for nioplexes based on lipids 1, 2 and 3, respectively). Our data showed a clear correlation between the cationic lipid/DNA ratios and the superficial charge of the nioplexes, as previously reported [15]. Hence, we can establish an appropriate ratio between cationic lipid and DNA (For lipid 1 and 3 at 6/1 ratio and for lipid 2 at 10/1 ratio (w/w)) to reach positive values, so that

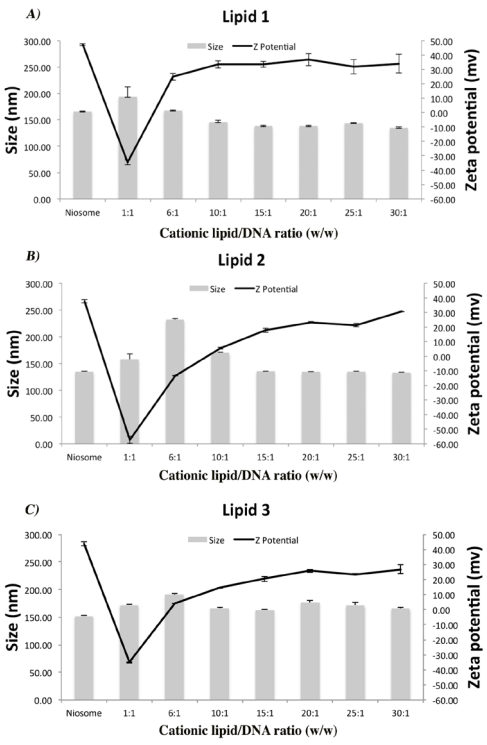

Figure 4. The influence of the cationic lipid/DNA ratio (w/w) on the particle Z-average (cumulants) size (bars) and zeta potential (lines) of nioplexes based on: (A) lipid 1, (B) lipid 2 and (C) lipid 3. Each value represents the mean ± standard deviation of three measurements.

nioplexes can interact easily with negatively charged cell membranes.

Concerning about the size of all nioplexes formed with the three niosome formulations (Fig. 4, bars), they did not show relevant differences at mass ratios from 1/1 to 30/1, except lipid 2 at ratio 6/1 (230 nm). Size of the nioplexes can depend on a fragile balance between the ability of cationic lipids to condense the DNA, which can reduce the particle size, and the space demanded by the lipid [7]. Thus, we can explain the slight variation of the size from the lowest to the highest ratio. In general, most of the nioplexes showed a final size below 200 nm, which is a suitable size to be internalized by the cells [30].

4.3.5. Agarose gel electrophoresis studies of nioplexes

In order to analyze the electrostatic interactions between the niosomes based on the cationic lipids 1, 2 and 3 and the DNA, we performed an agarose gel electrophoresis assay. Moreover, to study the DNA release, we added SDS to the formulations to simulate an ideal gene delivery condition, where all the cargo is released in the media. We also studied the capacity of niosomes to protect DNA against enzymatic digestion. Based on zeta potential and size data, we selected 6/1, 10/1, 20/1 and 30/1 cationic lipid/DNA ratios (w/w) to perform the agarose gel electrophoresis studies since at cationic lipid/DNA ratios below 6/1, the zeta potential values were negative. The agarose gel electrophoresis assays are shown in Fig. 5, where SC bands show the most bioactive DNA form and OC bands represent structural change of DNA of a less active form [31]. Nioplexes were analyzed in terms of condensation, release and protection of DNA.

First, regarding nioplexes based on cationic lipid 1 (Fig. 5A), the results showed deficient condensation of DNA (lanes 4, 7, 10 and 13), as SC bands were shown in the agarose gel. Moreover, DNA was easily released from the niosomes at mass ratios 6/1 and 10/1 (lanes 5 and 8) upon the addition of the tensoactive agent SDS, as a possible consequence of poor condensation. We also found that at mass ratios 20/1 and 30/1 there was a weak release of DNA, as white lines were observed at the top of the wells (lanes 11 and 14). This effect was probably due to high zeta potential values (around + 32mV) obtained at those ratios. In addition, protection of DNA can be observed at all mass ratios. The SC bands in lanes 6, 9, 12 and 15 showed that nioplexes protected the DNA from enzymatic digestion.

Second, regarding nioplexes based on the cationic lipid 2 (Fig. 5B), all ratios were able to condensate the DNA (lanes 4, 7, 10 and 13). The presence of several amino groups in this lipid may be the cause of this level of condensation. On the other hand, the release of DNA at all mass ratios was difficult (lanes 5, 8, 11 and 14), even at lower ratios. Concerning about DNA protection from DNase, we observed reasonable protection at all ratios. Intense OC bands can be observed especially at ratios 6/1, 10/1 and 20/1, which correspond to lanes

6, 9 and 12, as consequence of conformational change of DNA to open circular form due to DNase intervention.

Finally, nioplexes based on the cationic lipid 3 (Fig. 5C) indicated that high DNA condensation was only observed with nioplexes at 30/1 cationic lipid/DNA ratio (w/w) (lane 13), probably due to the high zeta potential values obtained at this ratio (+27 mV). Moreover, niosomes based on cationic lipid 3 were able to release the DNA especially at low ratios (6/1, lane 5 and 10/1, lane 8). Concerning about protection against enzymatic digestion, nioplexes showed that DNA was properly protected in all cases (lanes 6, 9, 12 and 15).

To summarize, data obtained from agarose gel electrophoresis studies, suggested that nioplexes based on the three cationic lipids, at low ratios (6/1) were less efficient to condensate, release and protect the DNA against enzymatic digestion. Thus, these outcomes indicated that nioplexes based on lipid 1, 2 and 3 at ratios (w/w) 10/1, 20/1 and 30/1 were more suitable to succeed in the transfection experiments.

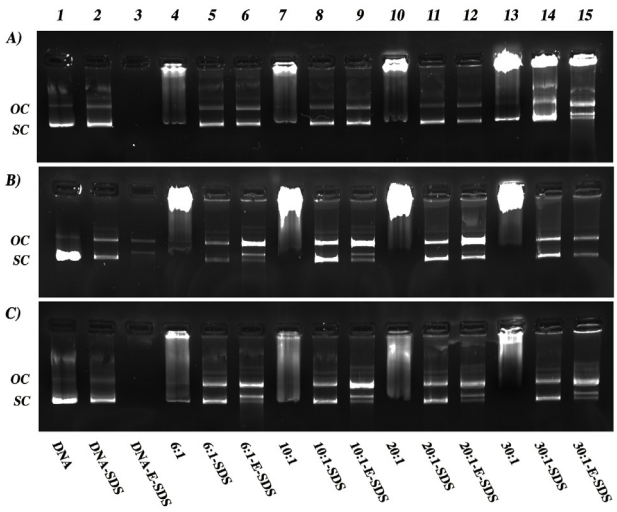

Figure 5. Binding, protection, and SDS-induced release of DNA from nioplexes at different lipid/DNA (w/w) ratios visualized by agarose electrophoresis. OC: open circular form, SC: supercoiled form. Lanes 1-3 correspond to free DNA; lanes 4-6, cationic lipid/DNA ratio 6/1; lanes 7-9, cationic lipid/DNA ratio 10/1; lanes 10-12, cationic lipid/DNA ratio 20/1; lanes 13-15, cationic lipid/DNA ratio 30/1. Nioplexes were treated with SDS (lanes 2,5,8,11 and 14) and DNase I + SDS (lanes 3,6,9,12 and 15). A) Nioplexes based on lipid 1, B) nioplexes based on lipid 2 and C) nioplexes based on lipid 3.

4.3.6. *In vitro* transfection experiments in HEK-293, ARPE-19 and PECC cells

We carried out further *in vitro* assays to analyze transfection efficiencies and toxicity of nioplexes in the following cells: HEK-293 cells, as general cell model, ARPE-19 cells, as

retinal cell model for possible *in vivo* applications in retina, and PECC cells, as neurons and glial model cells for the potential use of nioplexes in the brain (Fig. 6A).

The data obtained from the nioplexes based on the cationic lipid 1 showed that the highest percentage of transfection efficiencies were obtained in HEK-293 cells (around 21%) (Fig. 6A white bars) at mass ratios 20/1 and 30/1. Additionally, suitable transfection results were also observed for ARPE-19 cells, where the highest transfection values were around 18% at 20/1 mass ratio (Fig. 6A gray bars). It must be highlighted that previous work carried out with serinol-based cationic lipids modified with the same lipid tail showed null transfection efficiency in cell culture [15]. These findings suggest that small structural changes in the lipid (serinol by glycerol building block) are enough to influence dramatically on transfections efficiencies. On the other hand, transfection in PECC cells were around 3% for all mass ratios, which was the lowest percent observed within the three types of cells (Fig. 6A black bars). For nioplexes based on lipid 2, high percentage of transfected cells were observed again (13%) in HEK-293 cells at ratio 20/1 (w/w) (Fig. 6A white bars). However, low transfection efficiencies were registered in ARPE-19 and PECC cells at all cationic lipid/DNA mass ratios (Fig. 6A grey and black bars, respectively). Similar results also were observed in previous data reported [15] where the cationic lipid formed by longer polyamine chains and more amino nitrogen atoms did not precisely enhanced cell transfection in HEK-293 and ARPE-19 cells. These outcomes are probably due to self-folded conformation that disfavor effective interaction with DNA. It also must be emphasized that presence of more than one carbonyl group in the polar head-group seems to be also an impediment for efficient cell transfections [32,33]. Regarding nioplexes based on lipid 3, transfections around 20 % were obtained in HEK-293 cells at 30/1 mass ratio and lower transfections at 10/1 mass ratio (Fig. 6A white bars). Percentage of transfected cell levels in ARPE-19 cells also showed promising results (19%) at 30/1 mass ratio; similar to the data observed in HEK-293 cells. However, decrease in transfection efficiencies was observed at lower mass ratios (Fig. 6A gray bars). Furthermore, interesting data were obtained in PECC cells, especially at 30/1 mass ratio, where transfection was around 5% (Fig. 6A black bars). For further details regarding confocal microscopy images from transfected cerebral cortical cells, see Supplementary Data, Fig. S1. Cultured neurons are among the most difficult cells to be transfected due to their sensitivity to micro-environmental changes and they tend to die soon after transfection. Typical transfection efficiencies in this kind of cells are around 5% [34]. Interestingly, relevant transfection data in HEK-293, ARPE-19 and MSC-D1 cells were also observed with a similar cationic lipid that has the same molecular formula, but different structural conformation [15]. In addition, this structural relationship between lipids and transfection has been previously reported by different authors [32,33,35], which have

described that slight lipid structure modifications can provoke cell transfection variations.

Cell toxicity is another important issue that has to be addressed for the development of any novel drug delivery system including any desired cationic lipid for its use as non-viral vector. Therefore, we studied the cell viability with our formulations (Fig. 6B). The results indicated that only HEK-293 cells showed high viabilities with nioplexes prepared with lipid 1 (84%, 76% and 70% at 10/1, 20/1 and 30/1 mass ratios, respectively). On the other hand, the most toxic effect was observed with the lipid 2 (31% of viability) at 30/1 mass ratio (Fig. 6B white bars). Better toleration in ARPE-19 and PECC cells (Fig. 6B gray and black bars, respectively) was found with nioplexes at all studied ratios (100 % of viability) (Fig. 6B gray and black bars). It must be stressed that toxicity effect is, generally, a cell dependent process where every cell type shows different toleration levels [36]. Furthermore, the structure design of the cationic lipids also influences on the cell viability, such as small changes on the polar head-groups that can induce different levels of cytotoxicity [15,37]. It is worth mentioning that cationic lipids containing one or three hydrocarbonated alkyl chains tend to be more toxic and show poor transfection efficiencies [11].

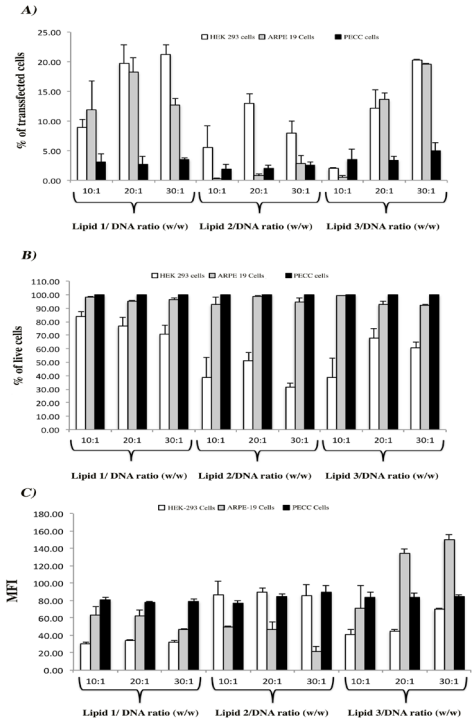

Figure 6. *In vitro* transfection experiments of nioplexes based on cationic lipid 1, 2 and 3 in HEK-293, ARPE-19 and PECC cells. A) Transfection efficiency at different cationic lipid/DNA ratios (w/w). B) Cell viability at different cationic lipid/DNA ratios (w/w). C) MFI of transfected cells with nioplexes based on cationic lipid 1, 2 and 3 in HEK-293, ARPE-19 and PECC cells at different cationic lipid/DNA ratios (w/w).

In order to describe more precisely the transfection efficiencies of our formulations, we analyzed the MFI of the EGFP expressed in the transfected cells. Results obtained from the nioplexes based on cationic lipid 1 showed that low MFI were observed in HEK-293 cells (around 30, Fig. 6C white bars) at all tested mass ratios. On the other hand, ARPE-19 and PECC cells showed higher MFI (over 40 and 80, respectively); high MFI in PECC cells were obtained at the three studied mass ratios (10/1, 20/1 and 30/1) (Fig. 6C black bars). Based on the data from nioplexes prepared with the cationic lipid 2, MFI in HEK-293 cells were

around 89 at the different analyzed mass ratios (10/1, 20/1 and 30/1, Fig. 6C white bars). Additionally, expression of EGFP was similar in PECC cells at all analyzed mass ratio (10/1, 20/1 and 30/1, Fig. 6C black bars). MFI results from nioplexes prepared with lipid 3 revealed that HEK-293 cells showed low EGFP expression (MFI around 60) when compared to ARPE-19 and PECC cells. Furthermore, ARPE-19 cells showed the highest MFI (149) at 30/1 mass ratio (Fig. 6C grey bars). The MFI obtained from PECC cells was around 80, which is similar to those observed with the other two cationic lipids (Fig. 6C black bars). Essentially, these results indicated that nioplexes based on cationic lipid 3 stimulated higher EGFP expression in ARPE-19 transfected cells and suitable expression of EGFP in PECC and HEK-293 transfected cells at 30/1 mass ratio. Likewise, differences in membrane composition among cell lines can also influence cellular uptake and posterior intracellular trafficking processes of vectors [38]. For further MFI information, see histograms in Supplementary Data Fig. S2.
Taking into account these data (Fig. 6), nioplexes based on cationic lipid 1 and 3 showed better percentages of transfection in ARPE-19 and PECC cells. These results also indicate that polar head-groups of the cationic lipids play a fundamental role in transfection efficiencies. In addition, cell toxicity assay showed a cell dependent toxicity effect rather than a polar head-group effect, where major toxicity effect was observed in HEK-293 cells. For MFI assay, the most relevant data were obtained from cationic lipid 3, which in general expressed high levels of EGFP in cells. Thus, we decided to use niosomes based on lipid 3 as the most appropriate system for further *in vivo* experiments.

Differences observed among the three cationic lipids on transfection efficiency could be explained, in part, by slight changes on their particle size and superficial charge that affect to their capacity to condense, protect and release the DNA against enzymatic digestion. Additionally, other physicochemical parameters related with the chemical structure of the polar-head group such as the balance between the cross-sectional area of the polar-head group (small end) and the hydrophobic domain (large end), or the pKa value should also be considered. The greater the imbalance between both the polar-head group and the hydrophobic domain, the more unstable the resulting lipid assembly and therefore, the greater the probability to undergo fusion with anionic vesicles [37]. Consequently, this hypothesis could explain the low percentages of transfected cells observed in nioplexes prepared with lipid 2. Regarding the pKa value, it has been suggested an optimal value slightly inferior to 7 in order to maintain a neutral surface charge density at pH 7.4 [39]. Previous results by our group have shown that dimethylaminoethyl pendent group provides pKa values that could fall in the optimal range for transfection (from 6.2 to 6.7) [15]. Consequently, cationic lipid 3 positive charge density should increase in the acidic environment of the endosome leading to a membrane-destabilizing process by forming ion pairs between the lipid 3 and phospholipids

in the endosomal membrane. This process might promote a lamellar to hexagonal transition in the lipid 3 which might disrupt the membrane and destabilize bilayers. Additionally, the presence of squalene in our formulation would facilitate this kind of transition [7]. The combination of these two effects would make this transfection process more efficient.

4.3.7. *In vivo* studies

We carried out *in vivo* studies to evaluate EGFP expression in the rat retina after both subretinal (Fig. 7) and intravitreal (Fig. 8) injections. Both administration routes are clinically viable options to deliver genetic material to the retina [40]. While classically, the effect of subretinal injection is localized around the injection site, intravitreal injections can carry the delivered material to a larger retinal surface [41]. In our results, subretinal injection of nioplexes based on cationic lipid 3 at 30/1 mass ratio resulted in substantial protein expression mainly observed in photoreceptors and in some nuclei in the outer nuclear layer (Fig. 7). Transfection at this level could be of great interest, since most of the inherited retinal diseases such as Stargat Disease, Retinitis Pigmentosa, Age-related Macular Degeneration or Leber Congenital Amaurosis are classically associated to mutations in genes expressed in photoreceptors and outer nuclear layers of the retina [17]. Therefore, subretinal administration of nioplexes based on cationic lipid 3 could be appropriate to treat aforementioned retinal inherited diseases. However, subretinal administration is frequently associated with high risk of retinal detachment or severe lesions in the retina, which often dissuade its clinical application. In any case, some promising results have been obtained in clinical trials after subretinal injection to treat many inherited retinal diseases such as Leber Congenital Amaurosis Type 2 [42].

By contrast, intravitreal injection is a safer technique in ophthalmology and

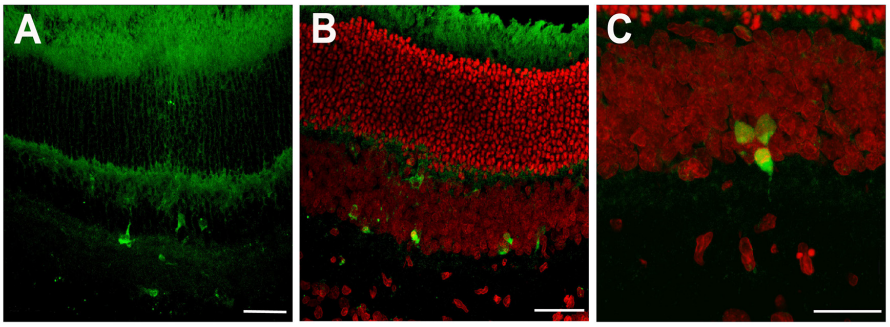

Figure 7. EGFP gene expression in retina 3 days after subretinal injection of nioplexes based on lipid 3 at mass ratio 30/1 cationic lipid/DNA. A), B) Retinal sections showing EGFP expression mainly in photoreceptors and in some nuclei in the outer nuclear layer (ONL). C) Detail of three EGFP+ cell nuclei located in the ONL. Cell nuclei were counterstained with Hoechst 33342 (red color) in B and C. Scale bars A, B= 40 μm; C= 25 μm.

is more widely used in the clinical practice. We found a good and uniformly distributed EGFP expression mainly in the ganglion cell layer and inner layers of the retina 3 days after intravitreal injection of nioplexes based on cationic lipid 3 at 30/1 mass ratio (Fig. 8), which suggests that nioplexes did not aggregate with the negatively charged components of the vitreous humor such as glycosamineglycanes and diffused through the inner layer of the retina, enhanced probably, by the ability of the PEG chains of the polysorbate 80 structure to prevent aggregations due to interaction with fibrilar structures in the vitreous [43,44]. Transfection at the inner layers of the retina could be of great interest to treat some genetic pathologies of the retina such us glaucoma [45] a progressive optic neuropathy that affect to retinal ganglion cells. Interestingly, we detected some protein expression in the retinal pigmented epithelium (Fig. 8E), which clearly represents a great challenge for retinal gene therapy in order to avoid subretinal injection to target the outer segments of the photoreceptors and the pigmented epithelium cells without causing harm to the sensitive neural tissue [2].

Additionally, we decided to evaluate the capacity of nioplexes based on lipid 3 at 30/1 ratio to transfect the rat cerebral cortex (Fig. 9). We identified by immunochemistry

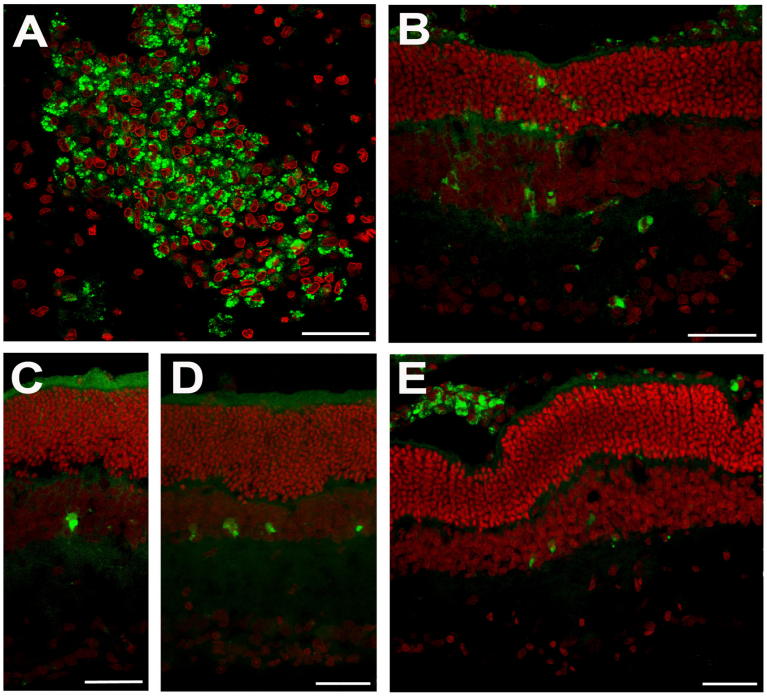

Figure 8. EGFP gene expression in retina 3 days after intravitreal injection of nioplexes based on lipid 3 at mass ratio 30/1 cationic lipid/DNA. A) Wholemount preparation showing EGFP+ cell bodies located in the ganglion cell layer (GCL). B), C), D) and E) Retinal cross sections. EGFP expression was detected throughout the whole retina although mainly in inner layers. Cell nuclei were counterstained with Hoechst 33342 (red color). Scale bar = 40μm.

analysis NeuN+ (red channel), NeuN- cells and GFP+ (green channel). The NeuN+ corresponded to neurons, NeuN- to non-neuronal cells, such as glial and endothelia population cells and GFP+ corresponded to cells expressing EGFP. Based on the analysis, we were able to identify neurons and non-neuronal cells that expressed EGFP in the area next to the injection site. Thus, on the one hand, Fig. 9A shows NeuN+ cells that corresponded to neurons expressing high levels of GFP in the cells bodies and in their dendritic trees (white arrows). On the other hand, Fig. 9B shows NeuN- cells with glial morphology that expressed high levels of GFP throughout the dendritic processes (yellow arrows). Briefly, it seems that there is a cell dependent effect for the nioplexes internalization and transfection process. Favorably, nioplexe injections did not affect the behavior of the animals and no loss of weight was detected during the 3 days of the experimental period. Even though delivering genetic material to the nervous system cells by non-viral vectors remains as a challenge, our nioplexes were able to transfect glial cells and identified neurons in the primary visual cortex *in vivo*. In this preliminary study, we determined that our nioplexes were able to transfect more glial cells than neurons. These results suggest that cell division of glial cells and the CMV promoter of pCMS-EGFP plasmid could be involved in the transfection process [46]. Therefore, the use of our nioplexes combined with plasmids holding different promoters might allow targeting different cell populations of the nervous system and enhance cell transfection in order to treat different genetic population deficits. Overall, our results open a safe alternative to the treatment of neurodegenerative diseases, such as Parkinson's disease. Despite the current advances to treat these types of diseases, neurodegenerative diseases still do not have effective pharmacotherapy treatments. Therefore, further research is required before these findings can reach the clinic.

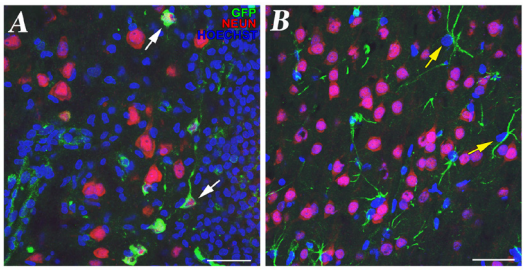

Figure 9. *In vivo* gene expression of EGFP 3 days after the administration of nioplexes based on lipid 3 at 30/1 mass ratio cationic lipid/DNA. A and B panels show triple labeling; nuclei are shown in blue (Hoechst), neurons in red (NeuN+), and EGFP expressed in cells (GFP+) in green. A) Several of the identified neurons (red) that express EGFP (green) in the membrane at their cell bodies and dendritic trees are indicated by white arrows. B) Several of the non-neuron cells (NeuN-) with glia morphology that express EGFP (green) through their processes are indicated by yellow arrows. Scale bar = 40µm.

4.4. CONCLUSION

In the present study, we designed niosomes prepared from squalene, as helper lipid, polysorbate 80, as non-ionic surfactant and three synthetized cationic lipids, which differed only in the polar head-group, to evaluate their transfection efficiency in retina and brain. Our results showed that the chemical composition of the cationic lipid head-groups clearly affects the physicochemical parameters of the niosomes and modifies the levels of transfection efficiencies of the nioplexes. We observed that niosomes based on cationic lipids with a dimethyl amino (lipid 3) and amino (lipid 1) head-groups showed remarkable percentages of transfection capacity when they were compared to their counterpart triglycine head-group (lipid 2). Regarding MFI, nioplexes based on the cationic lipid 3 showed higher protein expression in the transfected cells when they were compared to lipid 1. Moreover, *in vitro* results at different cationic lipid/DNA ratios (w/w) suggested that not only structural changes in the polar head-groups of these cationic lipids were involved in the success of these vectors, but also cationic lipid/DNA ratios were deeply involved in the interaction with the cells and their transfection efficiencies. *In vivo* results showed that after subretinal, intravitreal and brain injections, nioplexes transfected successfully the cells in rat retina and brain. Although this preliminary study highlights the flattering properties of nioplexes based on lipid 3 to deliver genetic material to the retina and brain, additional work, such as the long term evaluation of the transgene expression should also be investigated in order to translate preclinical results in animals to clinical trials.

4.5. ACKNOWLEDGMENTS

This project was partially supported by the University of the Basque Country UPV/EHU (UFI 11/32), the National Council of Science and Technology (CONACYT), Mexico, Reg. # 217101, the Spanish Ministry of Education (Grant CTQ2010-20541, CTQ2010-14897), the Basque Government (Department of Education, University and Research, predoctoral BFI-2011-2226 grant) and by Spanish grants MAT2012-39290-C02-01 and IPT-2012-0574-300000. Technical and human support provided by SGIker (UPV/EHU) is gratefully acknowledged. Authors also wish to thank the intellectual and technical assistance from the ICTS "NANBIOSIS", more specifically by the Drug Formulation Unit (U10) of the CIBER in Bioengineering, Biomaterials & Nanomedicine (CIBER-BBN) at the University of Basque Country (UPV/EHU).

4.6. REFERENCES

1. Yin H, Kanasty RL, Eltoukhy AA, Vegas AJ, Dorkin JR, Anderson DG. Non-viral vectors for gene-based therapy. Nat Rev Genet 2014;15:541-555.

2. Charbel Issa P, MacLaren RE. Non-viral retinal gene therapy: a review. Clin Experiment Ophthalmol 2012;40:39-47.

3. Agirre M, Zarate J, Ojeda E, Puras G, Rojas LA, Alemany R, et al. Delivery of an adenovirus vector plasmid by ultrapure oligochitosan based polyplexes. Int J Pharm 2015;479:312-319.

4. Zarbin MA, Montemagno C, Leary JF, Ritch R. Nanomedicine for the treatment of retinal and optic nerve diseases. Curr Opin Pharmacol 2013;13:134-148.

5. Arukuusk P, Parnaste L, Hallbrink M, Langel U. PepFects and NickFects for the Intracellular Delivery of Nucleic Acids. Methods Mol Biol 2015;1324:303-315.

6. Rajera R, Nagpal K, Singh SK, Mishra DN. Niosomes: a controlled and novel drug delivery system. Biol Pharm Bull 2011;34:945-953.

7. Puras G, Mashal M, Zarate J, Agirre M, Ojeda E, Grijalvo S, et al. A novel cationic niosome formulation for gene delivery to the retina. J Control Release 2014;174:27-36.

8. Couvreur P. "Squalenoylation": a new approach to the design of anticancer and antiviral nanomedicines. Bull Acad Natl Med 2009;193:663-73; discussion 673-4.

9. Chung H, Kim TW, Kwon M, Kwon IC, Jeong SY. Oil components modulate physical characteristics and function of the natural oil emulsions as drug or gene delivery system. J Controlled Release 2001;71:339-350.

10. Liu F, Yang J, Huang L, Liu D. New cationic lipid formulations for gene transfer. Pharm Res 1996;13:1856-1860.

11. Byk G, Dubertret C, Escriou V, Frederic M, Jaslin G, Rangara R, et al. Synthesis, activity, and structure--activity relationship studies of novel cationic lipids for DNA transfer. J Med Chem 1998;41:229-235.

12. Mahidhar YV, Rajesh M, Chaudhuri A. Spacer-arm modulated gene delivery efficacy of novel cationic glycolipids: design, synthesis, and *in vitro* transfection biology. J Med Chem 2004;47:3938-3948.

13. Karmali PP, Chaudhuri A. Cationic liposomes as non-viral carriers of gene medicines: resolved issues, open questions, and future promises. Med Res Rev 2007;27:696-722.

14. Zhi D, Zhang S, Wang B, Zhao Y, Yang B, Yu S. Transfection efficiency of cationic lipids with different hydrophobic domains in gene delivery. Bioconjug Chem 2010;21:563-577.

15. Ojeda E, Puras G, Agirre M, Zarate J, Grijalvo S, Pons R, et al. Niosomes based on synthetic cationic lipids for gene delivery: the influence of polar head-groups on the transfection efficiency in HEK-293, ARPE-19 and MSC-D1 cells. Org Biomol Chem 2015;13:1068-1081.

16. Bloquel C, Bourges JL, Touchard E, Berdugo M, BenEzra D, Behar-Cohen F. Non-viral ocular gene therapy: potential ocular therapeutic avenues. Adv Drug Deliv Rev 2006;58:1224-1242.

17. Lipinski DM, Thake M, MacLaren RE. Clinical applications of retinal gene therapy. Prog Retin Eye Res 2013;32:22-47.

18. Nagabhushan Kalburgi S, Khan NN, Gray SJ. Recent gene therapy advancements for neurological diseases. Discov Med 2013;15:111-119.

19. Worgall S, Sondhi D, Hackett NR, Kosofsky B, Kekatpure MV, Neyzi N, et al. Treatment of late infantile neuronal ceroid lipofuscinosis by CNS administration of a serotype 2 adeno-associated virus expressing CLN2 cDNA. Hum Gene Ther 2008;19:463-474.

20. Leone P, Shera D, McPhee SW, Francis JS, Kolodny EH, Bilaniuk LT, et al. Long-term follow-up after gene therapy for canavan disease. Sci Transl Med 2012;4:165ra163.

21. Muramatsu S. The current status of gene therapy for Parkinson's disease. Ann Neurosci 2010;17:92-95.

22. Soto-Sanchez C, Martinez-Navarrete G, Humphreys L, Puras G, Zarate J, Pedraz JL, et al. Enduring high-efficiency *in vivo* transfection of neurons with non-viral magnetoparticles in the rat visual cortex for optogenetic applications. Nanomedicine 2015;11:835-843.

23. Puras G, Zarate J, Aceves M, Murua A, Diaz AR, Aviles-Triguero M, et al. Low molecular weight oligochitosans

for non-viral retinal gene therapy. Eur J Pharm Biopharm 2012.
24. Jayaraman M, Ansell SM, Mui BL, Tam YK, Chen J, Du X, et al. Maximizing the potency of siRNA lipid nanoparticles for hepatic gene silencing *in vivo*. Angew Chem Int Ed Engl 2012;51:8529-8533.
25. Caracciolo G, Amenitsch H. Cationic liposome/DNA complexes: from structure to interactions with cellular membranes. Eur Biophys J 2012;41:815-829.
26. Rezvani Amin Z, Rahimizadeh M, Eshghi H, Dehshahri A, Ramezani M. The effect of cationic charge density change on transfection efficiency of polyethylenimine. Iran J Basic Med Sci 2013;16:150-156.
27. Caracciolo G, Caminiti R, Digman MA, Gratton E, Sanchez S. Efficient escape from endosomes determines the superior efficiency of multicomponent lipoplexes. J Phys Chem B 2009;113:4995-4997.
28. Gratton SE, Ropp PA, Pohlhaus PD, Luft JC, Madden VJ, Napier ME, et al. The effect of particle design on cellular internalization pathways. Proc Natl Acad Sci U S A 2008;105:11613-11618.
29. Heurtault B, Saulnier P, Pech B, Proust JE, Benoit JP. Physico-chemical stability of colloidal lipid particles. Biomaterials 2003;24:4283-4300.
30. Rejman J, Oberle V, Zuhorn IS, Hoekstra D. Size-dependent internalization of particles via the pathways of clathrin- and caveolae-mediated endocytosis. Biochem J 2004;377:159-169.
31. Stellwagen NC, Stellwagen E. Effect of the matrix on DNA electrophoretic mobility. J Chromatogr A 2009;1216:1917-1929.
32. Takeuchi K, Ishihara M, Kawaura C, Noji M, Furuno T, Nakanishi M. Effect of zeta potential of cationic liposomes containing cationic cholesterol derivatives on gene transfection. FEBS Lett 1996;397:207-209.
33. Fujiwara T, Hasegawa S, Hirashima N, Nakanishi M, Ohwada T. Gene transfection activities of amphiphilic steroid–polyamine conjugates. Biochimica et Biophysica Acta (BBA) - Biomembranes 2000;1468:396-402.
34. Karra D, Dahm R. Transfection Techniques for Neuronal Cells. The Journal of Neuroscience 2010;30:6171-6177.
35. Paecharoenchai O, Niyomtham N, Apirakaramwong A, Ngawhirunpat T, Rojanarata T, Yingyongnarongkul BE, et al. Structure relationship of cationic lipids on gene transfection mediated by cationic liposomes. AAPS PharmSciTech 2012;13:1302-1308.
36. Sohaebuddin SK, Thevenot PT, Baker D, Eaton JW, Tang L. Nanomaterial cytotoxicity is composition, size, and cell type dependent. Part Fibre Toxicol 2010;7:22-8977-7-22.
37. Martin B, Sainlos M, Aissaoui A, Oudrhiri N, Hauchecorne M, Vigneron JP, et al. The design of cationic lipids for gene delivery. Curr Pharm Des 2005;11:375-394.
38. Pozzi D, Marchini C, Cardarelli F, Salomone F, Coppola S, Montani M, et al. Mechanistic evaluation of the transfection barriers involved in lipid-mediated gene delivery: interplay between nanostructure and composition. Biochim Biophys Acta 2014;1838:957-967.
39. Semple SC, Akinc A, Chen J, Sandhu AP, Mui BL, Cho CK, et al. Rational design of cationic lipids for siRNA delivery. Nat Biotechnol 2010;28:172-176.
40. Conley SM, Naash MI. Nanoparticles for retinal gene therapy. Prog Retin Eye Res 2010;29:376-397.
41. Dureau P, Legat L, Neuner-Jehle M, Bonnel S, Pecqueur S, Abitbol M, et al. Quantitative analysis of subretinal injections in the rat. Graefes Arch Clin Exp Ophthalmol 2000;238:608-614.
42. Bennett J, Ashtari M, Wellman J, Marshall KA, Cyckowski LL, Chung DC, et al. AAV2 gene therapy readministration in three adults with congenital blindness. Sci Transl Med 2012;4:120ra15.
43. Ochoa GP, Sesma JZ, Diez MA, Diaz-Tahoces A, Aviles-Trigeros M, Grijalvo S, et al. A novel formulation based on 2,3-di(tetradecyloxy)propan-1-amine cationic lipid combined with polysorbate 80 for efficient gene delivery to the retina. Pharm Res 2014;31:1665-1675.
44. Peeters L, Sanders NN, Braeckmans K, Boussery K, Van de Voorde J, De Smedt SC, et al. Vitreous: a barrier to nonviral ocular gene therapy. Invest Ophthalmol Vis Sci 2005;46:3553-3561.
45. Liu X, Rasmussen CA, Gabelt BT, Brandt CR, Kaufman PL. Gene therapy targeting glaucoma: where are we? Surv Ophthalmol 2009;54:472-486.
46. Kugler S, Kilic E, Bahr M. Human synapsin 1 gene promoter confers highly neuron-specific long-term

transgene expression from an adenoviral vector in the adult rat brain depending on the transduced area. Gene Ther 2003;10:337-347.

5

The role of helper lipids in the intracellular disposition and transfection efficiency of niosome formulations for gene delivery to retinal pigment epithelial cells

The role of helper lipids in the intracellular disposition and transfection efficiency of niosome formulations for gene delivery to retinal pigment epithelial cells

Edilberto Ojeda[1,2]; Gustavo Puras[1,2]; Mireia Agirre[1,2]; Jon Zarate[1,2]; Santiago Grijalvo[2,3]; Ramon Eritja[2,3]; Luca DiGiacomo[4]; Giulio Caracciolo[4]; and Jose-Luis Pedraz[1,2]

[1] NanoBioCel Group, University of Basque Country (UPV/EHU), Vitoria-Gasteiz, Spain.

[2] Biomedical Research Networking Center in Bioengineering, Biomaterials and Nanomedicine (CIBER-BBN), Vitoria-Gasteiz, Spain

[3] Institute of Advanced Chemistry of Catalonia, IQAC-CSIC, Barcelona, Spain.

[4] Department of Molecular Medicine, "Sapienza" University of Rome, Viale Regina Elena, 324, 00161 Rome, Italy

International Journal of Pharmaceutics. 2016; 503: 115-126

ABSTRACT

In this work, we carried out a comparative study of four different niosome formulations based on the same cationic lipid and non-ionic tensoactive. The niosomes prepared by oil-in-water emulsion technique (o/w) only differed in the helper lipid composition: squalene, cholesterol, squalane or no helper lipid. Niosomes and nioplexes elaborated upon the addition of pCMS-EGFP reporter plasmid were characterized in terms of size, zeta potential and polydispersity index. The capacity of the niosomes to condense, release and protect the DNA against enzymatic degradation was evaluated by agarose gel electrophoresis. In vitro experiments were carried out to evaluate transfection efficiency and cell viability in retinal pigment epithelial cells. Moreover, uptake and intracellular trafficking studies were performed to further understand the role of the helper lipids in the transfection process. Interestingly, among all tested formulations, niosomes elaborated with squalene as helper lipid were the most efficient transfecting cells. Such transfection efficiency could be attributed to their higher cellular uptake and the particular entry pathways used, where macropinocytosis pathway and lysosomal release played an important role. Therefore, these results suggest that helper lipid composition is a crucial step to be considered in the design of niosome formulation for retinal gene delivery applications since clearly modulates the cellular uptake, internalization mechanism and consequently, the final transfection efficiency.

Keywords: Niosomes, non-viral vector, cationic lipid, transfection, helper lipid, intracellular trafficking

5.1. INTRODUCTION

Gene therapy represents a promising approach that aims to address the disease from the molecular point of view. This type of therapy is based on modified or normal functioning gene copies that are delivered into the cell nucleus to produce bioactive agents [1]. The delivery of naked DNA is an inefficient process due to the negatively charged nature of nucleic acids that difficult the passage through cell membrane and the presence of enzymes that can digest the naked DNA. Therefore, it is necessary the use of capable vectors to deliver efficiently the DNA inside the cells, such as non-viral vectors that are mainly based on cationic polymers and lipids. Compared to viral vectors, non-viral vectors show a reduced persistence of transfection and low transfection efficiencies in cells. On the other hand, non-viral vectors are cheaper, easy to elaborate, and the size of DNA inserted is hypothetically limitless. Moreover, they do not exhibit antigen-specific immune and inflammatory response [2]. Consequently, non-viral vectors have captured the attention of the research community in the last 20 years.

Niosomes are drug carrier systems similar to liposomes with a bilayer structure, where the phospholipids of the liposomes have been substituted by non-ionic surfactants. Compared to liposomes, niosomes show some significant advantages, such as low cost and high chemical and storage stabilities. Even though the application of niosomes in gene therapy has been poorly studied, some optimistic results have been recently reported in the literature that highlights the satisfactory properties of niosomes for gene delivery purposes [3,4].

Niosomes as gene delivery vectors are commonly based on non-ionic surfactants, cationic lipids and helper lipids. Over the years, several researchers have studied these components and their effect on the niosome formulations. Such studies have shown that non-ionic surfactants make niosome formulations stable, and prevent the formation of aggregates of the particles [5-7]. Cationic lipids handle the interaction with the negatively charged DNA and its condensation to form nioplexes by electrostatic interactions [8]. Additionally, it has been observed that cationic lipid chemical structures influence on the niosomes charge, toxicity, biodegradability, and transfection efficiencies [3,9,10]. Regarding helper lipids, it has been described that they are responsible for enhancing the physicochemical properties of the emulsion and the improvement of gene delivery [11,12]. However, the mechanisms that involve these improvements in cationic niosome formulations for gene delivery applications have not been completely understood, and more detailed studies are required.

The final impact on gene expression, among many other factors, clearly depends on the cell to be transfected and on the capacity of the vector to enter the cell and the posterior pathway employed to deliver its cargo into the nucleus [13]. Different endocytic

routes can mediate the cellular uptake and the final cargo delivery. Among these endocytic routes clathrin-mediated endocytosis (CME), caveolae-mediated endocytosis (CvME) and macropinocytosis are among the most studied [14-16]. Additionally to the uptake pathways, the particle transport mechanisms can determine the final intracellular fate of the vector, e.g., lysosomal degradation [17]. Such pathways have their particular characteristics and their intervention in the cellular uptake and further internal processing will depend on many factors related with the gene delivery vector such as the size, surface charge, morphology and composition [14,18,19]. Therefore, it is necessary to analyze and understand all these factors to develop more efficient non-viral vectors for gene delivery applications.

Thus, we carried out a comparative study of four different niosome formulations based on the same cationic lipid and non-ionic surfactant, but different helper lipid, to determine its role in the niosome formulations and the transfection process mediated by nioplexes upon the addition of pCMS-EGFP reporter plasmid. The niosome formulations only differed in the helper lipid: Squalene (Sque), cholesterol (Cho), squalane (Squa) or none helper lipid (None). Niosomes prepared by oil-in-water emulsion technique (o/w), and nioplexes were characterized in terms of size, zeta potential and polydispersity index. The capacity of the niosomes to condense, release and protect the DNA against enzymatic degradation was evaluated by agarose gel electrophoresis. In vitro experiments were performed in retinal pigment epithelial cells (ARPE-19) cells by flow cytometry to assess the transfection efficiency of nioplexes and cell viability. Additionally, we carried out cell uptake studies at 1 h after the addition of the nioplexes. To comprehend the internalization process, we analyzed cell trafficking of our formulations in different entry pathways (CME, CvME, macropinocytosis) and lysosomal compartment. Colocalization was analyzed through Mander's overlap coefficient between the nioplexes (niosomes/Cy3 stained DNA) and the above stained endocytic pathways.

5.2. MATERIAL AND METHODS

5.2.1. Preparation of niosomes

Cationic lipid 1-(2-dimethylaminoethyl)-3-[2,3-di(tetradecyloxy)propyl]urea was synthetized in the laboratory, see supporting information (Fig. SI 1), to elaborate all cationic niosome formulations. Niosomes based on the aforementioned cationic lipid (Fig. 1A), polysorbate 80 (Fig. 1B) (Tween 80, Sigma-Aldrich, Madrid, Spain) and different helper lipids were prepared using the o/w emulsification technique, as previously reported [3]. We prepared four niosome formulations, where three formulations were prepared with different helper lipids and one formulation without helper lipid (None). Briefly, 5 mg of the cationic lipid were gently grounded with either 23 µl of squalene (Sque) (Fig. 1C), 100 µl of

cholesterol (Cho) (Fig. 1D) or 24.69 µl of squalane (Squa) (Fig. 1E) (Sigma-Aldrich, Madrid, Spain). The concentration of all helper lipids in each formulation was 10 mM. Then, 1 ml of dichloromethane (DCM) (Panreac, Barcelona, Spain) was added to all four formulations and emulsified with 5 ml (0.5%, w/w) of the non-ionic surfactant aqueous solution of polysorbate 80. Sonication was used to obtain the emulsion (Branson Sonifier 250, Danbury) for 30 s at 50 W. The organic solvent was removed from the emulsion by evaporation under magnetic agitation for 3 h at room temperature inside the extraction hood. Upon DCM evaporation, a dispersion containing the nanoparticles was formed by precipitation of the nanoparticles in the aqueous medium. The final cationic lipid concentration obtained was 1mg/ml.

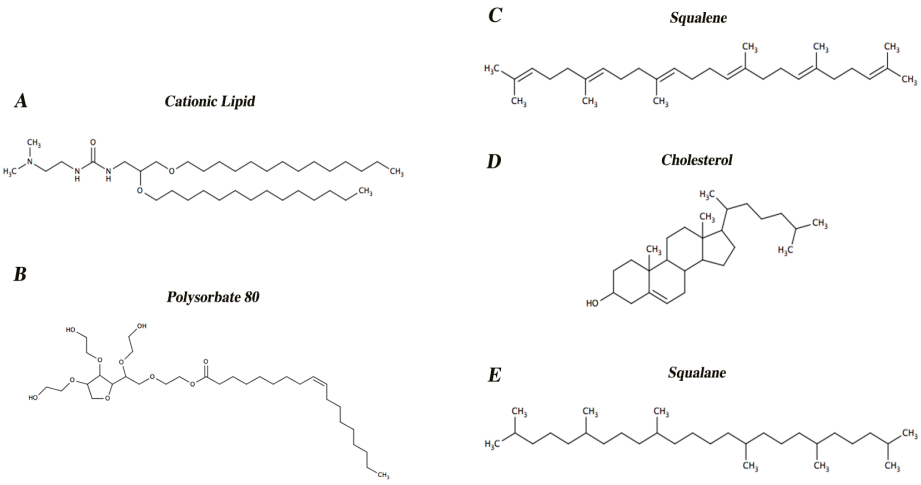

Figure 1. Chemical structures of niosome components.
A) Cationic lipid: 1-(2-dimethylaminoethyl)-3-[2,3-di(tetradecyloxy)propyl]urea
B) Polysorbate 80
C) Squalene: (6E,10E,14E,18E)-2,6,10,15,19,23-hexamethyltetracosa-2,6,10,14,18,22-hexaene
D) Cholesterol: 2,15-dimethyl-14-(6-methylheptan-2-yl) tetracyclo [8.7.0.02,7.011,15] heptadec-7-en-5-ol
E) Squalane: 2,6,10,15,19,23- hexamethyltetracosane.

5.2.2. Plasmid propagation and preparation of nioplexes

Escherichia coli DH5-α was used to propagate the pCMS-EGFP plasmid (PlasmidFactory, Bielefeld, Germany). According to the manufacturer's purification instructions, the plasmid was treated using the Qiagen endotoxin-free plasmid purification Maxi-prep kit (Qiagen, Santa Clarita, CA, USA). The concentration of pDNA was quantified using a NanoDrop® (ND-1000 spectrophotometer, Thermo Fisher Scientific Inc., Denver,

USA) measuring the absorbance at 260 nm. Agarose gel electrophoresis in Tris borate-EDTA buffer, pH 8.0 (TBE buffer) was used to verify the purity of the plasmid. DNA bands were detected using GelRedTM (Biotium, Hayward, California, USA) and images were observed with a ChemiDocTM MP imaging system (Bio-Rad, USA). The nioplexes formed by the addition of DNA to the niosomes and expressed as the ratio of cationic lipid/DNA (w/w) were elaborated by mixing cationic lipid/DNA at 30/1 (w/w) mass ratio. The mixture was left for 30 min at room temperature to enhance electrostatic interactions between the cationic lipid of the niosomes and the plasmid. The stock solution of plasmid pCMS-EGFP (0.5 mg/ml) was estimated to be around 0.137 micromolar (pCMS-EGFP, 5541 bp, average MW 3657060). For confocal fluorescence microscopy and uptake cytometry experiments, we used Cy3-labeled 2.7 kbp plasmid DNA (0.5 mg/ml) (Mirus Bio Corporation, Madison, WI, USA).

5.2.3. Size, polydispersity index and zeta potential measurements

The hydrodynamic diameter and the zeta potential of the niosomes and nioplexes were determined by Dynamic Light Scattering (DLS) and by Lasser Doppler Velocimetry (LDV), respectively. The data were obtained using a Zetasizer Nano ZS (Malvern Instrument, UK) as previously described [3]. Briefly, 50 µl of the niosomes and nioplexes were resuspended into 950 µl of 0.1 mM NaCl solution to determined size and polydispersity index (PDI). All measurements were carried out in triplicate. The particle size reported as hydrodynamic diameter was obtained by cumulative analysis. To determine the zeta potential, samples were resuspended (50 µl) into 0.1 mM NaCl (950 µl) using folded capillary cells for zeta analysis. The Smoluchowski approximation was used to support the calculation of the zeta potential from the electrophoretic mobility. Zeta potential measurements were run in triplicate. Only data that met the quality criteria according with the software program (DTS 5.0) were included in the study.

5.2.4. Agarose gel electrophoresis studies

Naked DNA and nioplexes based on different helper lipids and without helper lipid at 30/1 cationic lipid/DNA (w/w) mass ratio (containing 200 ng of the plasmid) were subjected to agarose gel electrophoresis. The agarose gel (0.8%) (Sigma-Aldrich, Madrid, Spain) was immersed in a Tris-acetate-EDTA buffer and exposed for 30 min to 120 V. GelRedTM (Biotium, Hayward, California, USA) was used to stain the DNA bands and images were observed with a ChemiDocTM MP Imaging System and analyzed by Image LabTM Software (BioRad, USA). To evaluate the release of DNA from the formulation, 12 µl of a 7% sodium dodecyl sulfate (SDS) (Sigma-Aldrich, Madrid, Spain) solution was added to the samples. The DNA protection capacity of the vectors against enzymatic digestion was

analyzed by adding the DNase I enzyme (Sigma-Aldrich, Madrid, Spain) to the formulations (final concentration of 1 U DNase I per 2.5 µg DNA). Afterward, the mixtures were incubated at 37 °C for 30 min. Finally, 12 µl of a 7% SDS solution was added to analyze the released DNA. Each sample contained 4 µl of loading buffer (BioRad, USA). Untreated DNA was used as a control to compare the integrity of the DNA in each sample.

5.2.5. Cell culture for transfection and cell uptake studies

ARPE-19 cells (ATCC) were grown in D-MEM/F-12 containing 10% bovine serum and supplemented with 5% penicillin-streptomycin (Gibco® San Diego, California, USA) and incubated at 37ºC and 5% CO2 atmosphere. Cells were split every 3-4 days to maintain monolayer coverage. For transfection and cell uptake assays, the cells were seeded in 24 well plates at initial density of 10×104 cells per well, with 300 µl of D-MEM/F-12 containing 10% bovine serum and incubated at 37ºC and 5% CO2 atmosphere. Cells were adhered overnight to achieve 70-90% of confluence at the time of transfection and cell uptake assays. For transfection assay, the regular growth medium was removed from ARPE-19 cells, and the cells were exposed to nioplexes based on the different helper lipids and without helper lipid (containing 1.25 µg of the plasmid for each well) resuspended in Opti-MEM® transfection medium (Gibco®, San Diego, California, USA). Each formulation was used in triplicate. After 4 h of incubation, the nioplexes were removed. Then, cells were washed twice with PBS (Sigma-Aldrich, Madrid, Spain) and 300 µl of regular growth medium was added to the cells [20]. Cells were allowed to grow for 72 h until flow cytometry analysis. For cell uptake assay, the regular growth medium was removed from ARPE-19 cells, and the cells were exposed to nioplexes prepared with different helper lipids and without helper lipid (containing 1.25 µg of Cy3-labeled plasmid for each well) resuspended in Opti-MEM® transfection medium. After 1 h of incubation, the nioplexes were removed. Then, cells were washed twice with PBS and detached for flow cytometry analysis. Each formulation was used in triplicate.

5.2.6. Transfection efficiency and cell viability assays

FACSCalibur system flow cytometer (Becton Dickinson Bioscience, San Jose, USA) was used to conduct flow cytometry analysis to quantify the % of EGFP and the mean fluorescence intensity (MFI) of positive cells. Cells were washed twice with PBS (Sigma-Aldrich, Madrid, Spain) and detached from the microplate with 200 µl of trypsin/EDTA (Gibco® San Diego, California, US). Once the cells were detached, 400 µl of normal growth medium was added and directly introduced into the flow cytometer tubes. Transfection efficiency was expressed as the percentage of EGFP positive cells at 525 nm (FL1) after excluding dead cells stained with 5 µL of diluted (1/20) Sytox® Blue reagent (Invitrogen,

Carlsbad, CA, USA). Control samples (non-transfected cells) were displayed on a forward scatter (FCS) versus side scatter (SSC) dot plot to establish a collection gate and exclude cell debris. The fluorescence corresponding to dead cells was measured at 444 nm (FL6). Mean fluorescence intensity (MFI) data were obtained from live positive cells (FL1). Control samples containing LipofectamineTM 2000 (Invitrogen, Carlsbad, CA, USA), transfected cells without Sytox® blue, and non-transfected cells with Sytox® blue were used to established the cytometer settings and channel compensations. For each sample, 10000 events were collected. Each formulation was used in triplicate. FlowJo software (Becton Dickinson, Mountain View, CA, USA) was used to analyze the data.

5.2.7. Cell uptake analysis

FACSCalibur system flow cytometer was used to conduct flow cytometry analysis to quantify the percentage of cells that contained Cy3-labeled plasmid DNA. Cells were washed twice with PBS and detached from the microplate with 200 µl of trypsin/EDTA. Once the cells were detached, 400 µl of normal growth medium were added and directly introduced into the flow cytometer. Cell uptake was expressed as the percentage of Cy3-labeled plasmid positive cells at 585 nm (FL2) after excluding dead cells as previously described. Mean fluorescence intensity (MFI) data were obtained from live positive cells (FL2). Control samples (non-transfected cells) were displayed on a forward scatter (FSC) versus side scatter (SSC) dot plot to establish a collection gate and exclude cells debris. For each sample, 10000 events were collected. Each formulation was used in triplicate. Data was analyzed by FlowJo software (Becton Dickinson, Mountain View, CA, USA).

5.2.8. Internalization mechanism assays

To identify the endocytic vesicles involved in nioplexes internalization, we performed colocalization assays in ARPE-19 cells. The cells were seeded in 12 well plates containing coverslips at an initial density of 20×104 cells per well. A volume of 600 µl of D-MEM/F-12 containing 10% bovine serum was added to each well and incubated at 37ºC and 5% CO2 atmosphere. Cells were adhered overnight to achieve 70-90% of confluence at the time of internalization assay. Then, the regular growth medium was removed to expose the cells to nioplexes based on the different helper lipids and without helper lipid (containing 0.625 µg of the Cy3 plasmid for each well) and fluorescent endocytic markers. Briefly, the markers were used as follows [16]: 60 µl (10 mg/ml) of Dextran Alexa Fluor 488, a fluid-phase uptake marker, incubated for 60 min to label macropinosomes; 96 µl (0.5 µM) of Lysotracker® Green incubated for 60 min to label lysosomes; 5 µl (1 mg/ml) of Cholera toxin B Alexa Fluor 488 incubated for 60 min to label CvME; and 5 µl (5 mg/ml) of Transferrin

Alexa Fluor 488 incubated for 60 min to label CME. All markers were purchased from Life Technologies, Eugene, OR, USA. Once the markers and the nioplexes were added, Opti-MEM® transfection medium was incorporated to obtain 600 µl final volume in each well. Cells were incubated for 1 h at 37ºC and 5% CO2 atmosphere. Next, the medium containing nioplexes was removed, and cells were washed twice with PBS. Then, the cells were fixed with 4% formaldehyde and mounted for their posterior examination by confocal microscopy. ImageJ software (NIH Image; http://rsbweb.nih.gov/ij/) was used to measure colocalization through Mander's overlap coefficient between red-labeled nioplexes and green stained endocytic pathways. (M=colocalized red/total red). Colocalization measurements were evaluated in 30 cells for each entry pathway.

5.2.9. Confocal laser scanning microscopy experiments (CLSM)

CLSM experiments were performed to evaluate qualitatively and quantitatively the colocalization between the different nioplexes formulations and the Cy3 stained DNA. Such assays were carried out with the Olympus Fluoview 1000 confocal microscope (Olympus, Tokyo, Japan) interfaced with a 405 nm diode laser, a 488 nm Argon laser, and 543 nm HeNe laser to excite the fluorescently labeled pDNA. Mounted slides were viewed with a 60x 1.25 numerical aperture (NA) water immersion objective. The following collection ranges were adopted: 500–540 nm (EGFP, Transferrin Alexa Fluor 488, Cholera toxin B Alexa Fluor 488 and Dextran Alexa Fluor 488), 555–655 nm (Cy3), and 460–530 (Lysotracker® Green). Images were collected in a sequential mode to eliminate emission crosstalk between the dyes.

5.3. RESULTS AND DISCUSSION

5.3.1. Synthesis of the ionizable cationic amino lipid

The evaluation of acid dissociation constants (pKa) in cationic lipids has become a useful parameter to design more efficient pH-responsive lipid-based drug delivery systems [21]. This mechanism normally benefits the release of the delivery system cargo in the presence of acid pH caused by late endosomes (pH 6.5) or lysosomes (pH 4.5). This property has allowed the design and synthesis of ionizable cationic lipid combinatorial libraries and formulations, which have shown a significant role on mediating cellular internalization and thereby causing the expected gene silencing in vitro and in vivo [21]. In our previous work [3], we found a tight correlation between acid dissociation constant (pKa) value and activity of cationic lipid-based combinatorial libraries, where an optimization was determined by several variables like lipid-chain unsaturation, linker chemistry and polar head nature. Interestingly, an optimum pKa (<7.0) for transfection was established as an ideal value to design new liposomal drug delivery systems [22]. Specifically, this optimal relationship

between pKa (6.72) and silencing activity was successfully found in the serinol isomer of the presented compound with the dimethylaminoethyl pendant group [3]. These findings made us to consider the possibility of introducing this potential modification to the presented cationic lipid: 1-(2-dimethylaminoethyl)-3-[2,3-di(tetradecyloxy)propyl]urea and continue with a deeper characterization. Moreover, this cationic lipid has already shown interesting transfection efficiencies in vivo in rats [20].

In light of the promising transfection results in vitro and in vivo recently obtained by our research group with optimized formulations based on the amino lipid 2,3-di(tetradecyloxy)propan-1-amine [4] (1, Fig. SI 1), we decided to chemically modify our glycerol-based cationic lipid lead compound with other potential polar head groups like this dimethylaminoethyl moiety used for gene delivery purposes.

The introduction of the dimethylamino derivative was accomplished by activating the amino lipid 1 with p-nitrophenyl-chloroformate according to well-stablished protocols [3]. Final nucleophilic reaction introduced the anticipated cationic head group and generated the expected urea derivative in moderate yields (65%) (Fig. SI 1). Having in hand the expected cationic lipid compound, we focused on evaluating the most appropriate niosomal formulation by adding squalene, cholesterol and squalane as helper lipids and its efficiency in gene transfection experiments.

5.3.2. Size polydispersity index and zeta potential measurements of niosomes and nioplexes

Combining size and zeta potential measurements is one of the most experimental strategies used to characterize the formation of vector /DNA complexes. Therefore, we investigated such parameters along with the polydispersity index (Fig. 2). Size characterization (Fig. 2A, white bars) indicated that niosomes based on squalene and cholesterol showed similar size (147 and 176 nm, respectively). Niosomes based on squalane showed the biggest size (259 nm) and niosomes prepared without helper lipid the smallest size (61 nm). As a homogeneity parameter for the niosome formulations, we determined the polydispersity index (PDI) (Fig. 2B). All niosome formulations showed appropriate size homogeneity with PDI values lower than 0.372. Zeta potential values of niosomes prepared with different helper lipids are shown in Fig. 2A (dot lines). The results showed that the zeta potential value obtained for niosomes prepared with squalene and squalane were similar (around +50 mV). For niosomes prepared with cholesterol, the zeta potential value was around +40 mV. Finally, the lowest values were observed with niosomes prepared without helper lipid (+32 mV).

The cationic lipid/DNA ratio w/w employed to form the nioplexes was the result from a previous characterization study (data not shown), where the ratio 30/1 was found the most appropriated. The size of the nioplexes (Fig. 2A gray bars) showed the following

results: Nioplexes based on squalene (150 nm), cholesterol (180 nm), squalane (254 nm), and without helper lipid (79 nm). These data indicate that the addition of DNA to niosomes to form nioplexes does not modify remarkably the original size of the niosomes, probably due to the high DNA condensation capacity of all formulations, with the exception of the niosome formulation prepared without helper lipid. All the formulations showed acceptable PDI values lower than 0.369 (Fig. 2B). The addition of the negatively charged DNA to niosomes decreased the zeta potential of all nioplexes formulations (Fig. 2A dash lines): Nioplexes based on squalene (from +50 to +40 mV), nioplexes based on cholesterol (from +38 to +35 mV), nioplexes based on squalane (from +51 to +46 mV) and, especially in nioplexes prepared without helper lipid (from +32 to +14 mV). This reduction on the superficial charge could be explained in part by the partial neutralization of the cationic charge carried by niosomes by the negatively charged DNA molecules. In any case, all nioplexes molecules were found to be positively charged (Fig. 2A dash lines), which suggest that at this cationic lipid/DNA mass ratio (30/1, w/w) free DNA is not present on the formulation and all the DNA is bound to the niosome. Collectively, our data shows that size and zeta-

A

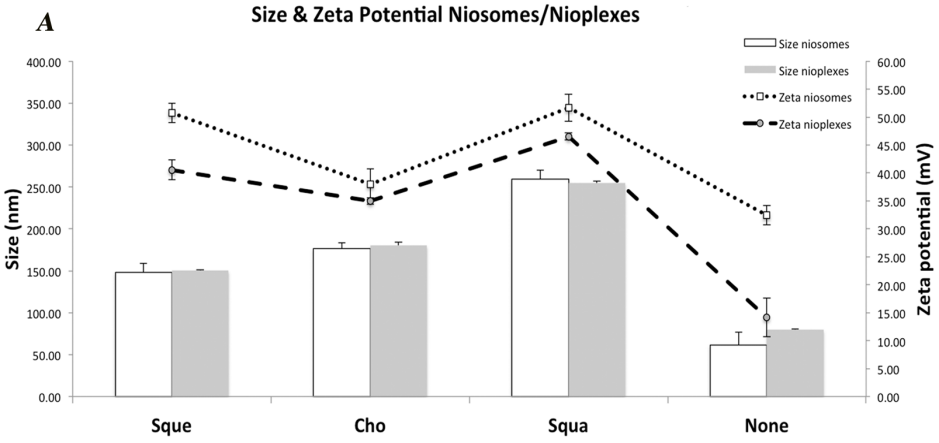

B

	PDI values			
	Niosomes		Nioplexes	
Helper lipid	PDI	SD	PDI	SD
Sque	0.235	0.011	0.232	0.007
Cho	0.372	0.014	0.361	0.010
Squa	0.279	0.023	0.369	0.006
None	0.355	0.043	0.194	0.010

Figure 2. Physico-chemical characterization of niosomes and nioplexes (niosome/DNA w/w ratio 30/1) prepared with different helper lipids: squelene (Sque), cholesterol (Cho), squalane (Squa) and without helper lipid (None). A) Size (white bars) and zeta potential (dot line) of niosomes. Size (gray bars) and zeta potential (dash lines) of nioplexes. B) PDI values of niosomes and nioplexes. Each value represents the mean ± standard deviation of three measurements.

potential results are compatible with DNA binding to niosome surfaces [23]. The addition of DNA to the niosomes did not remarkably modify the particle sizes, which are adequate for cellular uptake and internalization purposes [19,24-28]. Regarding zeta potential, it must be highlighted that all formulations showed positive zeta-potential values, which enhances not only the formation of stable suspensions due to the electrostatic repulsion between the positively charged particles [29] but also the interaction with negatively charged cell surfaces and the subsequences cell uptake processes [30]. In any case, we have to consider as well that both particle size and zeta potential values were measured as previously reported [4,20] in 0.1 mM NaCl medium to avoid saturation of the electrodes in the cuvettes. Therefore, although obtained values have significant importance for comparative purposes among the different formulations, absolute values could differ from those obtained in other fluids, such as transfection medium or other biological fluids, due to differences in the osmolarity or pH values to name a few.

5.3.3. Agarose gel electrophoresis studies

We investigated the electrostatic interactions of niosomes and DNA, the release of the DNA by SDS addition to the formulations and the capacity of niosomes to protect DNA against enzymatic digestion (Fig. 3) [3,31]The supercoiled (SC) bands in the gel show the most bioactive DNA form, and open circular (OC) bands represent the structural change of DNA of a less active form [32].

Nioplexes based on squalene showed deficient DNA condensation (lane 4), as a faint SC band was shown in the agarose gel. An easy release of DNA from the niosomes was detected (lane 5) upon the addition of the SDS surfactant agent, which could be the consequence of poor condensation. Due to the SC band observed in lane 6 (treatment with SDS plus DNase I), we can conclude that nioplexes based on squalene were able to protect the DNA from enzymatic digestion.

In the case of nioplexes based on cholesterol, we observed that they were able to condensate the DNA (lane 7). Moreover, we observed partial release of DNA upon the addition of SDS (lane 8) as all DNA content was not observed at the bottom of the well. Reasonable DNA protection was also observed as indicated by the detected SC band (lane 9). The analysis of nioplexes based on squalane, indicated high DNA condensation (lane 10), probably, due to their observed high zeta potential values (+46 mV, Fig 2A dash lines). Moreover, these nioplexes were able to release the DNA efficiently upon the addition of SDS (lane 11). Concerning about DNA protection against enzymatic digestion, these nioplexes showed that DNA was properly protected (lanes 12).

Finally, nioplexes prepared without helper lipid, despite their low zeta potential

values (+14 mV, Fig 2A dash lines), showed high DNA condensation capacity (lane 13). Thus, it seemed that the absence of helper lipids in the formulations could increase the condensation of DNA at low zeta potential values. Additionally, there was a satisfactory release and protection of DNA from enzymatic digestion, as SC bands were observed in lanes 14 and 15, respectively.

In brief, these studies showed that nioplexes prepared without helper lipid showed the highest level of DNA condensation whereas nioplexes based on squalene showed the lowest one. About DNA release, nioplexes based on squalene, squalane and without containing helper lipid showed an excellent capability to release the DNA. It is worth mentioning that both condensation and release of DNA are important parameters that need to be evaluated for the success of nioplexes as gene delivery vectors, where a delicate balance between these two factors for proper DNA delivery is required [4].

DNA protection is another factor to take into account due to the presence of enzymes in the cytosol since they can easily degrade the DNA and thus hamper the desired DNA delivery process [33]. This DNA protection was observed for all niosome formulations, which were able to protect the DNA against enzymatic digestion

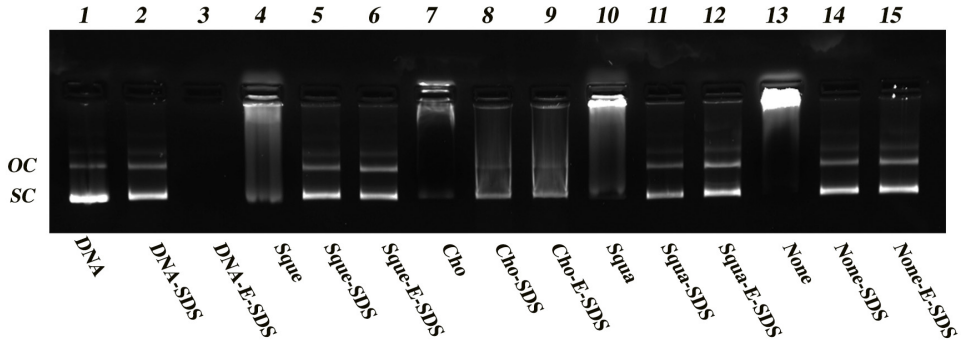

Figure 3. Binding, SDS-induced release and protection of DNA prepared with different helper lipids: squelene (Sque), cholesterol (Cho), squalane (Squa), without helper lipid (None). OC: open circular form, SC: supercoiled form. Lanes 1-3 correspond to free DNA; lanes 4-6, nioplexes based on squalene; lanes 7-9, nioplexes prepared with cholesterol; lanes 10-12, nioplexes based on squalane; lanes 13-15, nioplexes prepared without helper lipid. Naked DNA and nioplexes were treated with SDS (lanes 2,5,8,11 and 14) and DNase I + SDS (lanes 3,6,9,12 and 15).

5.3.4. *In vitro* transfection and cell uptake experiments

Percentages of transfected cells, cell viability, and cellular uptake studies were carried out in ARPE-19 cells as a retinal cell model for in vivo applications [31,34]. These pigmented epithelial cells of the retina play a major role in retinal diseases associated with

senescence and dystrophies of the photoreceptors. Mutations in genes of these cells can lead to photoreceptors death with dramatic consequences [35]. Therefore, the knowledge of the physicochemical and biological parameters that affect to the transfection efficiency on these particular cells merits special attention in order to design more efficient non-viral vectors for retinal gene delivery applications [20].

Gene expression in the cell nucleus is an indication that the DNA has been properly delivered by the vector. However, this process can involve, sometimes, few numbers of cells, which can be inadequate for gene therapy purposes. Therefore, our aim is to transfect as many cells as possible without compromising the cellular viability. The highest percentages values of transfected cells were observed for nioplexes prepared with squalene (31%), followed by nioplexes prepared with squalane (14%) (Fig. 4A bars). The lowest transfection values were obtained when nioplexes were prepared with cholesterol (2%) and without helper lipid (2%). For additional transfection data see histograms in supporting information (Fig. SI 2). Therefore, and as reported in the literature, transfection efficiency strongly depends on the chemical composition of the helper lipids [36,37]. The above results could be explained, in part, by the different endosomal scape ability of the helper lipids [38]. This capability has been attributed to the structural transition that helper lipids offer to the delivery system. Such structural transition usually goes from lamellar to inverse hexagonal due to the acid environment of the endosomes, where the transition induces the release of the DNA and its subsequent delivery into the cytoplasm [39,40]. Additionally, analyzed MFI data (Fig. 4B) showed that nioplexes prepared with squalene showed the higher MFI, around 70. On the other hand, despite of the low percentage of transfected cells observed with nioplexes prepared with the other three formulations (Fig. 4A bars), we found interesting MFI data that suggest that the few number of transfected cells were able to produce significant amounts of EGFP (Fig. 4B, Cho, Squa

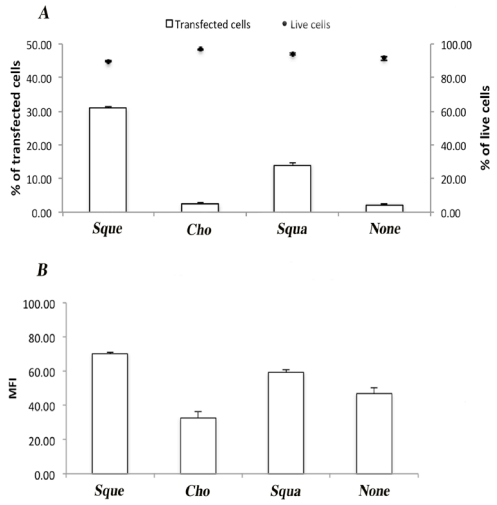

Figure 4. Transfection efficiencies at 72 h post-addition of nioplexes prepared with different helper lipids: squalene (Sque), cholesterol (Cho), squalane (Squa) and without helper lipid (None) in ARPE-19 cells. A) Percentage of transfection (bars) and viability (dots) of nioplexes. B) Mean fluorescence intensity (MFI) of cells with nioplexes prepared with different helpers. Each value represents the mean ± standard deviation of three measurements.

and None). The capacity of nioplexes based on squalene to transfect more efficiently ARPE-19 cells might also rely on the fact that squalene is usually synthesized in the cells, which may indicate that cells could easily recognize it and subsequently increase its cell permeability [41-43]. Therefore, we hypothesize that nioplexes prepared with squalene could take advantages of the properties of this helper lipid to obtained high transfection efficiencies. In any case, it could be interesting to perform further in vivo experiments, since transfection efficiency in vitro conditions may be strongly different than the efficiency observed in real biological fluids, mainly due to unspecific interactions between gene delivery vectors and biomolecules such as serum proteins that clearly affect to the stability and uptake of the formulations [34]. In any case, we have recently reported that niosomes based on squalene helper lipid transfected efficiently both the rat retina after intravitreal and subretinal administrations and the rat brain [4,20].

Additionally, to develop efficient drug delivery systems, it is important to consider the possible toxic effect of these vectors upon the targeted cells since cell viability generally depends on the vector composition [3,44]. Therefore, the effect of our niosome formulations on ARPE-19 cells was studied. Cell viability results (Fig. 4A dots) showed high viabilities with all the nioplexes formulations (around 90%), which indicated high cell tolerability with all the helper lipids used in each formulation.

Cell uptake analysis is another primary assay that helps to understand part of the transfection process and shows the capacity of the nioplexes to be internalized when they are in contact with the cells. Cell uptake percentages results (Fig. 5 black bars) showed that nioplexes based on squalene were practically internalized by all the cells (99 %), and nioplexes based cholesterol, squalane and without helper also showed worthy cell uptake levels (75 %, 85 % and 72 %, respectively). For additional uptake data see histograms in supporting information (Fig. SI 3). To show a better insight into the cell uptake process, we analyzed as well the mean MFI of the cells (Fig. 5 white bars). Our results showed that nioplexes based on squalene helper lipid showed higher MFI (around 200) compared to the rest of formulations (nioplexes based on

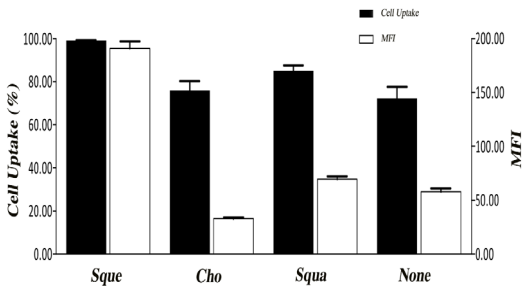

Figure 5. Cellular uptake at 1 h after the addition of nioplexes prepared with different helper lipids: squalene (Sque), cholesterol (Cho), squalane (Squa) and without helper lipid (None) in ARPE-19 cells. Uptake percentage of cells upon the addition of nioplexes (Black bars). Mean fluorescence intensity (MFI) of cells with nioplexes prepared with different helpers (White bars). Each value represents the mean ± standard deviation of three measurements.

cholesterol 32, squalane 69 and without helper lipid 58). Thus, our cellular uptake studies indicated that nioplexes based on squalene were internalized in most of the analyzed cell population, and the amount of nioplexes internalized in each cell was superior compared to the rest of formulations. Regarding this point, we could assume that the higher MFI value of niosomes based on squalene observed in Figure 5 (white bars) could be due to the higher particle size of this formulation rather than to the differences on number of particles internalized. However, data reported on Figure 2A, clearly discard this assumption. Moreover, we could discard the hypothesis that only Cy3-labelled DNA without the niosomes could enter the cell, since previous data reported on Figure 2A shows that at 30/1 cationic lipid/DNA mass ratio all the DNA is bound to the niosome. Additionally, fluorescent confocal microscopy images showed that immediately after administration (t<5 min), DNA appeared to be confined within punctate spot-like structure, while no evidence of diffuse fluorescence was found (see supporting information Figure SI 4). This finding unambiguously suggested that, at the early stages of internalization, DNA was encapsulated within niosomes vesicles.

Additionally, squalene has shown to increase the phagocytic activity of cells due to its capacity to potentiate the immune response in a non-toxic manner [45,46]. Furthermore, some authors have reported that squalene increases oxygenation in the cells, which results in a more efficient metabolic process [47]. Therefore, a more efficient and easy uptake of DNA could be performed when squalene is used as helper lipid in our niosome formulations.

Among many other parameters, cell uptake could also depends on physico-chemical parameters of the niosomes such as the particle size, where bigger size particles (>500 nm) are difficult and slowly taken, contrary to smaller particles (40 nm), which are easily and rapidly captured [48]. However, our results indicated that the lowest cell uptake value was obtained from the smallest particles (79 nm, nioplexes prepared without helper lipid), and the most efficient cellular uptake was obtained with bigger nioplexes (around 150 nm, nioplexes prepared with squalene and cholesterol). These data suggest that not only size is determinant in the cellular uptake but the helper lipid composition as well.

5.3.5. Intracellular trafficking

To develop more efficient non-viral vectors it is necessary to understand their intracellular trafficking mechanism and how their physical-chemical properties might trigger different internalization pathways. Thus, in the following experiments, we have investigated the intracellular traffic of nioplexes formulations and how this process influences the transfection efficiency. Fluorescence confocal microscopy allowed visualizing the intracellular trafficking of fluorescently labeled nioplexes (red) in ARPE-19 cells in the presence of various endocytic markers (green) (Fig. 6A). Since there was the possibility of

finding dextran-positive endosomes internalized by clathrin-mediated pathway (roughly 100–200 nm in size), the incubation time applied (60 min) was chosen to minimize accumulation of dextran in endosomes internalized by mechanisms other than macropinocytosis. The degree of colocalization was calculated by Mander´s overlap coefficient (Fig. 6B) to perform a quantitative analysis of confocal images. Colocalization analysis (Fig. 6B) showed that squalene-containing nioplexes mostly used macropinocytosis (M=0.480) followed by

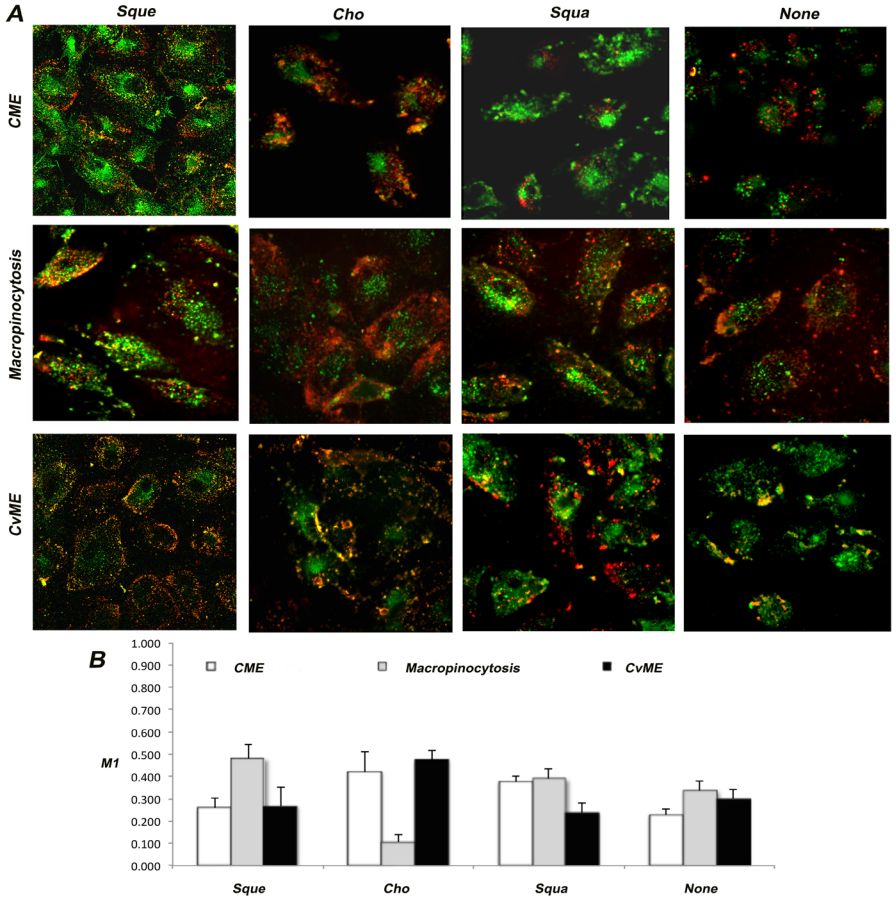

Figure 6. Cell trafficking results in ARPE-19 cells co-incubated with nioplexes prepared with squalene (Sque), cholesterol (Cho), squalane (Squa) and without helper lipid (None). A) Confocal microscopy merged images showing the cells co-incubated with nioplexes. Each image displayed in the optical section was representative of the cell population. Green coloring shows cells stained with Transferrin Alexa Fluor 488 for CME, Dextran Alexa Fluor 488 for macropinocytosis and Cholera toxin B Alexa Fluor 488 for CvME. Red coloring shows the DNA stained with Cy3. For interpretation of the referenced colors in this figure legend, the reader is referred to the web version of the article. B) Colocalization values were given as the fraction of cell-associated nanoparticles colocalizing with fluorescently labeled endocytic structures. M1 is equal to Mander´s overlap coefficient between the red signal from the stained DNA and the green fluorescence of the stained entry pathways. Each value represents the mean ± standard deviation of three measurements.6

CvME (M=0.266) and CME (M=0.258). On the other side, cholesterol-containing nioplexes were mainly located in CME (M=0.420) and CvME (M=0.475), while they were poorly processed throughout macropinocytosis (M=0.106). Nioplexes prepared with squalane, were internalized via macropinocytosis (M=0.388) and CME (M=0.376) and to a less extent via CvME (M=0.237). Lastly, in the absence of helper lipid nioplexes were also equally internalized via CME (M=0.227), macropinocytosis (M=0.336) and CvME (M=0.300). Our results indicated that each nioplexe formulation could use all the entry pathways simultaneously. Notably, transfection efficiencies did correlate to the internalization pathway: the larger the involvement of macropinocytosis, the higher the transfection efficiency.

To account for differences in transfection efficiency the ultimate intracellular fate of nioplexes was investigated (Fig. 7A). To this end, we used Lysosensor, which accumulates in acidic cell organelles, and is primarily a lysosome marker. Colocalization of fluorescently tagged nioplexes and Lysosensor reveals that highly efficient squalene-containing systems could efficiently escape from endosomal compartments (M=0.180), while poorly efficient cholesterol-containing nioplexes were largely degraded in the lysosomes (M=0.895). Nioplexes prepared either with squalane and with no helper lipid exhibited intermediate levels of lysosomal accumulation (M=0.330 and 0.247, respectively).

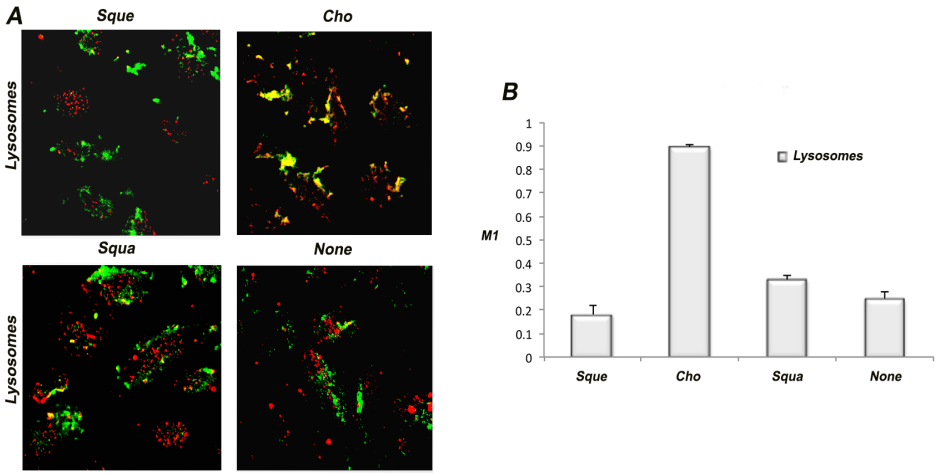

Figure 7. Lysosome colocalization results in ARPE-19 cells co-incubated with nioplexes prepared with squalene (Sque), cholesterol (Cho), squalane (Squa) and without helper lipid (None). Niosomes were complex with DNA stained with Cy3. A) Confocal microscopy merged images showing cells co-incubated with nioplexes prepared with different helper lipids. Each image displayed in the optical section was representative of the cell population. Green and red coloring show cells stained with Lysotracker® Green and the DNA, respectively. For interpretation of the referenced colors in this figure legend, the reader is referred to the web version of the article. B) The colocalization values were given as the fraction of cell-associated nanoparticles colocalizing with fluorescently labeled lysosomes, where M1 is equal to Mander´s overlap coefficient between the red signal from the stained DNA and the green fluorescence of the stained lysosomes. Each value represents the mean ± standard deviation of three measurements.

The precise correlation between the mechanism of cell uptake, final intracellular fate and transfection efficiency of nioplexes has been poorly investigated so far. It has been suggested that CME and macropinocytosis are correlated to the lysosomal fusion, which could partial or entirely degrade the content of their vesicles [18,19]. Moreover, it has been described that there is a recycling process of the vesicles when macropinocytosis is involved (i.e. macropinosome is sent back to the cell exterior) [26]. It also should be pointed out that CvME is mainly considered a non-digestive pathway. However, some findings suggest that this route is also involved in the lysosomal fusion [49].

In this regard, our results provided new views and insights into the relationship between intracellular trafficking and transfection efficiency of nioplexes. Squalene-containing nioplexes were largely internalized via macropinocytosis, exhibited minor lysosomal accumulation and showed high transfection efficiency. On the opposite, macropinocytosis was weakly activated when ARPE-19 cells were treated with poorly efficient cholesterol-containing nioplexes, which largely accumulated in lysosomes. Aside from clarifying the exact molecular aspects of this correlation, it seems that macropinocytosis could be a preferred internalization route of nioplexe formulations. This observation might explain the superior efficiency of nioplexes prepared with squalene (Fig. 4A bars, Sque) and provides a reasonable explanation for the low transfection efficiency of cholesterol-based nioplexes (Fig 4A bars, Cho). Notably, this suggestion is in excellent agreement with previous findings [16] showing that macropinocytosis is the main pathway of internalization of highly efficient liposome/DNA complexes. In any case, further experiments with specific inhibitors of the pathways studied such as chlorpromazine, filipin or EIPA (ethylisopropylamiloride) could help us to clarify our hypothesis.

Squalane-containing nioplexes exhibited an endocytic pattern similar to that of nioplexes prepared with squalene. Nevertheless, squalane-containing systems were less efficient (Fig 4A bars, Squa) than their squalene-enriched counterpart (Fig. 4A bars, Sque). This result was likely due to less involvement of macropinocytosis resulting in larger colocalization of complexes with lysosomes (Fig. 6 B). In the absence of helper lipid, nioplexes were poorly efficient (Fig. 4A bars, None), but this was not due to accumulation within acidic lysosomes (Fig. 7, None). These results suggest that despite being able to avoid lysosomal degradation this nioplexe formulation was unable to release their cargo effectively, which can be supported by the agarose gel results, where high DNA condensation was observed (Fig. 3 lane 13).

5.4. CONCLUSION

In this study, we investigated the role played by the helper lipid on the transfection efficiency of four niosome formulations in ARPE-19 cells. Our results showed that the helper lipid does affect not only to the physico-chemical properties of both bare and DNA-loaded niosomes, but also to important biological processes intimately related with the final transfection efficiency. Collectively, our data pointed out that the helper lipid composition has a deep influence on the cellular uptake of nioplexes that, in turn, affects final the fate and transfection efficiency. Niosomes elaborated with squalene as helper lipid showed the highest efficiency to transfect ARPE-19 cells, which could be attributed mainly to their high cellular uptake and posterior entry pathways used, where macropinocytosis pathway and lysosomal elution played an important role. Overall, these studies bring new insights into the role of helper lipids towards the development of highly efficient niosome formulations as non-viral gene delivery vectors for the treatment of inherited retinal diseases. However, we have to consider that both internalization mechanisms and intracellular trafficking processes can be highly modified by interaction of gene carriers with biological fluids, even for retinal application. Therefore, the knowledge of these biological processes that affect to the final transfection efficiency in vivo conditions represents a real challenge for the scientific community in order to design novel gene delivery systems based on non-viral vectors.

5.5. ACKNOWLEDGMENTS

This project was partially supported by the University of the Basque Country UPV/EHU (UFI 11/32), the National Council of Science and Technology (CONACYT), Mexico, Reg. # 217101, the Spanish Ministry of Education (Grant CTQ2010-20541, CTQ2010-14897), the Basque Government (Department of Education, University and Research, predoctoral BFI-2011-2226 grant) and by Spanish grants MAT2012-39290-C02-01 and IPT-2012-0574-300000. Technical and human support provided by SGIker (UPV/EHU) is gratefully acknowledged. Authors also wish to thank the intellectual and technical assistance from the ICTS “NANBIOSIS”, more specifically by the Drug Formulation Unit (U10) of the CIBER in Bioengineering, Biomaterials & Nanomedicine (CIBER-BBN) at the University of Basque Country (UPV/EHU). GC acknowledges support by the Italian Minister for University and Research (MIUR) (Futuro in Ricerca, Grant No. RBFR08TLPO).

5.6. REFERENCES

1. Anderson WF. Human gene therapy. Nature 1998;392:25-30.

2. Charbel Issa P, MacLaren RE. Non-viral retinal gene therapy: a review. Clin Experiment Ophthalmol 2012;40:39-47.

3. Ojeda E, Puras G, Agirre M, Zarate J, Grijalvo S, Pons R, et al. Niosomes based on synthetic cationic lipids for gene delivery: the influence of polar head-groups on the transfection efficiency in HEK-293, ARPE-19 and MSC-D1 cells. Org Biomol Chem 2015;13:1068-1081.

4. Puras G, Mashal M, Zarate J, Agirre M, Ojeda E, Grijalvo S, et al. A novel cationic niosome formulation for gene delivery to the retina. J Control Release 2014;174:27-36.

5. Moghassemi S, Hadjizadeh A. Nano-niosomes as nanoscale drug delivery systems: an illustrated review. J Control Release 2014;185:22-36.

6. Choi WJ, Kim JK, Choi SH, Park JS, Ahn WS, Kim CK. Low toxicity of cationic lipid-based emulsion for gene transfer. Biomaterials 2004;25:5893-5903.

7. Huang Y, Rao Y, Chen J, Yang VC, Liang W. Polysorbate cationic synthetic vesicle for gene delivery. J Biomed Mater Res A 2011;96:513-519.

8. Karmali PP, Chaudhuri A. Cationic liposomes as non-viral carriers of gene medicines: resolved issues, open questions, and future promises. Med Res Rev 2007;27:696-722.

9. Byk G, Dubertret C, Escriou V, Frederic M, Jaslin G, Rangara R, et al. Synthesis, activity, and structure--activity relationship studies of novel cationic lipids for DNA transfer. J Med Chem 1998;41:229-235.

10. Zhi D, Zhang S, Wang B, Zhao Y, Yang B, Yu S. Transfection efficiency of cationic lipids with different hydrophobic domains in gene delivery. Bioconjug Chem 2010;21:563-577.

11. Dabkowska AP, Barlow DJ, Campbell RA, Hughes AV, Quinn PJ, Lawrence MJ. Effect of helper lipids on the interaction of DNA with cationic lipid monolayers studied by specular neutron reflection. Biomacromolecules 2012;13:2391-2401.

12. Mochizuki S, Kanegae N, Nishina K, Kamikawa Y, Koiwai K, Masunaga H, et al. The role of the helper lipid dioleoylphosphatidylethanolamine (DOPE) for DNA transfection cooperating with a cationic lipid bearing ethylenediamine. Biochim Biophys Acta 2013;1828:412-418.

13. Agirre M, Ojeda E, Zarate J, Puras G, Grijalvo S, Eritja R, et al. New Insights into Gene Delivery to Human Neuronal Precursor NT2 Cells: A Comparative Study between Lipoplexes, Nioplexes, and Polyplexes. Mol Pharmaceutics 2015;12:4056-4066.

14. Zhao F, Zhao Y, Liu Y, Chang X, Chen C, Zhao Y. Cellular uptake, intracellular trafficking, and cytotoxicity of nanomaterials. Small 2011;7:1322-1337.

15. Marchini C, Pozzi D, Montani M, Alfonsi C, Amici A, Amenitsch H, et al. Tailoring lipoplex composition to the lipid composition of plasma membrane: a Trojan horse for cell entry? Langmuir 2010;26:13867-13873.

16. Cardarelli F, Pozzi D, Bifone A, Marchini C, Caracciolo G. Cholesterol-dependent macropinocytosis and endosomal escape control the transfection efficiency of lipoplexes in CHO living cells. Mol Pharm 2012;9:334-340.

17. Pozzi D, Marchini C, Cardarelli F, Salomone F, Coppola S, Montani M, et al. Mechanistic evaluation of the transfection barriers involved in lipid-mediated gene delivery: interplay between nanostructure and composition. Biochim Biophys Acta 2014;1838:957-967.

18. Luzio JP, Parkinson MD, Gray SR, Bright NA. The delivery of endocytosed cargo to lysosomes. Biochem Soc Trans 2009;37:1019-1021.

19. Xiang S, Tong H, Shi Q, Fernandes JC, Jin T, Dai K, et al. Uptake mechanisms of non-viral gene delivery. J Control Release 2012;158:371-378.

20. Ojeda E, Puras G, Agirre M, Zarate J, Grijalvo S, Eritja R, et al. The influence of the polar head-group of synthetic cationic lipids on the transfection efficiency mediated by niosomes in rat retina and brain. Biomaterials 2015;77:267-279.

21. Jayaraman M, Ansell SM, Mui BL, Tam YK, Chen J, Du X, et al. Maximizing the potency of siRNA lipid

nanoparticles for hepatic gene silencing in vivo. Angew Chem Int Ed Engl 2012;51:8529-8533.
22. Semple SC, Akinc A, Chen J, Sandhu AP, Mui BL, Cho CK, et al. Rational design of cationic lipids for siRNA delivery. Nat Biotechnol 2010;28:172-176.
23. Caracciolo G, Caminiti R. DNA–DNA electrostatic interactions within cationic lipid/DNA lamellar complexes. Chemical Physics Letters 2004;400:314-319.
24. Caracciolo G, Caminiti R, Digman MA, Gratton E, Sanchez S. Efficient escape from endosomes determines the superior efficiency of multicomponent lipoplexes. J Phys Chem B 2009;113:4995-4997.
25. Gratton SE, Ropp PA, Pohlhaus PD, Luft JC, Madden VJ, Napier ME, et al. The effect of particle design on cellular internalization pathways. Proc Natl Acad Sci U S A 2008;105:11613-11618.
26. Lim JP, Gleeson PA. Macropinocytosis: an endocytic pathway for internalising large gulps. Immunol Cell Biol 2011;89:836-843.
27. Rejman J, Oberle V, Zuhorn IS, Hoekstra D. Size-dependent internalization of particles via the pathways of clathrin- and caveolae-mediated endocytosis. Biochem J 2004;377:159-169.
28. Gillard M, Jia Z, Hou JJ, Song M, Gray PP, Munro TP, et al. Intracellular trafficking pathways for nuclear delivery of plasmid DNA complexed with highly efficient endosome escape polymers. Biomacromolecules 2014;15:3569-3576.
29. Caracciolo G, Amenitsch H. Cationic liposome/DNA complexes: from structure to interactions with cellular membranes. Eur Biophys J 2012;41:815-829.
30. Rezvani Amin Z, Rahimizadeh M, Eshghi H, Dehshahri A, Ramezani M. The effect of cationic charge density change on transfection efficiency of polyethylenimine. Iran J Basic Med Sci 2013;16:150-156.
31. Ochoa GP, Sesma JZ, Diez MA, Diaz-Tahoces A, Aviles-Trigeros M, Grijalvo S, et al. A novel formulation based on 2,3-di(tetradecyloxy)propan-1-amine cationic lipid combined with polysorbate 80 for efficient gene delivery to the retina. Pharm Res 2014;31:1665-1675.
32. Stellwagen NC, Stellwagen E. Effect of the matrix on DNA electrophoretic mobility. J Chromatogr A 2009;1216:1917-1929.
33. Midoux P, Monsigny M. Efficient gene transfer by histidylated polylysine/pDNA complexes. Bioconjug Chem 1999;10:406-411.
34. Puras G, Zarate J, Diaz-Tahoces A, Aviles-Trigueros M, Fernandez E, Pedraz JL. Oligochitosan polyplexes as carriers for retinal gene delivery. Eur J Pharm Sci 2013;48:323-331.
35. Bejjani RA, BenEzra D, Cohen H, Rieger J, Andrieu C, Jeanny JC, et al. Nanoparticles for gene delivery to retinal pigment epithelial cells. Mol Vis 2005;11:124-132.
36. Chung H, Kim TW, Kwon M, Kwon IC, Jeong SY. Oil components modulate physical characteristics and function of the natural oil emulsions as drug or gene delivery system. J Controlled Release 2001;71:339-350.
37. Kim YJ, Kim TW, Chung H, Kwon IC, Sung HC, Jeong SY. The effects of serum on the stability and the transfection activity of the cationic lipid emulsion with various oils. Int J Pharm 2003;252:241-252.
38. Pozzi D, Marchini C, Cardarelli F, Amenitsch H, Garulli C, Bifone A, et al. Transfection efficiency boost of cholesterol-containing lipoplexes. Biochim Biophys Acta 2012;1818:2335-2343.
39. Zuhorn IS, Bakowsky U, Polushkin E, Visser WH, Stuart MC, Engberts JB, et al. Nonbilayer phase of lipoplex-membrane mixture determines endosomal escape of genetic cargo and transfection efficiency. Mol Ther 2005;11:801-810.
40. Allain V, Bourgaux C, Couvreur P. Self-assembled nucleolipids: from supramolecular structure to soft nucleic acid and drug delivery devices. Nucleic Acids Res 2012;40:1891-1903.
41. Liu GC, Ahrens EH,Jr, Schreibman PH, Crouse JR. Measurement of squalene in human tissues and plasma: validation and application. J Lipid Res 1976;17:38-45.
42. Koivisto PV, Miettinen TA. Increased amounts of cholesterol precursors in lipoproteins after ileal exclusion. Lipids 1988;23:993-996.
43. Stewart ME. Sebaceous gland lipids. Semin Dermatol 1992;11:100-105.
44. Martin B, Sainlos M, Aissaoui A, Oudrhiri N, Hauchecorne M, Vigneron JP, et al. The design of cationic lipids

for gene delivery. Curr Pharm Des 2005;11:375-394.
45. Seubert A, Monaci E, Pizza M, O'Hagan DT, Wack A. The adjuvants aluminum hydroxide and MF59 induce monocyte and granulocyte chemoattractants and enhance monocyte differentiation toward dendritic cells. J Immunol 2008;180:5402-5412.
46. Allison AC, Byars NE. An adjuvant formulation that selectively elicits the formation of antibodies of protective isotypes and of cell-mediated immunity. J Immunol Methods 1986;95:157-168.
47. Reddy LH, Couvreur P. Squalene: A natural triterpene for use in disease management and therapy. Adv Drug Deliv Rev 2009;61:1412-1426.
48. dos Santos T, Varela J, Lynch I, Salvati A, Dawson KA. Quantitative assessment of the comparative nanoparticle-uptake efficiency of a range of cell lines. Small 2011;7:3341-3349.
49. Kiss AL, Botos E. Endocytosis via caveolae: alternative pathway with distinct cellular compartments to avoid lysosomal degradation? J Cell Mol Med 2009;13:1228-1237.

6

General Discussion

6. GENERAL DISCUSSION

Currently, gene delivery has become a tangible option for the treatment of several diseases [1-3]. However, there are few available options in the market, where viral vectors are the preferred option due to their high transduction efficiency. Despite the advantages that viral vectors offer, there are still many concerns about their safety. To overcome this issue, non-viral vectors have rouse interesting expectations, specifically on particles based on cationic lipids, where niosomes are a promising approach due to recent findings. Unfortunately, more research is needed before niosomes, as gene delivery vectors, can emulate transfection efficiencies obtained with viral vectors and be launched into the market. In the present study, we have prepared and characterized *in vitro* niosome formulations based on different cationic lipids for their *in vivo* application in retina and brain.

6.1. THE INFLUENCE OF POLAR HEAD-GROUPS OF SERINOL BASED CATIONIC LIPIDS ON THE TRANSFECTION EFFICIENCY OF NIOSOMES

One fundamental component of niosomes is the cationic lipid, where the structure design of such cationic lipid can determine the success of the gene delivery. Therefore, as a first step for the design of cationic niosomes for gene delivery purposes, three novel ionizable amino lipids (1, 2 and 3) were synthesized (Fig. 1). These three lipids contained two identical fully hydrocarbonated alkyl chains, the same serinol backbone and linker group, only varying the cationic head structure. Once the cationic lipids were synthetized, they were subjected to small angle X-ray scattering analysis (SAXS) to obtain information about their structures. The results indicated that lipid 2 showed a more fluid hydrophobic domain compared to lipid 1 and 3, and that the polar region of lipid 3 contained almost no water.

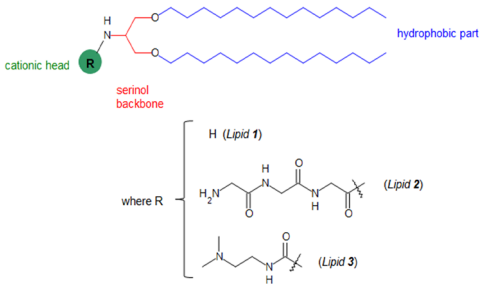

Figure 1. General structure for the novel amino lipid-based serinol derivatives (lipids 1, 2 and 3) that contain the same backbone, linker group, hydrophobic part and different cationic head-groups

Lipid pKa has been used to predict the efficacy of formulations that contain ionizable amino lipids to encapsulate and mediate delivery of different cargoes into cells [4]. This parameter has been used in rational design of lipids [5] and structure activity relationship (SAR) studies to analyze combinatorial libraries of lipids by varying the amino cationic head-group, linker or hydrophobic chains. Thus, we measured the amino lipid pKa values at different pH values (from 2.5 to 11.0)

to determine the acid dissociation constant of our niosome formulations containing the ionizable amino lipids 1, 2 and 3. The modification of the head-group of the amino lipids (1, 2 and 3) was sufficient to affect the pKa value for the corresponding niosomes (lipid 1, pKa=7.00; lipid 2, pKa=6.63 and lipid 3, pKa=6.72). It has been suggested that the optimal pKa of cationic lipid for transfection purposes should be inferior to 7.0 as in this way, a large number of amino groups would be neutral at physiological pH 7.4 [5]. If this suggestion is correct, the pKa of the amino lipids described in this work could fall into the optimal range for transfection.

The uptake and transfection efficiency of non-viral vectors strongly depend on the method of elaboration, which clearly impact on some physicochemical parameters such as size, zeta potential and morphology [6]. Therefore, we prepared niosomes based on the lipids 1, 2 and 3 by o/w emulsion and film-hydration techniques. Resulted niosomes were characterized in terms of size, zeta potential and morphology. We observed that zeta potential values were similar between both techniques for the three niosome formulations (Fig. 2 lines). Interestingly, the highest zeta potential values were obtained when niosomes were based on lipid 3 (+30 mV), independently of the elaboration technique. Regarding particle size values (Fig. 2 bars), we did not find differences between the niosomes when these were elaborated by both techniques (values around 200 nm). In addition to the size and charge, the homogeneity of the dispersion that contains the nanoparticles should be also considered since this parameter affects to the formation of the nioplexes (after the addition of plasmid) and the subsequent cell internalization processes [7]. We determined the polydispersity index (PDI) as a measure of homogeneity. Our data clearly revealed that the lowest PDI values were obtained when niosomes were prepared by the o/w emulsion technique (0.20, 0.20 and 0.21 for lipid 1, 2 and 3, respectively). On the other hand, when niosomes were elaborated

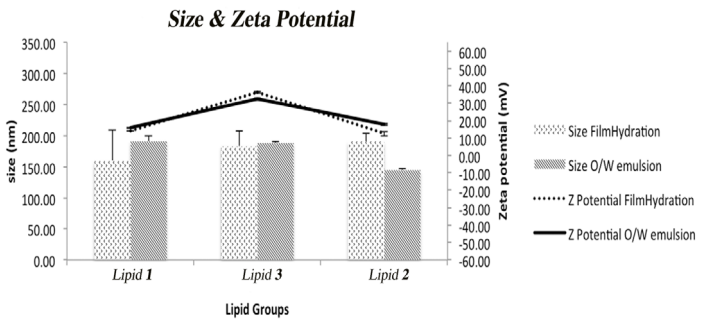

Figure 2. Physicochemical characterization of niosomes based on lipids 1, 3 and 2. Size and zeta potential values of niosomes prepared by film-hydration and o/w emulsion techniques. Each value represents the mean ± standard deviation of three measurements.

by the film-hydration technique, PDI values were extremely high, which indicates that these suspensions showed a very broad size distribution (0.9, 0.3 and 0.9 for lipid 1, 2 and 3, respectively). Consequently, we discarded for the next experiments the niosomes that were prepared using film-hydration technique.

To obtain a direct evidence of the niosomes formation, we examined niosomes elaborated by the o/w emulsion technique with the three cationic lipids under a Cryo-TEM microscopy. In our experimental conditions, all niosomes, especially those elaborated with the lipid 3, adopted a spherical and homogeneous morphology, which is the most favorable structure from an energetic point of view.

Stability of niosomes can be seen as a merging of one or more particles (aggregates) that could result in an increase on the particle size throughout the testing period, which can end in an unstable niosomal system. Normally, the electrostatic repulsions among the vesicles are due to the surface charge, where high surface charges of the vesicles (above +20 mV) should provide enough electrostatic repulsion to prevent the formation of aggregates [8]. Therefore, we measured the physical stability of niosomes based on the three cationic lipids by monitoring the particle size and the zeta potential throughout 100 days at 4°C and 25°C respectively. Our data showed that stability of niosomes strongly depended on the storage temperature and on the polar head-group of the cationic lipid, where at 25°C we observed unstable niosomes due to the reduction of the electrostatic repulsions [9], except on the case of niosomes prepared with lipid 3. However, when samples were stored at 4°C, we only observed a clear decrease on the zeta potential on niosomes based on lipid 2, which also showed an increase of the particle size probably as the consequence of the zeta potential decrease. In conclusion, niosomes based on lipids 1, 2 and 3 were more stable when they were stored at 4°C, specially niosomes based on the lipid 3, which size and zeta potential values did not strongly vary along all the storage period. Moreover, these data indicated that the polar head-group of the cationic lipid strongly affects to the niosome stabilities.

To select the appropriate cationic lipid/DNA ratios for the *in vitro* assays, we added DNA to the niosomes at different cationic lipid/DNA ratios (w/w) to form the nioplexes that were characterized by charge and size. A clearer decrease in the zeta potential value was observed in the three niosome formulations when DNA was added at a cationic lipid/DNA mass ratio of 1/1 (Fig. 3 lines). Interestingly, in all nioplexes formulations, zeta potential values increased proportionally to the cationic lipid/DNA mass ratio, reaching the maximum values at the highest cationic lipid/DNA ratio 30/1 (+8 mV, +10 mV and +22 mV for nioplexes based on lipid 1, 2 and 3, respectively). Positively charged nioplexes can easily interact with the negatively charged cell surface, which induces early steps of the endocytosis process and increases transfection efficiency [10]. Regarding the size of nioplexes, results

showed that the increase of the cationic lipid /DNA ratios from 1:1 to 30:1 did not significantly affect to the final size (Fig. 3 bars). In general, most of the nioplexes showed a final size value less than 200 nm, which has been reported to be adequate for intracellular uptake and transfection purposes [11].

As an optimum balance between DNA condensation and release is mandatory to both enhance transfection efficiency [12] and protect DNA against enzymatic digestion [13], we performed an agarose gel electrophoresis assay to analyze the interaction between the niosomes based on the three cationic lipids and the DNA. At cationic lipid/DNA mass ratios 6/1, the zeta potential values of nioplexes were slightly negatives for lipid 1 and 2 and positive for lipid 3. Therefore, we selected 6/1, 10/1, 20/1 and 30/1 ratios to perform the agarose gel electrophoresis studies (Fig. 4).

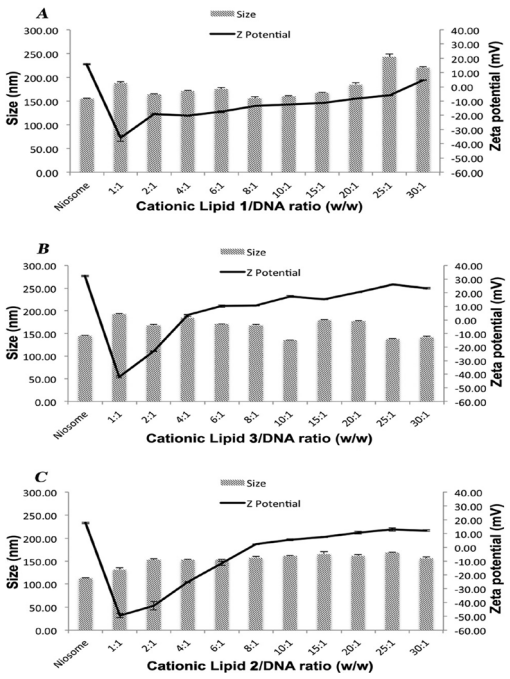

Figure 3. The influence of the cationic lipid/DNA ratio (w/w) on the particle size (bars) and zeta potential (lines) of niosomes based on: A) lipid 1, B) lipid 3 and C) lipid 2. Each value represents the mean ± standard deviation of three measurements.

The data showed that all studied ratios of nioplexes based on cationic lipid 1 failed to condense the DNA (Fig. 4A). Subsequently, deficient protection of DNA against enzymatic digestion and an easy DNA release were observed (Fig. 4A). Based on these data, we could anticipate the poor performance of nioplexes based on lipid 1 for the next *in vitro* transfection experiments. Nioplexes based on the cationic lipid 2 clearly failed to protect the DNA at all ratios (Fig. 4C), despite the fact that niosomes properly condensed and released the DNA (Fig. 4C). Therefore, we hypothesize that electrostatic interactions between the cationic lipid 2 and DNA are effective to condense the DNA, but are not strong enough to protect the DNA against enzymatic digestion. Regarding nioplexes based on the lipid 3, we observed a proportionally protection and condensation increase with the increase of cationic lipid/DNA mass ratios (Fig. 4B). Moreover, the nioplexes at all cationic lipid mass ratios were able to release the DNA. These results reveals that electrostatic interactions between niosomes based on the lipid 3 and DNA are strong enough to condense DNA (Fig. 4B), but at the same

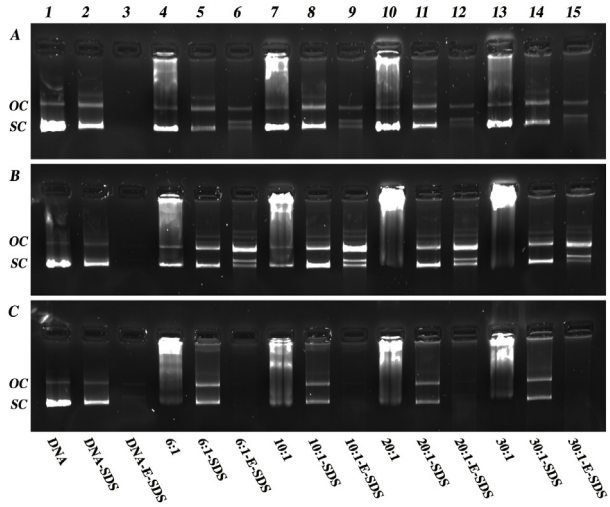

Figure 4. Binding, protection, and SDS-induced release of DNA from niosomes at different cationic lipid/DNA ratios (w/w) visualized by agarose electrophoresis. OC: open circular form, SC: supercoiled form. Lanes 1-3 correspond to free DNA; lanes 4-6, cationic lipid/DNA ratio 6/1; lanes 7-9, cationic lipid/DNA ratio 10/1; lanes 10-12, cationic lipid/DNA ratio 20/1; lanes 13-15, cationic lipid/DNA ratio 30/1. Nioplexes were treated with SDS (lanes 2,5,8,11 and 14) and DNase I + SDS (lanes 3,6,9,12 and 15). A) Nioplexes based on cationic lipid 1, B) Nioplexes based on cationic lipid 3, C) Nioplexes based on cationic lipid 2.

time DNA can be easily released from the niosomes, which is an optimal condition for gene delivery purposes [14].

One single vector is unlikely to be optimal for all applications since gene delivery is a cell dependent process [15,16]. Therefore, it is necessary to study and evaluate the transfection efficiency of the vectors in different cell lines, as we have presented in the current study. Human embryonic kidney cells (HEK-293) have been extensively used as a well known and easy to transfect cell model [17]. Human retinal pigment epithelial cells (ARPE-19), which are more difficult to transfect cells [18], are essential cells for neural retina homeostasis and play a major role in genetic ocular diseases associated with senescence and dystrophies of the photoreceptors [19]. Finally, mesenchymal stem cells (MSC-D1) have shown flattering characteristics for different medicine applications due to their capacity for differentiation (osteocytes, chondrocytes or adipocytes) and their ability to produce immunosuppression upon transplantation. Therefore, MSC-D1 cells represent an attractive model for the development of safe non-viral vectors carriers [20].

Transfection results indicated that only those nioplexes based on cationic lipid 3 showed relevant percentages of transfection (Fig. 5A). At different cationic lipid/DNA mass ratio studied, the highest percentages were obtained in HEK-293, reaching 33% of transfection at the cationic lipid/DNA ratio 10/1. This value is clearly superior to the

maximum transfection values obtained in both ARPE-19 (8% at 10/1 ratio) and MSC-D1 cells (1% at 20/1 ratio). Such differences found on transfection values among the cells could be explained by the different cell line dependent barriers that nucleic acids need to face before reaching the cellular machinery for protein synthesis, such as cellular uptake, structural changes caused by interactions with cellular lipids and posterior intracellular trafficking processes [21-24]. We can also mention that these differences observed in the transfection efficiency mediated by the different niosome formulations could also be attributed to several causes, such as particle hydrophobicity, electrostatic interactions, lipid structures, or formation of aggregates between nioplexes [25,26], which can be directly related to the chemical structure of the polar head-group of the cationic lipid. Therefore, minor structural changes performed in the cationic lipid head-groups, for example the inclusion of one additional methylene moiety, were able to change significantly gene transfer efficiencies [27].

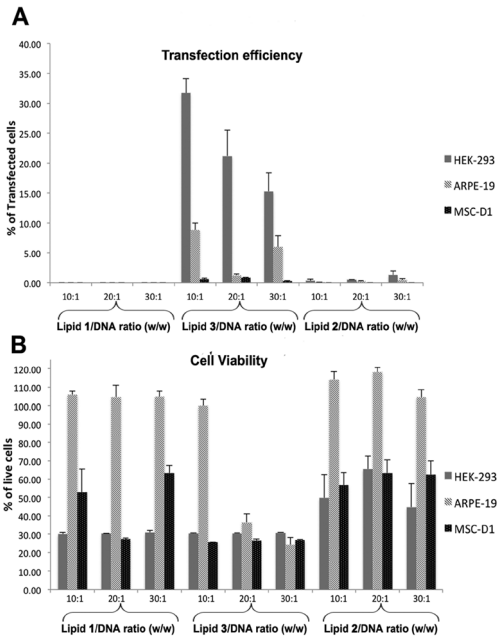

Figure 5. *In vitro* transfection experiments of nioplexes based on cationic lipids 1, 3 and 2 in HEK-293, ARPE-19 and MSC-D1 cells. A) Transfection efficiency at different cationic lipid/DNA ratios (w/w). B) Cell viability at different cationic lipid/DNA ratio (w/w).

Moreover, we hypothesized that the presence of dimethylamino derivatives, as hydrophilic cationic head-group (lipid 3, Fig. 1), were able to show efficient cellular uptake of pDNA, probably, due to the easiness of these amino lipids to ionize, based on pKa=6.72 of lipid 3, and the tendency to interact with biomembranes [28,29]. It must be highlighted that this possible effect could not only depend on the cationic lipid 3 since other compounds, such as the helper lipid, squalene, can also help and increase the gene delivery by promoting the hexagonal phase for membrane fusion and endosome swelling [30]. On the other hand, the lack of cell transfection activity of nioplexes based on lipid 1 and 2 could be attributed to the molecular shape of the cationic lipids that might be unable to adopt the hexagonal morphology and become more stabilized [31]. Moreover, these results also evidenced that pKa constant is a necessary, but not sufficient condition to achieve worthy DNA delivery into the cell [29].

The introduction of foreign DNA into the cell is not a natural process. Therefore, transfection is an inherent toxic process by itself. Additionally, cationic lipids toxicity is a highly cell dependent process that has been classically attributed to the induction of apoptosis and could limit the application in the clinic [32]. Regarding cell viability results, we observed a clearly cell-dependent toxicity effect, where toleration of ARPE-19 cells was higher compared to HEK-293 and MSC-D1 cells in most cationic lipid/DNA ratios studied (Fig. 5B). Cell-dependent toxicity effect observed could be caused due to differences in membrane composition as well as differences in phagocytic activity and processing of the nioplexes among the studied cells. Regarding the cytotoxic effect among our three nioplexes formulations, we clearly observed that nioplexes based on the cationic lipid 3 showed a more deleterious effect than their counterparts, especially in ARPE-19 cells (Fig. 5B). This toxic effect of nioplexes based on the cationic lipid 3 could be explained by the higher zeta potential of these vectors (Fig. 2 line), which could destabilize cell membranes.

To summarize, our data revealed that cationic lipid chemical structure of the hydrophilic head-group clearly influenced not only on transfection efficiency, but also on cell viability. Therefore, the detailed study of this domain is a mandatory issue for the research community to design more efficient and safe non-viral vectors based on cationic lipids.

6.2. THE INFLUENCE OF THE POLAR HEAD-GROUP OF GLYCEROL BASED SYNTHETIC CATIONIC LIPIDS ON THE TRANSFECTION EFFICIENCY MEDIATED BY NIOSOMES

Since the previously obtained results with the serinol based backbone cationic lipids showed promising transfection results (Fig. 1), but at the same time these cationic lipids exhibited a toxic effect on the studied cell lines, we decided, in this second approach, to made structural modification to the previous three cationic lipids. Specifically, these changes were made within the structural backbone, where the serinol backbones of the cationic lipids were substituted by glycerol backbones (Fig. 6) for their study as glycerol building block cationic lipids and to investigate further additional effects that could govern transfection efficiency processes when increased the polar-pendent group.

Once the glycerol backbone cationic lipids 1, 2 and 3 were successfully synthesized (Fig. 6), we prepared the niosomes by o/w emulsion and film-hydration techniques to determine the most suitable technique to prepare niosomes. Resulted niosomes were characterized in terms of size, PDI, zeta potential and morphology. The characterization results showed that zeta potential values were similar in both techniques for the niosomes based on lipid 1 and 3 (Fig. 7 lines). On the other hand, for the niosomes prepared with the lipid 2, there was a considerable difference of 20 mV in the zeta potential between the two

techniques. In any case, all niosome formulations exhibited positive zeta values over 30 mV (Fig. 7 lines), which enhanced the formation of stable suspensions due to the repulsion among the positively charged particles [9]. Additionally, these positive charges also allow an easy interaction with the negatively charged cell surfaces to increase cell uptake [33].

Regarding particle size, we did not find remarkable differences between the niosomes when they were elaborated by the o/w emulsion or film-hydration technique (Fig.7 bars). In all cases, the particle size was around 200 nm. As a homogeneity parameter of the suspensions, we determined the PDI (see chapter 4 fig. 2B). Additionally, these results are similar to those obtained with the serinol backbone cationic lipids (Fig. 2), which suggest that the size of the niosomes is not strictly related to the modification of the backbone structure. Results indicated that lower PDI values were found in niosomes prepared by o/w emulsion technique (0.19, 0.17 and 0.21 for lipid 1, 2 and 3, respectively), which showed that the size distribution was narrower than the size distribution obtained by film-hydration technique (0.35, 0.99 and 0.56 for lipid 1, 2 and 3, respectively). Since it has been previously reported that narrow distribution of the PDI values enhances the uptake and posterior internalization process of the nanoparticles [7,34], we decided to discard the niosomes prepared by the film-hydration technique for the following experiments and continue with the niosomes prepared by o/w emulsion technique. The morphology of niosomes based on the three cationic lipids elaborated by the o/w emulsion technique was analyzed by Cryo-TEM,

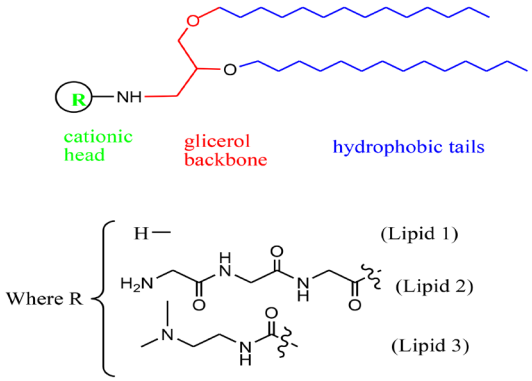

Figure 6. Chemical structures of cationic lipids.
Lipid 1: 2, 3-bis (tetradecyloxy) propan-1-amine
Lipid 2: 2-amino-N-(((((2, 3-bis (tetradecyloxy) propyl) carbamoyl) methyl) carbamoyl) methyl) acetamide
Lipid 3: 1-(2-dimethylaminoethyl)-3-[2,3-di (tetradecoxy) propyl] urea

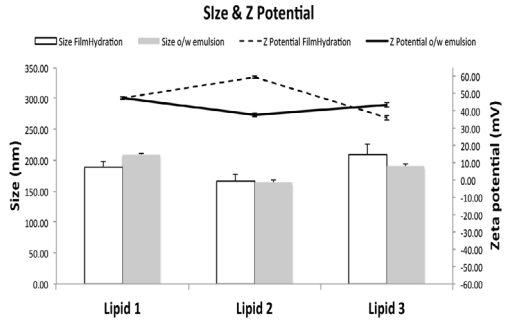

Figure 7. Physicochemical characterization of niosomes based on lipid 1, 2 and 3. A) Z-average (cumulants) size (white and gray bars, which correspond to niosomes prepared by film-hydration and o/w emulsion techniques, respectively) and zeta potential values (dotted and continuous lines which correspond to niosomes prepared by film-hydration and o/w emulsion techniques, respectively). Each value represents the mean ± standard deviation of three measurements.

and it was observed that all niosomes adopted a spherical and homogeneous morphology.

As previously mentioned, the physical stability of niosomes can vary according to the temperature, storage time and the cationic lipid chemical structure. Since structural modifications were effectuated in these new cationic lipids, we performed the stability assay of the niosomes. The analysis was determined as previously described. Regarding zeta potential data, all the niosomes stored at 4ºC did not show relevant changes. On the other hand, when formulations were stored at 25ºC, remarkable decreases on the zeta potential values were found in all niosome formulations. This decrease of zeta potential values at 25ºC can be explained by the re-orientation of crystalline structure of the lipids at high temperatures that is followed by a change on the particle surface, which reduces the zeta potential [35]. Concerning about the size of the niosomes, they remained stable for all conditions at 4ºC. However at 25ºC storage temperature, niosomes based on lipid 3 increased their size to 250 nm after 100 days. This increase of the particle size can be caused by gradual diminution of the positive charges of the particles that decreases electrostatic repulsion and generates aggregates [9]. In general, more stable formulations over the time in terms of size and charge were achieved at 4ºC. At this temperature condition, the high charges avoid the formation of niosome aggregates due to electrostatic repulsion forces. These findings about the zeta potential and size of the niosomes suggest that storage temperature plays an important role in the stability of our niosomes. Moreover, these data also highlighted the influence of the polar head-groups in the physical stability of niosomes, where the effect is more evident in the zeta potential values at 25ºC. These results are similar to those observed in previous reported data with the serinol backbone cationic lipids [36].

To determine an appropriate cationic lipid/DNA ratio, we prepared different nioplexes by the addition of DNA to the niosomes at different cationic lipid/DNA ratios (w/w) and characterized them in terms of charge and size (Fig. 8). The results showed a significant decline in zeta potential values in the three niosomes formulations when DNA was added at 1/1 cationic lipid/DNA mass ratio (w/w) (Fig. 8 lines). However, we observed a constant increment of the zeta potential values in all nioplexes formulations with the increment of cationic lipid/DNA proportion. The maximum positive zeta potential values were observed at 30/1 cationic lipid/DNA ratio (w/w) (+35 mV, +31 mV and +27 mV for nioplexes based on lipids 1, 2 and 3, respectively). Our data showed a clear correlation between the cationic lipid/DNA ratios and the superficial charge of the nioplexes, as previously reported with the serinol cationic lipid backbones [36]. Hence, we could establish an appropriate ratio between cationic lipid and DNA to reach positive values, so that nioplexes could interact easily with negatively charged cell membranes. Concerning about the size, the three niosome formulations did not present relevant differences at mass ratios from 1/1 to 30/1 (Fig. 8 bars). In general, most of

the nioplexes showed a final size below 200 nm, which is a suitable size for the cell internalization process [37].

To analyze the electrostatic interactions between the niosomes based on the cationic lipids 1, 2 and 3 and the DNA, we performed an agarose gel electrophoresis assay to study the DNA condensation, DNA release and the capacity of niosomes to protect DNA against enzymatic digestion (Fig. 9). Based on zeta potential and size data, we selected 6/1, 10/1, 20/1 and 30/1 cationic lipid/DNA ratios (w/w) to perform the agarose gel electrophoresis studies since at cationic lipid/DNA ratios below 6/1, the zeta potential values were negative (Fig. 8 lines). First, regarding nioplexes based on cationic lipid 1 (Fig. 9A), the results showed deficient condensation of DNA. Moreover, DNA was easily released from the niosomes at mass ratios 6/1 and 10/1, as a possible consequence of poor condensation. We also found that at mass ratios 20/1 and 30/1 there was a weak release of DNA. This effect was probably due to high zeta potential values (around +32mV) obtained at those ratios. In addition, protection of DNA was observed at all mass ratios. Second, regarding nioplexes based on the cationic lipid 2 (Fig. 9B), all ratios were able to condensate the DNA. The presence of several amino groups in this lipid may be the cause of this level of condensation. On the other hand, the release of DNA at all mass ratios was difficult, even at lower ratios. Concerning about DNA protection from DNase, we observed reasonable protection at all ratios. Finally, nioplexes based on the cationic lipid 3 (Fig. 9C) indicated that high DNA condensation was only observed with nioplexes at 30/1 cationic lipid/DNA ratio (w/w), probably due to the zeta potential values obtained at this ratio (+27 mV). Moreover, niosomes based on cationic lipid 3 were able to release the DNA, especially at low ratios (6/1 and 10/1). Concerning about protection against enzymatic digestion, nioplexes showed that DNA was properly protected in all cases. To

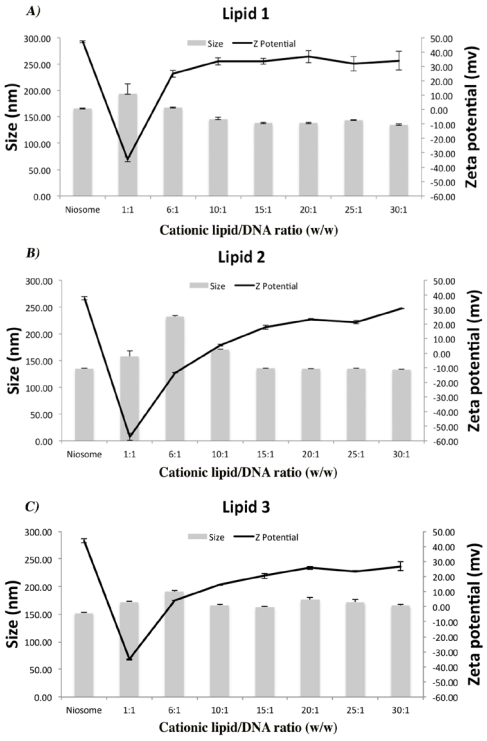

Figure 8. The influence of the cationic lipid/DNA ratio (w/w) on the particle Z-average (cumulants) size (bars) and zeta potential (lines) of nioplexes based on: (A) lipid 1, (B) lipid 2 and (C) lipid 3. Each value represents the mean ± standard deviation of three measurements.

summarize, data obtained from agarose gel electrophoresis studies, suggested that nioplexes based on the three cationic lipids, at low ratios (6/1) were less efficient to condensate, release and protect the DNA against enzymatic digestion. Thus, these outcomes indicated that nioplexes based on lipid 1, 2 and 3 at ratios (w/w) 10/1, 20/1 and 30/1 were more suitable to succeed in further transfection experiments.

To analyze the transfection efficiencies and toxicity of the selected nioplexes, we carried out *in vitro* assays in the following cells: HEK-293 cells, as general cell model, ARPE-19 cells, as retinal cell model for possible *in vivo* applications in retina, and PECC

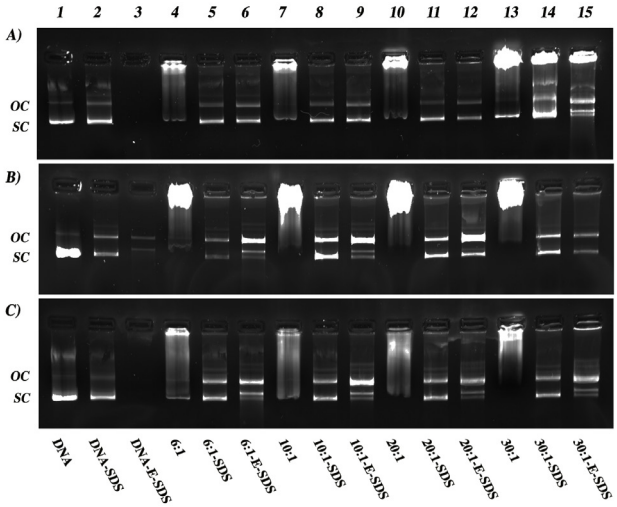

Figure 9. Binding, protection, and SDS-induced release of DNA from nioplexes at different lipid/DNA (w/w) ratios visualized by agarose electrophoresis. OC: open circular form, SC: supercoiled form. Lanes 1-3 correspond to free DNA; lanes 4-6, cationic lipid/DNA ratio 6/1; lanes 7-9, cationic lipid/DNA ratio 10/1; lanes 10-12, cationic lipid/DNA ratio 20/1; lanes 13-15, cationic lipid/DNA ratio 30/1. Nioplexes were treated with SDS (lanes 2,5,8,11 and 14) and DNase I + SDS (lanes 3,6,9,12 and 15). A) Nioplexes based on lipid 1, B) nioplexes based on lipid 2 and C) nioplexes based on lipid 3.

primary cells from rat embryonic cerebral cortex, as neurons and glial model cells for the potential use of nioplexes in the brain. The data obtained from the nioplexes based on the cationic lipid 1 showed that the highest percentage of transfection efficiencies were obtained in HEK-293 cells (around 21%), followed by ARPE-19 cells (around 18%) at 20/1 mass ratio (Fig. 10A). It must be highlighted that in our previous work, this same lipid 1, but with serinol-based backbone cationic lipid (Fig. 1), showed null transfection efficiency in HEK-293, ARPE-19 and MSC-D1 cell lines (Fig. 5A) [36]. These findings suggest that small structural changes in the lipid (serinol by glycerol building block) (Fig. 1 and 6) are enough

to influence dramatically on transfections efficiencies (Fig. 5A and 10A). On the other hand, transfection in PECC cells were around 3% for all mass ratios, which was the lowest percent observed within the three types of cells. For nioplexes based on lipid 2, the highest percentage of transfected cells (13%) was observed in HEK-293 cells at 20/1 mass ratio (Fig. 10A). However, low transfection efficiencies were registered in ARPE-19 and PECC cells. Similar results were also observed in previous reported data with its analogous serinol backbone cationic lipid [36], where the cationic lipid formed by longer polyamine chains and more amino nitrogen atoms did not precisely enhanced cell transfection in HEK-293 and ARPE-19 cells (Fig. 5A). These outcomes are probably due to self-folded conformation that disfavor effective interaction with DNA. It also must be emphasized that presence of more than one carbonyl group in the polar head-group seems to be also an impediment for efficient cell transfections [38,39]. Regarding nioplexes based on lipid 3, high transfection percentages (around 20%) were obtained in HEK-293 and ARPE-19 cells at 30/1 mass ratio. Furthermore, interesting data were obtained in PECC cells, especially at 30/1 mass ratio, where transfection was around 5% (Fig. 10A). Cultured neurons are among the most difficult cells to transfect since they tend to die soon after transfection due to their sensitivity to micro-environmental changes. Typical transfection efficiencies in this kind of cells have been reported around 5% [40]. Interestingly, relevant transfection data in HEK-293, ARPE-19 and MSC-D1 cells were also observed with a similar cationic lipid that has the same molecular formula, but different structural backbone conformation (serinol backbone, fig. 5A) [36]. In addition, this structural relationship between lipids and transfection has been previously reported by different authors [38,39,41], which have described that slight lipid structure modification can provoke cell transfection variations.

Cell toxicity is another important issue that has to be addressed for the development of any novel drug delivery system. Therefore, we studied the cell viability with our formulations (Fig. 10B). The results indicated that only HEK-293 cells showed high viabilities with nioplexes prepared with lipid 1 at all mass ratios. On the other hand, the most toxic effect was observed with the lipid 3 followed by the lipid 2. Better toleration in ARPE-19 and PECC cells was found with nioplexes at all studied ratios (100 % of viability). It must be stressed that toxicity effect is, generally, a cell dependent process, where every cell type shows different tolerance levels [42]. Furthermore, the structure design of the cationic lipids also influences on the cell viability, such as small changes on the polar head-groups or backbones can induce different levels of cytotoxicity [36,43]. This cell toxicity level is clearly observed in our previous work with similar cationic lipids, but with a structural modification in the backbone structure, where cationic lipids with serinol backbone resulted in less cell viability percentages (Fig 5B and 10B). It is worth mentioning that cationic lipids

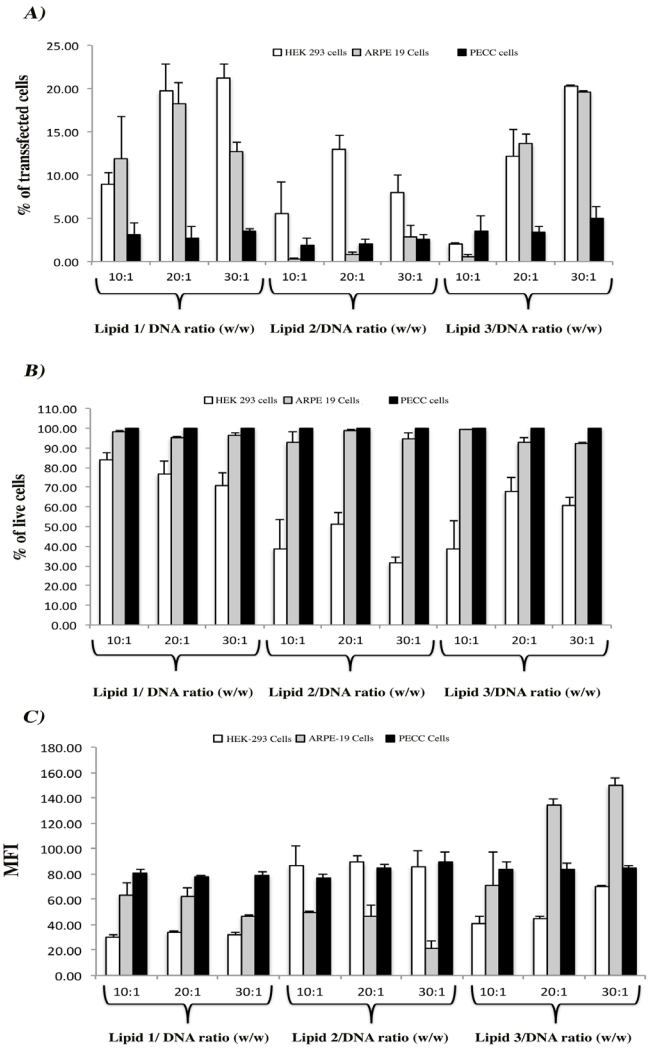

Figure 10. *In vitro* transfection experiments of nioplexes based on cationic lipid 1, 2 and 3 in HEK-293, ARPE-19 and PECC cells. A) Transfection efficiency at different cationic lipid/DNA ratios (w/w). B) Cell viability at different cationic lipid/DNA ratios (w/w). C) MFI of transfected cells with nioplexes based on cationic lipid 1, 2 and 3 in HEK-293, ARPE-19 and PECC cells at different cationic lipid/DNA ratios (w/w).

that contain one or three hydrocarbonated alkyl chains tend to be more toxic and show poor transfection efficiencies [44].

To describe more precisely the transfection efficiencies of our formulations, we analyzed the MFI of the EGFP expressed in the transfected cells (Fig. 10C). Results obtained from the nioplexes based on cationic lipid 1 showed that low MFI were observed in HEK-293 (around 30) and in ARPE-19 cells (around 40) at all tested mass ratios. On the other

hand, PECC cells showed higher MFI (around 80) at the three studied mass ratios. Based on the data from nioplexes prepared with the cationic lipid 2, MFI in HEK-293 and PECC cells were around 89 at the different analyzed mass ratios On the other hand, ARPE-19 cells showed the lowest MFI. Results from nioplexes prepared with lipid 3 revealed that HEK-293 cells showed lower EGFP expression (MFI around 60). However, ARPE-19 cells showed the highest MFI (149) at 30/1 mass ratio. The MFI obtained from PECC cells was around 80, which was similar to those observed with the other two cationic lipids. Essentially, these results indicated that nioplexes based on cationic lipid 3 stimulated higher EGFP expression in ARPE-19 transfected cells and suitable expression of EGFP in PECC and HEK-293 transfected cells at 30/1 mass ratio. Likewise, differences in membrane composition among cell lines can also influence cellular uptake and posterior intracellular trafficking processes of the vectors [24].

Taking into account these data, nioplexes based on cationic lipid 1 and 3 showed better percentages of transfection in ARPE-19 and PECC cells (Fig. 10A). These results also indicate that polar head-groups of the cationic lipids play a fundamental role in transfection efficiencies. In addition, cell toxicity assay showed a cell dependent toxicity effect rather than a polar head-group effect, where major toxicity effect was observed in HEK-293 cells (Fig. 10B). For MFI assay, the most relevant data were obtained from cationic lipid 3 (Fig. 10C), which in general expressed high levels of EGFP in the cells. Thus, we decided to use niosomes based on lipid 3 as the most appropriate system for further *in vivo* experiments.

We carried out *in vivo* studies to evaluate EGFP expression in the rat retina after subretinal and intravitreal injections (Fig. 11, 12), which are clinically viable options to deliver genetic material to the retina [45]. Results of the subretinal injection of nioplexes based on cationic lipid 3 at 30/1 mass ratio revealed substantial protein expression, mainly observed in photoreceptors and in some nuclei in the outer nuclear layer (Fig. 11). Transfection at this level could be of great interest since most of the inherited retinal diseases, such as Stargat Disease, Retinitis Pigmentosa, Age-related Macular Degeneration or Leber Congenital Amaurosis, are classically associated to mutations in genes expressed in photoreceptors and outer nuclear layers of the retina [1]. Concerning intravitreal injection, we

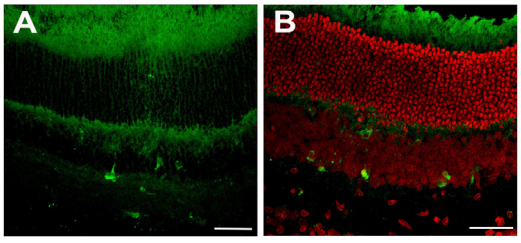

Figure 11. EGFP gene expression in retina 3 days after subretinal injection of nioplexes based on lipid 3 at mass ratio 30/1 cationic lipid/DNA. A), B) Retinal sections showing EGFP expression mainly in photoreceptors and in some nuclei in the outer nuclear layer (ONL). Cell nuclei were counterstained with Hoechst 33342 (red color) in B and C. Scale bars A, B= 40 μm; C= 25 μm.

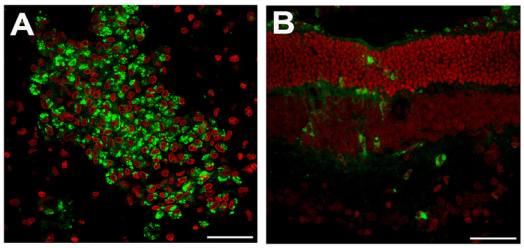

Figure 12. EGFP gene expression in retina 3 days after intravitreal injection of nioplexes based on lipid 3 at mass ratio 30/1 cationic lipid/DNA. A) Wholemount preparation showing EGFP+ cell bodies located in the ganglion cell layer (GCL). B) Retinal cross sections. EGFP expression was detected throughout the whole retina although mainly in inner layers. Cell nuclei were counterstained with Hoechst 33342 (red color). Scale bar = 40μm.

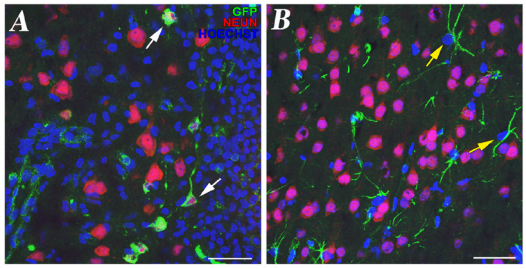

Figure 13. *In vivo* gene expression of EGFP 3 days after the administration of nioplexes based on lipid 3 at 30/1 mass ratio cationic lipid/DNA. A and B panels show triple labeling; nuclei are shown in blue (Hoechst), neurons in red (NeuN+), and EGFP expressed in cells (GFP+) in green. A) Several of the identified neurons (red) that express EGFP (green) in the membrane at their cell bodies and dendritic trees are indicated by white arrows. B) Several of the non-neuron cells (NeuN-) with glia morphology that express EGFP (green) through their processes are indicated by yellow arrows. Scale bar = 40μm.

found a good and uniformly distributed EGFP expression, mainly in the ganglion cell layer and inner layers of the retina 3 days after intravitreal injection of nioplexes based on cationic lipid 3 at 30/1 mass ratio (Fig. 12). These outcomes suggest that nioplexes did not aggregate with the negatively charged components of the vitreous humor, such as glycosamineglycanes, due to the possible effect of the PEG chains of the polysorbate 80 to prevent aggregations that could interact with fibrilar structures in the vitreous [14,46]. These results could be of great interest to treat some genetic pathologies of the retina such as glaucoma [47]. Interestingly, we detected some protein expression in the retinal pigmented epithelium, which after intravitreal injection clearly represents a great challenge for retinal gene therapy to avoid the subretinal injection and the subsequent possible harm to the sensitive neural tissue [48]. Additionally, we decided to evaluate the capacity of nioplexes based on lipid 3 at 30/1 mass ratio to transfect the rat cerebral cortex. Based on the analysis, we identified high levels of GFP expression in neurons, including dendritic trees, and glial cells throughout the dendritic processes in the area next to the injection site (Fig. 13). Even though the delivery of genetic material to the nervous system cells by non-viral vectors remains as a challenge, our nioplexes were able to transfect glial cells and neurons in the primary visual cortex *in vivo* without affecting the animals during the 3 days of the experimental period. Since in this preliminary study nioplexes transfected more glial cells than neurons, we suggest that cell division of glial cells and the CMV promoter of pCMS-EGFP plasmid could be involved in the transfection

process [49]. Therefore, the use of our nioplexes combined with plasmids holding different promoters might allow targeting different cell populations of the nervous system and enhance cell transfection to treat different genetic population deficits. Overall, our results open a safe alternative to the treatment of neurodegenerative diseases, such as Parkinson or Alzheimer, where effective pharmacotherapy treatments are still under development [3,50].

6.3. THE ROLE OF HELPER LIPIDS IN THE INTRACELLULAR DISPOSITION AND TRANSFECTION EFFICIENCY OF NIOSOME FORMULATIONS

Interestingly, the dimethylaminoethyl pendant group (Fig. 1 and 6, lipid 3) has shown optimal pKa values, which normally benefits the release of the delivery system cargo in the presence of acid pH caused by late endosomes (pH 6.5) or lysosomes (pH 4.5). Thus, obtaining favorable transfection efficiencies. Moreover, this mechanism does not only concern to the cationic lipids, but also to the rest of the niosome compounds, such as the helper lipid. In light of the promising transfection results *in vitro* and *in vivo* obtained with optimized formulations based on the glycerol-based cationic lipid with dimethylaminoethyl polar head-group, we decided to analyze the role of the helper lipids by alternating squalene, cholesterol, squalane or non-helper lipid in the niosome formulations.

Size characterization (Fig. 14 bars) indicated that niosomes based on squalene and cholesterol showed similar size (147 and 176 nm, respectively). Niosomes based on squalane showed the biggest size (259 nm) and niosomes prepared without helper lipid the smallest size (61 nm). As a homogeneity parameter for the niosome formulations, we determined the polydispersity index. Such results indicated PDI values below 0.372, which showed appropriate size homogeneity. Zeta potential values indicated that all niosome formulations were positively charged (Fig. 14 lines) (squalene-niosomes and squalane-niosome +50 mV, cholesterol-niosomes +40 mV and non-helper-niosomes +32 mV).

The cationic lipid/DNA ratio w/w employed to form the nioplexes was the result from the previous characterization study, where the ratio 30/1 was the most appropriated [51]. The size of the nioplexes showed that the addition of DNA to niosomes to form nioplexes does not remarkably modify the original size of the niosomes (Fig. 14 bars), probably due to the high DNA condensation capacity of all formulations. All the nioplexes showed acceptable PDI values lower than 0.369. The addition of the negatively charged DNA to niosomes decreased the zeta potential of all nioplexes formulations, especially in the case of nioplexes prepared without helper lipid (Fig. 14 lines). This reduction on the superficial charge could be explained, in part, by the partial neutralization of the cationic charge carried by niosomes by the negatively charged DNA molecules. In any case, all nioplexes were positively charged (Fig. 14 lines), which suggest that at this cationic lipid/DNA mass ratio (30/1, w/w) free

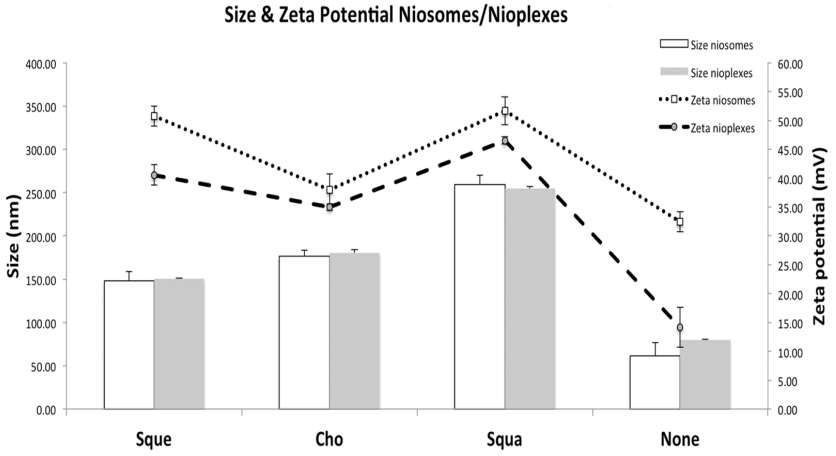

Figure 14. Physico-chemical characterization of niosomes and nioplexes (niosome/DNA w/w ratio 30/1) prepared with different helper lipids: squelene (Sque), cholesterol (Cho), squalane (Squa) and without helper lipid (None). Size (white bars) and zeta potential (dot line) of niosomes. Size (gray bars) and zeta potential (dash lines) of nioplexes. Each value represents the mean ± standard deviation of three measurements.

DNA was not present on the formulation. Collectively, our data shows that size and zeta potential results are compatible with DNA binding to niosome surfaces [52]. The addition of DNA to the niosomes did not remarkably modify the particle sizes, which were adequate for cellular uptake and internalization purposes [53,54]. Regarding zeta potential, it must be highlighted that all formulations showed positive zeta potential values, which enhances not only the formation of stable suspensions due to the electrostatic repulsion between the positively charged particles [9] but also the interaction with negatively charged cell surfaces and the subsequences cell uptake processes [33].

Since a delicate balance between the DNA bound to niosomes, release and protection is necessary for gene delivery applications, we performed an agarose gel assay to analyze such parameters (Fig 15). The results indicated that nioplexes based on squalene showed deficient DNA condensation and easy release of DNA, which could be the consequence of poor condensation. DNA enzymatic digestion data showed that nioplexes based on squalene were able to protect the DNA. In the case of nioplexes based on cholesterol, we observed that they were able to condensate the DNA, to partially release it and to protect it from enzymatic digestion. The analysis of nioplexes based on squalane, indicated high DNA condensation, probably, due to their high zeta potential values (+46 mV). Moreover, these nioplexes were able to release the DNA efficiently. Concerning DNA protection against enzymatic digestion, these nioplexes showed that DNA was properly protected. Finally, nioplexes prepared without helper lipid, despite their low zeta potential values (+14 mV), showed

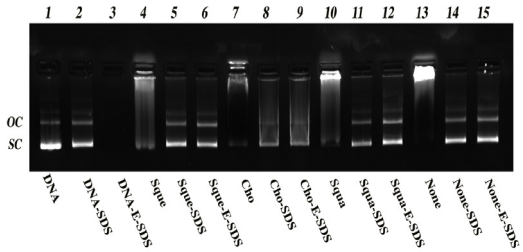

Figure 15. Binding, SDS-induced release and protection of DNA prepared with different helper lipids: squelene (Sque), cholesterol (Cho), squalane (Squa), without helper lipid (None). OC: open circular form, SC: supercoiled form. Lanes 1-3 correspond to free DNA; lanes 4-6, nioplexes based on squalene; lanes 7-9, nioplexes prepared with cholesterol; lanes 10-12, nioplexes based on squalane; lanes 13-15, nioplexes prepared without helper lipid. Naked DNA and nioplexes were treated with SDS (lanes 2,5,8,11 and 14) and DNase I + SDS (lanes 3,6,9,12 and 15).

high DNA condensation capacity, where it seemed that the absence of helper lipids in the formulations could increase the condensation of DNA at low zeta potential values (Fig. 14 lines). Additionally, there was a satisfactory release and protection of DNA from enzymatic digestion.

In vitro assays were carried out in ARPE-19 cells since these retinal cells play a major role in retinal diseases associated with senescence and dystrophies of the photoreceptors [19]. Therefore, to gain knowledge in the gene carrier design, we conducted transfection, viability and cellular uptake studies of niosomes in this cell line. Gene expression in the cell nucleus is an indication that the DNA has been properly delivered by the vector. However, this process can involve, sometimes, few number of cells, which can be inadequate for gene therapy purposes. Therefore, our aim is to transfect as many cells as possible without compromising the cellular viability.

Our results showed that the highest percentages values of transfected cells were obtained with squalene-nioplexes (31%), followed by squalane-nioplexes (14%). The lowest transfection values were obtained with cholesterol-nioplexes and non-helper lipid-nioplexes (2%) (Fig. 16A bars). Therefore, as reported in the literature, transfection efficiency is strongly linked to the chemical composition of the helper lipids [55,56]. The above results could be explained, in part, by the endosomal scape capacity of the helper lipids [57]. This capability has been attributed to the structural transition that helper lipids offer to the delivery system. Such structural transition usually goes from lamellar to inverse hexagonal due to the acid environment of the endosomes, where the transition induces the release of the DNA and its subsequent delivery into the cytoplasm [58,59]. Additionally, analyzed MFI data showed that nioplexes prepared with squalene showed the highest MFI, around 70 (Fig. 16B). On the other hand, despite the low percentage of transfected cells observed with nioplexes prepared with the other three formulations, we found interesting MFI data that suggested that the few number of transfected cells were able to produce significant amounts of EGFP. The capacity of nioplexes based on squalene to transfect more efficiently ARPE-

19 cells might also rely on the fact that squalene is usually synthesized in the cells, which could indicate that cells easily recognized it and subsequently increased its cell permeability [60-62]. Since we have recently reported that niosomes based on squalene helper lipid transfected efficiently the rat retina and brain [51,63], we hypothesize that nioplexes prepared with squalene could have taken the advantages of this helper lipid properties.

Additionally, to develop efficient drug delivery systems, it is important to consider the possible toxic effect of these vectors upon the targeted cells since cell viability can depend on the vector composition [36,43]. Therefore, the effect of our niosome formulations on ARPE-19 cells was studied (Fig 16A dots). Cell viability results showed high viabilities with all the nioplexes formulations (around 90%), which indicated high cell tolerability with all the helper lipids used in each formulation.

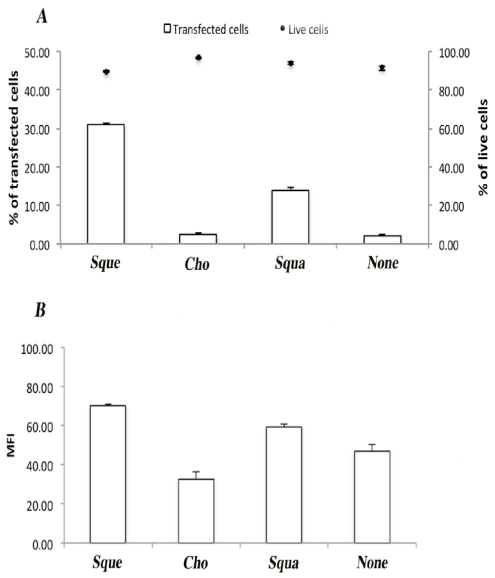

Figure 16. Transfection efficiencies at 72 h post-addition of nioplexes prepared with different helper lipids: squalene (Sque), cholesterol (Cho), squalane (Squa) and without helper lipid (None) in ARPE-19 cells. A) Percentage of transfection (bars) and viability (dots) of nioplexes. B) Mean fluorescence intensity (MFI) of cells with nioplexes prepared with different helpers. Each value represents the mean ± standard deviation of three measurements.

Cell uptake analysis is another important assay that helps to understand part of the transfection process and shows the capacity of the nioplexes to be internalized when they are in contact with the cells. Cell uptake results showed that squalene-nioplexes were practically internalized by all the cells, while the other nioplexes also showed worthy cell uptake levels (around 75 %) (Fig. 17 black bars). To show a better insight into the cell uptake process, we analyzed the MFI as well. Our results showed that squalene-nioplexes showed the highest MFI (Fig. 17 white bars). Thus, our cellular uptake studies indicated that nioplexes based on squalene were internalized in most of the analyzed cell population, and the amount of nioplexes internalized in each cell was superior compared to the rest of formulations. Regarding this point, we can discard the possibility that the high MFI value of niosomes based on squalene could be due to the high particle size rather than the number of particles internalized since size data showed homogeneous size around 150 nm. Moreover, we could

discard the hypothesis that only Cy3-labelled DNA enters the cell without the niosomes since agarose gel assay showed that all DNA was bound to the niosomes. Additionally, fluorescent confocal microscopy images showed that immediately after administration (t<5 min) (Data not shown), DNA appeared to be confined within punctate spot-like structure, while no evidence of diffuse fluorescence was found. This finding unambiguously suggested that, at the early stages of internalization, DNA was encapsulated within niosomes vesicles.

Additionally, squalene has shown, in other studies, to increase the phagocytic activity of cells due to its capacity to potentiate the immune response in a non-toxic manner [64,65]. Furthermore, some authors have reported that squalene increases oxygenation in the cells, which results in a more efficient metabolic process [66]. Therefore, a more efficient and easy uptake of nioplexes could be performed when squalene was used as helper lipid in the formulations.

Among many other parameters, cell uptake could also depend on physico-chemical parameters of the niosomes such as the particle size, where bigger size particles (>500 nm) are difficult and slowly taken, contrary to smaller particles (40 nm), which are easily and rapidly captured [67]. However, our results indicated that the lowest cell uptake value was obtained from the smallest particles (79 nm, non-helper lipid-nioplexes), and the most efficient cellular uptake was obtained with bigger nioplexes (around 150 nm, squalene and cholesterol-nioplexes) (Fig. 14 bars). These data suggest that not only size is determinant in the cellular uptake but the helper lipid composition as well.

To develop more efficient non-viral vectors it is also necessary to understand their intracellular trafficking mechanism and how their physico-chemical properties might trigger

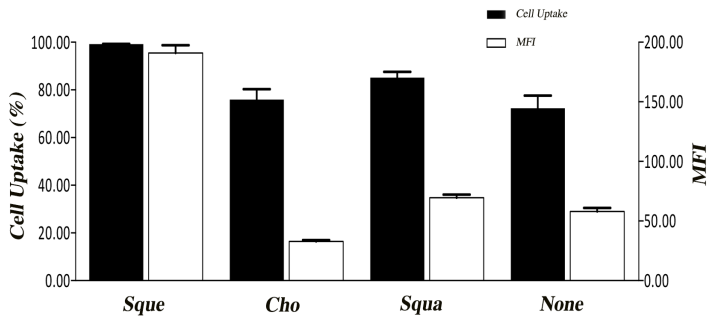

Figure 17. Cellular uptake at 1 h after the addition of nioplexes prepared with different helper lipids: squalene (Sque), cholesterol (Cho), squalane (Squa) and without helper lipid (None) in ARPE-19 cells. Uptake percentage of cells upon the addition of nioplexes (Black bars). Mean fluorescence intensity (MFI) of cells with nioplexes prepared with different helpers (White bars). Each value represents the mean ± standard deviation of three measurements.

different internalization pathways. Thus, in the following experiments, we have investigated the intracellular traffic of nioplexes formulations and how this process influences the transfection efficiency in ARPE-19 cells in the presence of various endocytic markers (Fig. 18A and 19A). The degree of colocalization was calculated by Mander´s overlap coefficient to perform a quantitative analysis of confocal images (Fig. 18B and 19B).

The precise correlation between the mechanism of cell uptake, final intracellular fate and transfection efficiency of nioplexes has been poorly investigated so far. In this regard, our results provided new insights into the relationship between intracellular trafficking and transfection efficiency of nioplexes. Squalene-containing nioplexes were largely internalized via macropinocytosis, followed in minor degree by CvME and CME (Fig. 18B Sque), while they efficiently exhibited scape from endosomal compartments (Fig. 19B Sque) and

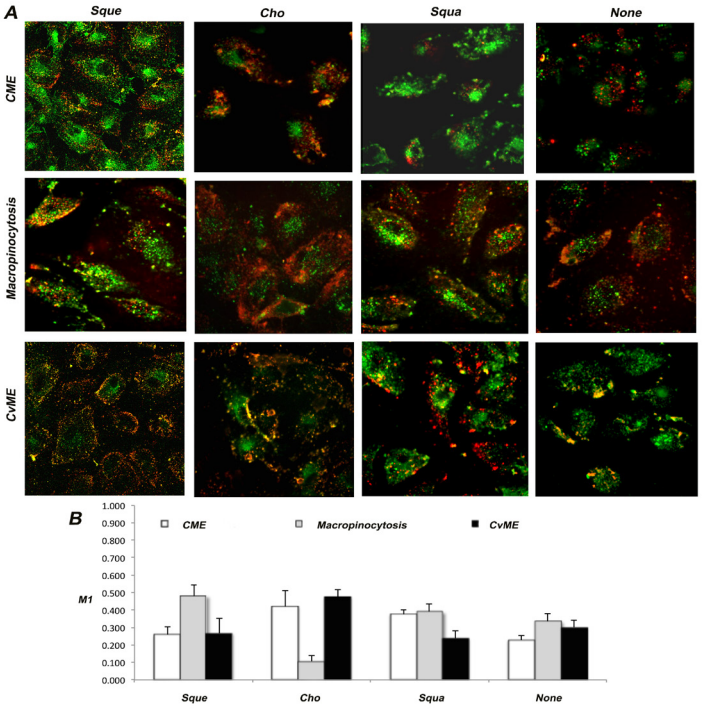

Figure 18. Cell trafficking results in ARPE-19 cells co-incubated with nioplexes prepared with squalene (Sque), cholesterol (Cho), squalane (Squa) and without helper lipid (None). A) Confocal microscopy merged images showing the cells co-incubated with nioplexes. Each image displayed in the optical section was representative of the cell population. Green coloring shows cells stained with Transferrin Alexa Fluor 488 for CME, Dextran Alexa Fluor 488 for macropinocytosis and Cholera toxin B Alexa Fluor 488 for CvME. Red coloring shows the DNA stained with Cy3. For interpretation of the referenced colors in this figure legend, the reader is referred to the web version of the article. B) Colocalization values were given as the fraction of cell-associated nanoparticles colocalizing with fluorescently labeled endocytic structures. M1 is equal to Mander´s overlap coefficient between the red signal from the stained DNA and the green fluorescence of the stained entry pathways. Each value represents the mean ± standard deviation of three measurements.

showed high transfection efficiency (Fig. 16A Sque). On the opposite, poorly efficient cholesterol-containing nioplexes, CME and CvME were highly involved (Fig. 18B Cho), and macropinocytosis was weakly activated. Moreover cholesterol-containing nioplexes were largely degraded in lysosomes (Fig. 19B Cho). It also should be pointed out that CvME is mainly considered a non-digestive pathway. However, some findings suggest that this route is also involved in the lysosomal fusion [68]. Aside from clarifying the exact molecular aspects of this correlation, it seems that macropinocytosis could be a preferred internalization route of efficient nioplexe formulations. This observation might explain the superior transfection efficiency of nioplexes prepared with squalene and provides a reasonable explanation for the low transfection efficiency of cholesterol-based nioplexes (Fig. 16A bars). However, it has been suggested that CME and macropinocytosis are correlated to the lysosomal fusion, which could partial or entirely degrade the content of their vesicles [53,69]. Nevertheless, our findings suggest, in excellent agreement with previous data [70], that macropinocytosis is the main pathway of internalization of highly efficient niosome/DNA complexes, where it has been also described that there is a recycling process of the vesicles when macropinocytosis is involved (i.e. macropinosome is sent back to the cell exterior) [71]. In any case, further experiments with specific inhibitors of the pathways studied, such as chlorpromazine, filipin or ethylisopropylamiloride, could help us to clarify our hypothesis. Squalane-containing nioplexes exhibited an endocytic pattern similar to nioplexes prepared with squalene. Nevertheless, squalane-containing systems were less efficient than their squalene-enriched

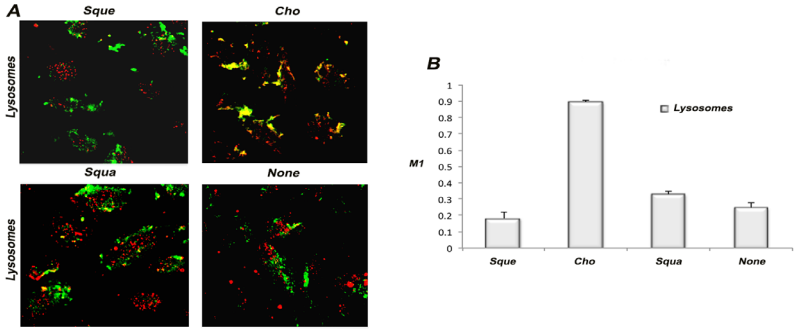

Figure 19. Lysosome colocalization results in ARPE-19 cells co-incubated with nioplexes prepared with squalene (Sque), cholesterol (Cho), squalane (Squa) and without helper lipid (None). Niosomes were complex with DNA stained with Cy3. A) Confocal microscopy merged images showing cells co-incubated with nioplexes prepared with different helper lipids. Each image displayed in the optical section was representative of the cell population. Green and red coloring show cells stained with Lysotracker® Green and the DNA, respectively. For interpretation of the referenced colors in this figure legend, the reader is referred to the web version of the article. B) The colocalization values were given as the fraction of cell-associated nanoparticles colocalizing with fluorescently labeled lysosomes, where M1 is equal to Mander´s overlap coefficient between the red signal from the stained DNA and the green fluorescence of the stained lysosomes. Each value represents the mean ± standard deviation of three measurements.

counterpart. This result was, likely, due to less involvement of macropinocytosis, as larger colocalization of complexes with lysosomes (Fig. 19B Squa) was observed. In the absence of helper lipid, results showed that despite all entry pathways were used simultaneously (Fig. 18B None), at the same degree, and low accumulation within acidic lysosomes (Fig. 19 None), the nioplexes were poorly efficient. These results suggest that to circumvent the lysosomal degradation with well condensate DNA, which is supported by the agarose gel results, is not enough to release the cargo effectively.

In general, we have hypothesized that the larger the involvement of macropinocytosis, the higher the transfection efficiency. Moreover, the transfection efficiency of squalene-containing nioplexes was probably due to the positive charge density of the cationic lipid that increased in the acidic environment of the endosome, which destabilizes the cell membrane, letting the formation of pairs of ions between the cationic lipid and phospholipids in the endosomal membrane. Along with the squalene, this process could have also promoted from a lamellar to hexagonal transition in the cationic lipid that might disrupt the membrane and destabilize bilayers [63].

6.4. REFERENCES

1. Lipinski DM, Thake M, MacLaren RE. Clinical applications of retinal gene therapy. Prog Retin Eye Res 2013;32:22-47.

2. Bennett J, Ashtari M, Wellman J, Marshall KA, Cyckowski LL, Chung DC, et al. AAV2 gene therapy readministration in three adults with congenital blindness. Sci Transl Med 2012;4:120ra15.

3. Simonato M, Bennett J, Boulis NM, Castro MG, Fink DJ, Goins WF, et al. Progress in gene therapy for neurological disorders. Nat Rev Neurol 2013;9:277-291.

4. Kanasty R, Dorkin JR, Vegas A, Anderson D. Delivery materials for siRNA therapeutics. Nat Mater 2013;12:967-977.

5. Semple SC, Akinc A, Chen J, Sandhu AP, Mui BL, Cho CK, et al. Rational design of cationic lipids for siRNA delivery. Nat Biotechnol 2010;28:172-176.

6. Tros de Ilarduya C, Sun Y, Duzgunes N. Gene delivery by lipoplexes and polyplexes. Eur J Pharm Sci 2010;40:159-170.

7. Caracciolo G, Caminiti R, Digman MA, Gratton E, Sanchez S. Efficient escape from endosomes determines the superior efficiency of multicomponent lipoplexes. J Phys Chem B 2009;113:4995-4997.

8. Huang Y, Rao Y, Chen J, Yang VC, Liang W. Polysorbate cationic synthetic vesicle for gene delivery. J Biomed Mater Res A 2011;96:513-519.

9. Caracciolo G, Amenitsch H. Cationic liposome/DNA complexes: from structure to interactions with cellular membranes. Eur Biophys J 2012;41:815-829.

10. Resina S, Prevot P, Thierry AR. Physico-chemical characteristics of lipoplexes influence cell uptake mechanisms and transfection efficacy. PLoS One 2009;4:e6058.

11. Ferrari A, Pellegrini V, Arcangeli C, Fittipaldi A, Giacca M, Beltram F. Caveolae-mediated internalization of extracellular HIV-1 tat fusion proteins visualized in real time. Mol Ther 2003;8:284-294.

12. Delgado D, del Pozo-Rodriguez A, Solinis MA, Rodriguez-Gascon A. Understanding the mechanism of protamine in solid lipid nanoparticle-based lipofection: the importance of the entry pathway. Eur J Pharm Biopharm 2011;79:495-502.

13. Midoux P, Monsigny M. Efficient gene transfer by histidylated polylysine/pDNA complexes. Bioconjug Chem 1999;10:406-411.

14. Ochoa GP, Sesma JZ, Diez MA, Diaz-Tahoces A, Aviles-Trigeros M, Grijalvo S, et al. A novel formulation based on 2,3-di(tetradecyloxy)propan-1-amine cationic lipid combined with polysorbate 80 for efficient gene delivery to the retina. Pharm Res 2014;31:1665-1675.

15. Gao X, Huang L. A novel cationic liposome reagent for efficient transfection of mammalian cells. Biochem Biophys Res Commun 1991;179:280-285.

16. Leventis R, Silvius JR. Interactions of mammalian cells with lipid dispersions containing novel metabolizable cationic amphiphiles. Biochim Biophys Acta 1990;1023:124-132.

17. Thomas P, Smart TG. HEK293 cell line: a vehicle for the expression of recombinant proteins. J Pharmacol Toxicol Methods 2005;51:187-200.

18. del Pozo-Rodriguez A, Delgado D, Solinis MA, Gascon AR, Pedraz JL. Solid lipid nanoparticles for retinal gene therapy: transfection and intracellular trafficking in RPE cells. Int J Pharm 2008;360:177-183.

19. Bejjani RA, BenEzra D, Cohen H, Rieger J, Andrieu C, Jeanny JC, et al. Nanoparticles for gene delivery to retinal pigment epithelial cells. Mol Vis 2005;11:124-132.

20. Corsi K, Chellat F, Yahia L, Fernandes JC. Mesenchymal stem cells, MG63 and HEK293 transfection using chitosan-DNA nanoparticles. Biomaterials 2003;24:1255-1264.

21. del Pozo-Rodriguez A, Pujals S, Delgado D, Solinis MA, Gascon AR, Giralt E, et al. A proline-rich peptide improves cell transfection of solid lipid nanoparticle-based non-viral vectors. J Control Release 2009;133:52-59.

22. Pozzi D, Caracciolo G, Caminiti R, De Sanctis SC, Amenitsch H, Marchini C, et al. Toward the rational design of lipid gene vectors: shape coupling between lipoplex and anionic cellular lipids controls the phase evolution of

lipoplexes and the efficiency of DNA release. ACS Appl Mater Interfaces 2009;1:2237-2249.
23. Pozzi D, Marchini C, Cardarelli F, Rossetta A, Colapicchioni V, Amici A, et al. Mechanistic understanding of gene delivery mediated by highly efficient multicomponent envelope-type nanoparticle systems. Mol Pharm 2013;10:4654-4665.
24. Pozzi D, Marchini C, Cardarelli F, Salomone F, Coppola S, Montani M, et al. Mechanistic evaluation of the transfection barriers involved in lipid-mediated gene delivery: interplay between nanostructure and composition. Biochim Biophys Acta 2014;1838:957-967.
25. Brunner S, Sauer T, Carotta S, Cotten M, Saltik M, Wagner E. Cell cycle dependence of gene transfer by lipoplex, polyplex and recombinant adenovirus. Gene Ther 2000;7:401-407.
26. Lin AJ, Slack NL, Ahmad A, George CX, Samuel CE, Safinya CR. Three-dimensional imaging of lipid gene-carriers: membrane charge density controls universal transfection behavior in lamellar cationic liposome-DNA complexes. Biophys J 2003;84:3307-3316.
27. Singh RS, Chaudhuri A. Single additional methylene group in the head-group region imparts high gene transfer efficacy to a transfection-incompetent cationic lipid. FEBS Lett 2004;556:86-90.
28. Heyes J, Palmer L, Bremner K, MacLachlan I. Cationic lipid saturation influences intracellular delivery of encapsulated nucleic acids. J Control Release 2005;107:276-287.
29. Jayaraman M, Ansell SM, Mui BL, Tam YK, Chen J, Du X, et al. Maximizing the potency of siRNA lipid nanoparticles for hepatic gene silencing *in vivo*. Angew Chem Int Ed Engl 2012;51:8529-8533.
30. Goni FM, Alonso A. Membrane fusion induced by phospholipase C and sphingomyelinases. Biosci Rep 2000;20:443-463.
31. Smisterova J, Wagenaar A, Stuart MC, Polushkin E, ten Brinke G, Hulst R, et al. Molecular shape of the cationic lipid controls the structure of cationic lipid/dioleylphosphatidylethanolamine-DNA complexes and the efficiency of gene delivery. J Biol Chem 2001;276:47615-47622.
32. Yingyongnarongkul BE, Radchatawedchakoon W, Krajarng A, Watanapokasin R, Suksamrarn A. High transfection efficiency and low toxicity cationic lipids with aminoglycerol-diamine conjugate. Bioorg Med Chem 2009;17:176-188.
33. Rezvani Amin Z, Rahimizadeh M, Eshghi H, Dehshahri A, Ramezani M. The effect of cationic charge density change on transfection efficiency of polyethylenimine. Iran J Basic Med Sci 2013;16:150-156.
34. Gratton SE, Ropp PA, Pohlhaus PD, Luft JC, Madden VJ, Napier ME, et al. The effect of particle design on cellular internalization pathways. Proc Natl Acad Sci U S A 2008;105:11613-11618.
35. Heurtault B, Saulnier P, Pech B, Proust JE, Benoit JP. Physico-chemical stability of colloidal lipid particles. Biomaterials 2003;24:4283-4300.
36. Ojeda E, Puras G, Agirre M, Zarate J, Grijalvo S, Pons R, et al. Niosomes based on synthetic cationic lipids for gene delivery: the influence of polar head-groups on the transfection efficiency in HEK-293, ARPE-19 and MSC-D1 cells. Org Biomol Chem 2015;13:1068-1081.
37. Rejman J, Oberle V, Zuhorn IS, Hoekstra D. Size-dependent internalization of particles via the pathways of clathrin- and caveolae-mediated endocytosis. Biochem J 2004;377:159-169.
38. Takeuchi K, Ishihara M, Kawaura C, Noji M, Furuno T, Nakanishi M. Effect of zeta potential of cationic liposomes containing cationic cholesterol derivatives on gene transfection. FEBS Lett 1996;397:207-209.
39. Fujiwara T, Hasegawa S, Hirashima N, Nakanishi M, Ohwada T. Gene transfection activities of amphiphilic steroid–polyamine conjugates. Biochimica et Biophysica Acta (BBA) - Biomembranes 2000;1468:396-402.
40. Karra D, Dahm R. Transfection Techniques for Neuronal Cells. The Journal of Neuroscience 2010;30:6171-6177.
41. Paecharoenchai O, Niyomtham N, Apirakaramwong A, Ngawhirunpat T, Rojanarata T, Yingyongnarongkul BE, et al. Structure relationship of cationic lipids on gene transfection mediated by cationic liposomes. AAPS PharmSciTech 2012;13:1302-1308.
42. Sohaebuddin SK, Thevenot PT, Baker D, Eaton JW, Tang L. Nanomaterial cytotoxicity is composition, size, and cell type dependent. Part Fibre Toxicol 2010;7:22-8977-7-22.

43. Martin B, Sainlos M, Aissaoui A, Oudrhiri N, Hauchecorne M, Vigneron JP, et al. The design of cationic lipids for gene delivery. Curr Pharm Des 2005;11:375-394.
44. Byk G, Dubertret C, Escriou V, Frederic M, Jaslin G, Rangara R, et al. Synthesis, activity, and structure--activity relationship studies of novel cationic lipids for DNA transfer. J Med Chem 1998;41:229-235.
45. Conley SM, Naash MI. Nanoparticles for retinal gene therapy. Prog Retin Eye Res 2010;29:376-397.
46. Peeters L, Sanders NN, Braeckmans K, Boussery K, Van de Voorde J, De Smedt SC, et al. Vitreous: a barrier to nonviral ocular gene therapy. Invest Ophthalmol Vis Sci 2005;46:3553-3561.
47. Liu X, Rasmussen CA, Gabelt BT, Brandt CR, Kaufman PL. Gene therapy targeting glaucoma: where are we? Surv Ophthalmol 2009;54:472-486.
48. Charbel Issa P, MacLaren RE. Non-viral retinal gene therapy: a review. Clin Experiment Ophthalmol 2012;40:39-47.
49. Kugler S, Kilic E, Bahr M. Human synapsin 1 gene promoter confers highly neuron-specific long-term transgene expression from an adenoviral vector in the adult rat brain depending on the transduced area. Gene Ther 2003;10:337-347.
50. Tsuji S. Genetics of neurodegenerative diseases: insights from high-throughput resequencing. Hum Mol Genet 2010;19:R65-70.
51. Ojeda E, Puras G, Agirre M, Zarate J, Grijalvo S, Eritja R, et al. The influence of the polar head-group of synthetic cationic lipids on the transfection efficiency mediated by niosomes in rat retina and brain. Biomaterials 2015;77:267-279.
52. Caracciolo G, Caminiti R. DNA–DNA electrostatic interactions within cationic lipid/DNA lamellar complexes. Chemical Physics Letters 2004;400:314-319.
53. Xiang S, Tong H, Shi Q, Fernandes JC, Jin T, Dai K, et al. Uptake mechanisms of non-viral gene delivery. J Control Release 2012;158:371-378.
54. Gillard M, Jia Z, Hou JJ, Song M, Gray PP, Munro TP, et al. Intracellular trafficking pathways for nuclear delivery of plasmid DNA complexed with highly efficient endosome escape polymers. Biomacromolecules 2014;15:3569-3576.
55. Chung H, Kim TW, Kwon M, Kwon IC, Jeong SY. Oil components modulate physical characteristics and function of the natural oil emulsions as drug or gene delivery system. J Controlled Release 2001;71:339-350.
56. Kim YJ, Kim TW, Chung H, Kwon IC, Sung HC, Jeong SY. The effects of serum on the stability and the transfection activity of the cationic lipid emulsion with various oils. Int J Pharm 2003;252:241-252.
57. Pozzi D, Marchini C, Cardarelli F, Amenitsch H, Garulli C, Bifone A, et al. Transfection efficiency boost of cholesterol-containing lipoplexes. Biochim Biophys Acta 2012;1818:2335-2343.
58. Zuhorn IS, Bakowsky U, Polushkin E, Visser WH, Stuart MC, Engberts JB, et al. Nonbilayer phase of lipoplex-membrane mixture determines endosomal escape of genetic cargo and transfection efficiency. Mol Ther 2005;11:801-810.
59. Allain V, Bourgaux C, Couvreur P. Self-assembled nucleolipids: from supramolecular structure to soft nucleic acid and drug delivery devices. Nucleic Acids Res 2012;40:1891-1903.
60. Liu GC, Ahrens EH,Jr, Schreibman PH, Crouse JR. Measurement of squalene in human tissues and plasma: validation and application. J Lipid Res 1976;17:38-45.
61. Koivisto PV, Miettinen TA. Increased amounts of cholesterol precursors in lipoproteins after ileal exclusion. Lipids 1988;23:993-996.
62. Stewart ME. Sebaceous gland lipids. Semin Dermatol 1992;11:100-105.
63. Puras G, Mashal M, Zarate J, Agirre M, Ojeda E, Grijalvo S, et al. A novel cationic niosome formulation for gene delivery to the retina. J Control Release 2014;174:27-36.
64. Seubert A, Monaci E, Pizza M, O'Hagan DT, Wack A. The adjuvants aluminum hydroxide and MF59 induce monocyte and granulocyte chemoattractants and enhance monocyte differentiation toward dendritic cells. J Immunol 2008;180:5402-5412.
65. Allison AC, Byars NE. An adjuvant formulation that selectively elicits the formation of antibodies of protective

isotypes and of cell-mediated immunity. J Immunol Methods 1986;95:157-168.
66. Reddy LH, Couvreur P. Squalene: A natural triterpene for use in disease management and therapy. Adv Drug Deliv Rev 2009;61:1412-1426.
67. dos Santos T, Varela J, Lynch I, Salvati A, Dawson KA. Quantitative assessment of the comparative nanoparticle-uptake efficiency of a range of cell lines. Small 2011;7:3341-3349.
68. Kiss AL, Botos E. Endocytosis via caveolae: alternative pathway with distinct cellular compartments to avoid lysosomal degradation? J Cell Mol Med 2009;13:1228-1237.
69. Luzio JP, Parkinson MD, Gray SR, Bright NA. The delivery of endocytosed cargo to lysosomes. Biochem Soc Trans 2009;37:1019-1021.
70. Cardarelli F, Pozzi D, Bifone A, Marchini C, Caracciolo G. Cholesterol-dependent macropinocytosis and endosomal escape control the transfection efficiency of lipoplexes in CHO living cells. Mol Pharm 2012;9:334-340.
71. Lim JP, Gleeson PA. Macropinocytosis: an endocytic pathway for internalising large gulps. Immunol Cell Biol 2011;89:836-843.

7

Conclusions

7. CONCLUSIONS

According with the results obtained in the previously described experiments, the main conclusions of this work include:

1. The chemical composition of the cationic head-groups, clearly, affects the physicochemical parameters of the niosomes along with their transfection efficiency and cell viability. Only niosomes based on cationic lipids with dimethyl amino head-group showed acceptable transfection efficiencies when it was compared to their counterparts amino and tripeptide head-groups. In any case, the most efficient polar head-group was the worst tolerated by the cells. Such toxicity could be attributed to the ether bonds in the serinol structural backbones of the cationic lipids which are poorly biodegradable.

2. Niosomes based on cationic lipid with the glycerol backbone and the dimethyl amino head-group transfected efficiently *in vitro* brain and retinal cells. Moreover, these niosomes were able to transfect *in vivo* brain cells after administration in the cerebral cortex and retinal cells after subretinal and intravitreal administrations. The subretinal administration mainly transfected photoreceptors and the outer nuclear layer and the intravitreal administration mainly transfected the inner layers.

3. The helper lipids in the niosome formulations affected not only to the physicochemical properties of bared and DNA loaded niosomes, but also to relevant biological processes related to the transfection efficiencies. Niosomes elaborated with squalene as helper lipid showed the highest efficiency to transfect ARPE-19 cells that could be mainly attributed to their high cellular uptake and the posterior employed entry pathway, where macropinocytosis and lysosomal elution played an important role. Overall, our study brings new insights into the role of helper lipids towards the development of highly efficient niosome formulations as non-viral gene delivery vectors for the treatment of inherited retinal diseases.

ANNEX I

Elaboration and physicochemical characterization of niosome-based nioplexes for gene delivery purposes

Elaboration and physicochemical characterization of niosome-based nioplexes for gene delivery purposes

Ojeda, E[1,2], Agirre, M[1,2], Villate, I[1,2], Mashal, M[1], Puras, G[1,2], Zarate, J[1,2] and Pedraz, JL[1,2]

[1]NanoBioCel Group, University of the Basque Country (UPV-EHU), Vitoria-Gasteiz, Spain
[2]Biomedical Research Networking Center in Bioengineering, Biomaterials and Nanomedicine (CIBER-BBN), Vitoria-Gasteiz, Spain

Accepted for publication: Springer 2016

SUMMARY

Niosomes formulations for gene delivery purposes are based on non-ionic surfactants, helper lipids and cationic lipids that interact electrostatically with negatively charged DNA molecules to form the so-called nioplexes. Niosomes are elaborated by different techniques, such as solvent emulsion-evaporation, thin film hydration, hand-shaking, dissolvent injection and microfluidization method, among many others. In this chapter, we have described some protocols for the elaboration of niosomes and nioplexes and their physicochemical characterization that guarantees the quality criteria of the formulation in terms of size, morphology, ζ-potential and stability.

Keywords: Niosomes, gene delivery, non-viral vector, cationic lipid, non-ionic surfactant, transfection

1. INTRODUCTION

Niosomes are drug delivery systems that form vesicles with a bilayer structure and represent an alternative to liposomes where the phospholipids of the liposomes have been substituted by non-ionic surfactants [1]. Compared to liposomes, niosomes are recognized for their low cost and superior chemical and storage stabilities. Niosomes have been widely used as carrier vectors to deliver chemotherapy drugs, peptides, antigens and hormones. Additionally, niosomes are also recognized as gene delivery vectors to promote the desirable gene expression [2]. Consequently, many research groups have focused their attention on the use of niosomes as non-viral carriers for gene delivery [3].

Niosomes formulations for gene delivery purposes are based on 1) non-ionic surfactants, such as tween 80, brij, span, that play an important role in terms of toxicity and stability. Moreover, these non-ionic surfactants do not have any charge in their head-groups, which makes no interference with the charge of the niosomes [2]. 2) helper lipids, such as cholesterol or squalene, which enhance the physicochemical properties of the lipid emulsion as they can modify the morphology, permeability, storage time, nucleic acid release and stability of the formulation [4,5] and finally, 3) cationic lipids that interact electrostatically with negatively charged nucleic acid to form nioplexes, whose structural and physical properties clearly influence the transfection efficiency and toxicity of the final nioplexes [6]. These cationic lipids contain four functional domains: 1) Hydrophobic group: this group is usually derived from aliphatic hydrocarbon chains and often contains two linear aliphatic chains because it has been reported that cationic lipids containing one or three carbon chains tend to be more toxic and show poor transfection efficiencies [7]. 2) Linker group: this part affects the flexibility, stability, and biodegradability of the cationic lipid and, its length determines the level of hydration. Thus, it has been hypothesized that the replacement of the ether bonds by ester bonds in the cationic lipids could lead to a better tolerated niosome formulation since ether bonds are too stable to be biodegraded [8]. 3) Backbone: it separates the polar head-group from the hydrophobic group; serinol and glycerol groups are the most popular units [9]. 4) Hydrophilic head-group: this domain is responsible for the interaction and condensation of the nucleic acid to form nioplexes due to electrostatic interactions. Additionally, this domain especially affects transfection efficiencies and it clearly affects to the stability and physicochemical parameters of the niosomes [6,10].

Once the niosomes and nioplexes are prepared, it is important to characterize them to ensure that the formulations meet our needs. Such characterization can be defined in terms of size, size distribution, morphology, ζ-potential and stability, among many others [6].
In this chapter, we will describe step by step our laboratory protocols to prepare niosomes for gene delivery purposes, formation of nioplexes and their subsequent characterization.

2. MATERIALS AND METHODS

2.1. Material

Prepare and use all reagents at room temperature (RT). Carefully follow all the waste disposal regulations when disposing waste materials. Prepare all solutions using ultrapure water (dH2O).

1. 5 mg of the desirable cationic lipid (Fig. 2 A).
2. Polysorbate 80 (0.5% (w/w) Tween 80) (see Note 1).
3. Squalene.
4. Distilled water (dH2O).
5. Dichloromethane (DCM).
6. Sonicator (Branson Sonifier 250, Danbury) (Fig. 1 A2).
7. Microfluidizer (Microfluidics LV1) (Fig. 1 B).
8. Magnetic stirrer (Fig. 1 C2).
9. Magnetic stirring bar 1.2 cm L x 0.4 cm Ø (Fig. 1 D3).
10. Magnetic stirring bar 4 cm L x 0.8 cm Ø (Fig. 1 D2).
11. 10 mL glass beaker.
12. Spatula (Fig. 1 D1).
13. Parafilm®.
14. Two 5 mL syringes (Fig. 3 A).
15. Filters 0.05 µm Ø (spectrum laboratories, California, USA) (Fig. 1 F).
16. Clear disposable size and ζ-cell (Fig. 4 A).
17. Plasmid DNA (pDNA) pCMS-EGFP 0.5 mg/mL (PlasmidFactory).
18. Zetasizer-nano (Malvern Instruments)
19. Transfection medium Opti-MEM®

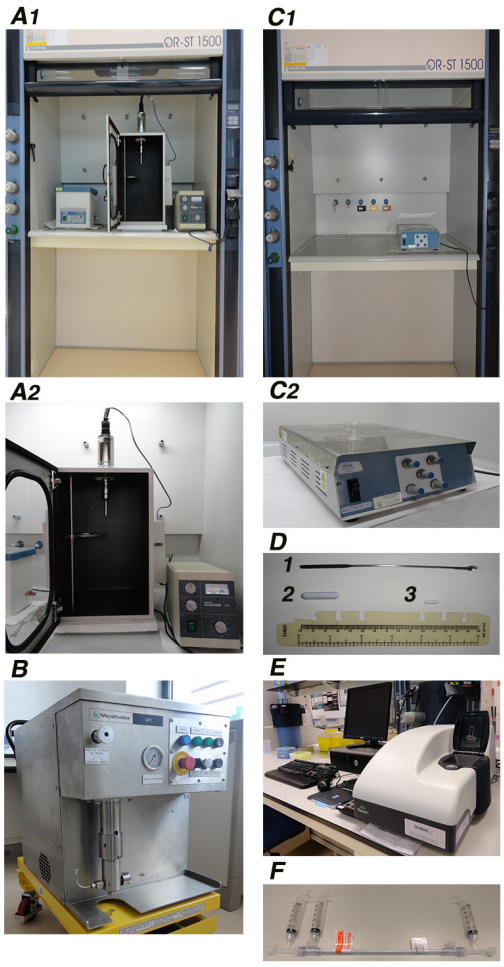

Figure 1. Required material and equipment for niosome preparation. A1) Extraction hood and sonicator, A2) sonicator, B) microfluidics, C1) extraction hood and magnetic stirrer, C2) magnetic stirrer, D1) spatula, D2) magnetic stirring bar 4 cm L x 0.8 cm Ø, D3) magnetic stirring bar 1.2 cm L x 0.4 cm Ø, E) nano Zetasizer and F) filters.

2.2. Methods

It is important to acknowledge that the techniques described below can be combined to obtain the desirable niosomes, such as the preparation of niosomes based on cationic lipids by thin film-hydration and microfluidization methods.

According to our criteria and experience preparing niosome formulations, the following techniques have been adapted from the original methods to specifically prepare cationic niosome formulations for gene delivery purposes. However, these techniques can be modified according to the employed components.

2.2.1. Niosome elaboration techniques

2.2.1.1. Solvent emulsion-evaporation technique

1. Weigh 5 mg of the cationic lipid in a 10 mL glass beaker.
2. Add 23 µL of squalene (Fig. 2 B, C).
3. Gently mix the squalene with the cationic lipid (Fig. 2 D).
4. Add, quickly, 1 mL of DCM and mix it by placing a magnetic stirring bar in the glass (Fig. 1 D3). The glass beaker must be inside the extraction hood (Fig. 1 C1).
5. When the lipid and squalene are dissolved, remove the magnetic stirring bar with the help of another magnetic stirring bar (Fig. 1 D2).
6. Add 5 mL of aqueous phase containing the non-ionic surfactant tween 80 (0.5% w/w) (Fig. 2 E).
7. Once the two phases are observed in the beaker (Fig. 2 F, G), sonicate them for 30 sec at 50 W to obtain the final emulsion (Fig. 2 H). The sonicator must be inside the extraction hood (Fig. 1 A1).
8. Remove the organic solvent from the

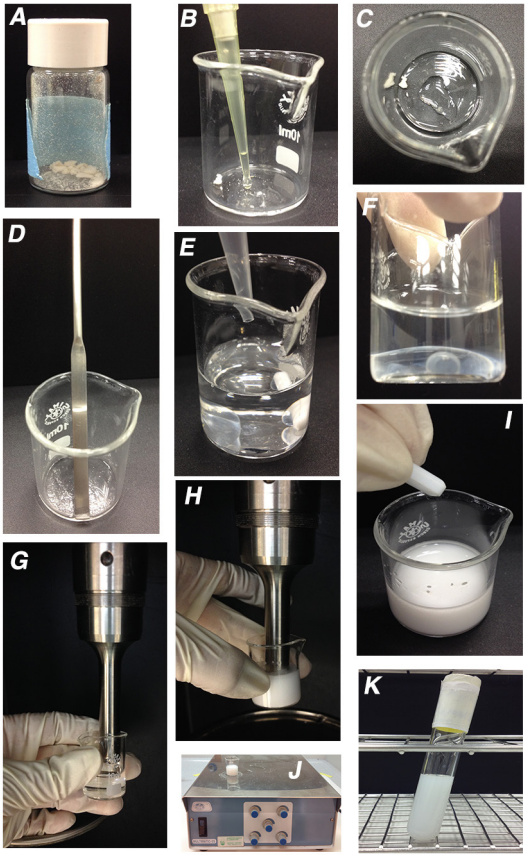

Figure 2. Material and preparation procedure for niosome elaboration. A) Cationic lipid, B) addition of squalene to cationic lipid, C) cationic lipid, squalene added, D) mix of squalene and cationic lipid, E) addition of tween 80 to the mix of squalene, cationic lipid and DCM, F) organic (at the bottom) and aqueous (at the top) phases, G) formulation previous to sonication, H) formulation post sonication, I) placing magnetic stirring bar into the formulation, J) placing the glass beaker with the emulsion on the magnetic stirrer and K) niosome formulation.

emulsion by evaporation under magnetic agitation for 3 h. (Fig. 2 I, J). The magnetic stirrer must be inside the extraction hood (Fig. 1 C1).

9. Upon DCM evaporation, a dispersion containing the nanoparticles is formed by precipitation of the cationic nanoparticles in the aqueous medium (Fig. 2 K).

10. Store the niosomes at 4ºC to keep their properties (stability depends on the storage time and temperature).

11. The final concentration is 1 mg of cationic lipid/mL (see Note 2, 3).

12. The niosomes are ready to be characterized in terms of size, PDI, ζ-potential (Fig. 1 E) and stability over the time.

2.2.1.2. Thin film-hydration technique

1. Weigh 5 mg of the cationic lipid in a 10 mL glass beaker.

2. Add 23 µL of squalene (Fig. 2 B, C).

3. Gently mix the squalene with the cationic lipid (Fig. 2 D).

4. Add, quickly, 1 mL of DCM and thoroughly mix it with a magnetic stirring bar (Fig. 1 D3) to obtain the organic phase.

5. Evaporate the solvent under magnetic agitation for 3 h. The glass beaker and magnetic stirrer must be inside the extraction hood (Fig. 1 C1).

6. When DCM has been evaporated, remove the magnetic stirring bar with the help of another magnetic stirring bar (Fig. 1 D2).

7. Hydrate the obtained lipid film with 5 mL of aqueous phase containing the non-ionic surfactant, 0.5% (w/w) tween 80.

8. Sonicate the mix for 30 sec at 50 W to obtain the emulsion (Fig. 2 H).

9. Store the niosomes at 4ºC to keep their properties (stability depends on the storage time and temperature).

10. The final concentration of cationic lipid in the formulations is 1 mg cationic lipid/mL (see Note 2 and 3).

11. Characterize the niosomes by size, PDI, ζ-potential (Fig. 1 E) and stability over the time.

2.2.1.3. Hand shaking method

1. Weigh 5 mg of the cationic lipid in a 10 mL glass beaker.

2. Add 23 µL of squalene (Fig. 2 B, C).

3. Gently mix the squalene with the lipid (Fig. 2 D).

4. Add quickly 1 mL of DCM and thoroughly mix it with a magnetic stirring bar (Fig. 1 D3) to obtain the organic phase.

5. Evaporate the solvent under magnetic agitation for 3 h. The glass beaker and magnetic

stirrer must be inside the extraction hood (Fig. 1 C1).

6. When DCM has been evaporated, remove the magnetic stirring bar with the help of another magnetic stirring bar (Fig. 1 D2).

7. Hydrate the obtained lipid film with 5 mL of aqueous phase containing the non-ionic surfactant, 0.5% (w/w) tween 80.

8. Cover the top of the beaker with parafilm and gently agitate it to form the niosomes.

9. Store the niosomes at 4ºC to keep their properties (stability dependents on storage time and temperature).

10. The final concentration is 1 mg of cationic lipid/mL (see Note 2 and 3).

11. Characterize the niosomes by size, PDI, ζ-potential (Fig. 1 E) and stability over the time.

2.2.1.4. Dissolvent injection method

1. Weigh 5 mg of the cationic lipid in a 10 mL glass beaker.

2. Add 23 μL of squalene (Fig. 2 B, C).

3. Gently mix the squalene with the lipid (Fig. 2 D).

4. Add quickly 1 mL of DCM and mix it by placing a magnetic stirring bar in the glass (Fig. 1 D3). The glass beaker must be inside the extraction hood (Fig. 1 C1).

5. When the lipid and squalene are dissolved, remove the magnetic stirring bar with the help of another magnetic stirring bar (Fig. 1 D2).

6. Pipe all the solution contained in the glass beaker.

7. In another glass beaker with one magnetic stirring bar, add 5 mL of aqueous phase containing the non-ionic surfactant 0.5% (w/w) tween 80.

8. Under magnetic agitation, slowly add the previously piped solution to the non-ionic surfactant solution glass.

9. Evaporate the solvent under magnetic agitation for 3 h. The glass beaker and magnetic stirrer must be inside the extraction hood (Fig. 1 C1).

10. Upon DCM evaporation, a dispersion containing the nanoparticles is formed by precipitation of the cationic nanoparticles in the aqueous medium (Fig. 2 K).

11. Store the niosomes at 4ºC to keep their properties (stability depends on the storage time and temperature).

12. The final concentration is 1 mg of cationic lipid/mL (see Note 2, 3).

13. The niosomes are ready to be characterized by size, PDI, ζ-potential (Fig. 1 E) and stability over the time.

2.2.1.5. Microfluidization technique

This technique is used to decrease the PDI values of the niosome preparation. Thus, resulted niosomes are more homogeneous.

1. Place the emulsion in the microfluidics (Fig. 1 B).
2. Attach the two syringes to the microfluidics conducts.
3. For the entry conduit, attach the syringe without the syringe plunger and pour the sample into it (Fig. 3 B).
4. Attach the second syringe with the syringe plunger into the exit conduit to collect the sample (Fig. 3 B).
5. Establish the desirable pressure on the central control (Fig. 3 C).
6. Load the sample into the microfluidics system (Fig. 3 D).

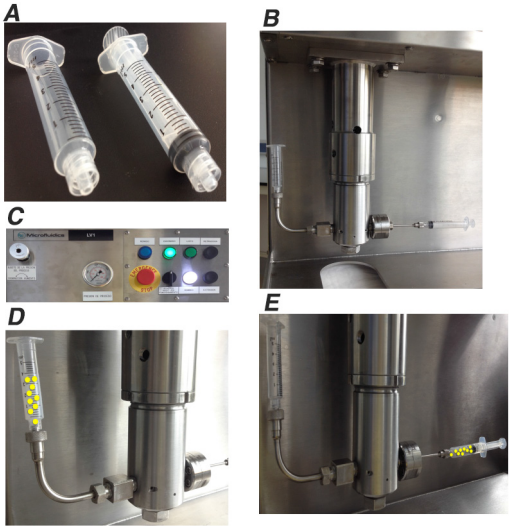

Figure 3. Material and procedure for microfluidization. A) Two 5 mL syringes, B) syringes attached to the entry and exit conduits, C) control center, D) loaded sample into the syringe in the entry conduit and E) collected niosomes in the syringe in the exit conduit.

7. The sample is ready to pass through the microfluidics.
8. When the sample has been processed, collect the niosomes in the syringe connected to the exit conduit (Fig. 3 E).
9. Store the niosomes at 4ºC to keep their properties (stability dependents on the storage time and temperature).
10. Characterize the niosomes by size, PDI, ζ-potential (Fig. 1 E) and stability over the time.

2.2.2. Preparation of nioplexes

Once the niosomes are prepared, they can be complexed with DNA to form nioplexes. The niosome/DNA proportions are expressed as the ratio of cationic lipid/DNA (w/w). In order to exemplify the preparation of nioplexes, we will use 30:1 cationic lipid:DNA ratio. Stock niosome formulation contains 1 mg cationic lipid/mL and stock pDNA solution 0.5 mg/mL.

1. In a small tube, add 30 µL of niosome formulation (30 µL = 30 µg) and add 20 µL of dH2O or transfection medium to obtain a final volume of 50 µL (see Note 4).
2. In a separate tube, add 2.5 µL of pDNA stock solution (2.5 µL =1.25 µg) and add 47.5 µL of dH2O or transfection medium to obtain a final volume of 50 µL (see Note 4).

3. Pipe all pDNA solution (50 µL) and add it to niosome solution. The final volume obtained is 100 µL (see Note 5).
4. Pipe the mix up and down 3-4 times.
5. Leave the mix 30 min. at RT to enhance electrostatic interactions between the cationic lipids and the negatively charged pDNA (see Note 6).
6. Characterize the nioplexes by size, PDI and ζ-potential (Fig. 1 E).

2.2.3. Characterization of niosomes-nioplexes

2.2.3.1. Size and polydispersity index (PDI)

Niosomes are usually spherical (Fig. 4 C) and they show different sizes according to the technique and materials used for their preparation. Additionally, differences in terms of size are also found in the same niosome suspension due to high polydispersity of the preparation. In order to analyze the size and polydispersity, we can use different instruments, such as the zetasizer-nano that measure the size of the particles by dynamic light scattering (DLS).

1. Turn the zetasizer-nano on and open the software.
2. In a small tube, add 50 µL of niosome or nioplexes (see Note 7).
3. Add 950 µL of 0.1 mM NaCl.
4. Pipepette up and down 3-4 times and add the mix (1 mL) in a size/ ζ-cell (see Note 8) (Fig. 4 A).
5. Place the cell into the instrument.
6. Measure the size according to the equipment protocol for size and PDI characterization (see Note 9).

2.2.3.2. ζ-potential

ζ-potential is the measurement obtained by the combination of electrophoresis and laser doppler velocimetry techniques, where the data obtained indicates the charge of our niosome formulation or nioplexes (Fig. 4 B). We can also use instruments, such as the previously mentioned to obtain this information.

1. Turn on the zetasizer-nano and open the software.

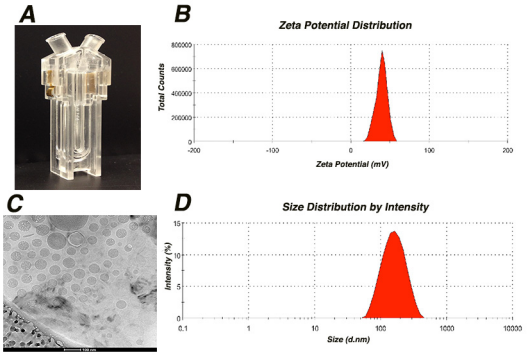

Figure 4. Material and data for characterization of niosomes. A) Clear disposable size and ζ-cell, B) graph indicating ζ-potential distribution of the niosomes, C) Cryo-TEM image of niosomes and D) characterizing graph of size distribution of niosomes in nanometers.

2. In a small tube, add 50 μL of niosome or nioplexes (see Note 10).
3. Add 950 μL 0.1 mM of NaCl (see Note 11).
4. Pipe up and down 3-4 times and add the mix (1 mL) in a size/ζ-cell (see Note 12) (Fig. 4 A).
5. Place the cell into the instrument.
6. Measure the ζ-potential according to the equipment protocol (see Note 9 and 13).

2.2.3.2. Stability

Periodic measurements of size, PDI and ζ-potential of niosomes at different storage temperatures are necessary to avoid unwanted process, such as aggregation that could hamper the performance of the formulation.

1. Pipe 800 μL of niosomes from the main batch.
2. Separate the 800 μL in two small tubes.
3. Use 400 μL for RT storage and the other 400 μL for 4ºC storage.
4. Perform the first size and ζ-potential measurement right after the niosomes are prepared.
5. Label both tubes and store them at their corresponding temperatures.
6. Perform periodic measurements of size, PDI and ζ potential of the niosomes (e.g. every 30 d up to 100 d) as previously indicated (see Subheading 3.3) (see Note 14, 15).

3. NOTES

1. We find that it is best to prepare fresh non-ionic surfactant solution each time.
2. The evaporation technique can be used to obtain a higher concentrated formulation. When the niosomes have been formed, keep the sample under magnetic agitation until desirable concentration is reached (e.g. three more h). The rpm of the magnetic stirrer will affect the evaporation time; we suggest employing around 1400 rpm. Attach the glass to the stirrer plate with adhesive tape to avoid spilling the sample.
3. The filtration technique is employed to obtain higher concentrated formulation. When the niosomes have been formed, place the sample inside the filters (Fig. 1 F) (filters can be found at different diameters) and drain the sample through the filters until the desirable concentration is reached (go to manufacturer website, spectrumlabs.com, to obtain protocol details).
4. Use dH2O or transfection medium to prepare the nioplexes. If the nioplexes are prepared for characterization purposes (e.g. size, ζ-potential, agarose gel assays), we use dH2O. If the nioplexes are prepared for transfection purposes (e.g. cell transfection, cell uptake, cell viability), we use transfection medium, such as Opti-MEM® [6].
5. Same niosomes and DNA volumes are preferred to enhance the cationic lipid-pDNA

interaction.

6. Use nioplexes as soon as possible to avoid DNA degradation.

7. Smaller amounts of niosomes or nioplexes can be used to measure the size and PDI, especially for those niosome formulations that have been concentrated. The zetasizer-nano is able to measure size and PDI with small amounts of sample. So, if you exceed the required amount of sample, the size and PDI might not be accurate. The polydispersity index (PDI) indicates the size distribution of the particles, where the maximum value is 1.0. A sample that shows a PDI value close to 1.0 suggests that there are a broad size distribution and possible large particles or aggregates. In such case, the sample is not suitable for DLS measurements.

8. If you do not want to waste valuable sample, we suggest using the ζ-potential cell. Additionally, the ζ-potential cell only requires 1 mL of final volume compared to other cells that require greater amounts of sample.

9. It is recommendable to measure the same sample at least three times.

10. Smaller amounts of niosomes or nioplexes can be used to measure the ζ-potential, especially for those niosome formulations that have been concentrated. The zatasizer-nano is able to measure employing small amounts of sample. So, if you exceed the required amount of sample, the ζ-potential might not be accurate.

11. Conductivity can be a problem when the saline solution used to measure the ζ-potential is highly concentrated. In order to avoid wrong ζ-potential data, we suggest using 0.1 mM NaCl.

12. Before pouring the sample into the cell, make sure that the electrodes are not black. Due to the constant use of the cells, the electrodes turn black (burned aspect) impeding accurate measurements.

13. The ζ-potential is an important factor to consider for niosome aggregation. The ζ-potential is also important when the niosomes are bound with DNA through electrostatic interactions to form nioplexes. Moreover, positively charged nioplexes are desired to facilitate their interaction with the negatively charged cell surfaces and encourage the endocytic process.

14. The stability of niosomes is a relevant aspect that might cause concern if it has not been taken into consideration when the niosome formulation has been prepared and stored for their later use. Over the time, niosomes can show modifications due to poor stability that directly affects their size, ζ-potential and polydispersity.

15. Acquisition times of size and ζ-potential data will depend on the desired storage time. We recommend to measure size and ζ-potential up to 100 d.

4. ACKNOWLEDGMENTS

This project was partially supported by the University of the Basque Country UPV/EHU (UFI 11/32), the National Council of Science and Technology (CONACYT), Mexico, Reg. # 217101, the Spanish Ministry of Education (Grant CTQ2010-20541, CTQ2010-14897), the Basque Government (Department of Education, University and Research, pre-doctoral PRE-2014-1-433 and BFI-2011-2226 grants) and by Spanish grants MAT2012-39290-C02-01 and IPT-2012-0574-300000. Technical and human support provided by SGIker (UPV/EHU) is gratefully acknowledged. Authors also wish to thank the intellectual and technical assistance from the ICTS "NANBIOSIS", more specifically by the Drug Formulation Unit (U10) of the CIBER in Bioengineering, Biomaterials & Nanomedicine (CIBER-BBN) at the University of Basque Country (UPV/EHU).

5. REFERENCES

1. Rajera R, Nagpal K, Singh SK, Mishra DN. Niosomes: a controlled and novel drug delivery system. Biol Pharm Bull 2011;34:945-953.

2. Moghassemi S, Hadjizadeh A. Nano-niosomes as nanoscale drug delivery systems: an illustrated review. J Control Release 2014;185:22-36.

3. Puras G, Mashal M, Zarate J, Agirre M, Ojeda E, Grijalvo S, et al. A novel cationic niosome formulation for gene delivery to the retina. J Control Release 2014;174:27-36.

4. Junyaprasert VB, Teeranachaideekul V, Supaperm T. Effect of charged and non-ionic membrane additives on physicochemical properties and stability of niosomes. AAPS PharmSciTech 2008;9:851-859.

5. Spanova M, Zweytick D, Lohner K, Klug L, Leitner E, Hermetter A, et al. Influence of squalene on lipid particle/droplet and membrane organization in the yeast Saccharomyces cerevisiae. Biochim Biophys Acta 2012;1821:647-653.

6. Ojeda E, Puras G, Agirre M, Zarate J, Grijalvo S, Pons R, et al. Niosomes based on synthetic cationic lipids for gene delivery: the influence of polar head-groups on the transfection efficiency in HEK-293, ARPE-19 and MSC-D1 cells. Org Biomol Chem 2015;13:1068-1081.

7. Byk G, Dubertret C, Escriou V, Frederic M, Jaslin G, Rangara R, et al. Synthesis, activity, and structure--activity relationship studies of novel cationic lipids for DNA transfer. J Med Chem 1998;41:229-235.

8. Mahidhar YV, Rajesh M, Chaudhuri A. Spacer-arm modulated gene delivery efficacy of novel cationic glycolipids: design, synthesis, and in vitro transfection biology. J Med Chem 2004;47:3938-3948.

9. Zhi D, Zhang S, Wang B, Zhao Y, Yang B, Yu S. Transfection efficiency of cationic lipids with different hydrophobic domains in gene delivery. Bioconjug Chem 2010;21:563-577.

10. Karmali PP, Chaudhuri A. Cationic liposomes as non-viral carriers of gene medicines: resolved issues, open questions, and future promises. Med Res Rev 2007;27:696-722.